The University of New Mexico
Dept. of Physics and Astronomy
PHYSICS 307L: Junior Laboratory
Fall 2006

Professor Michael Gold
office: 1111 (277-2086) , lab: 131 (277-3604)
E-mail: mgold@unm.edu

Contents

1. Purpose of this Course:

Physics is science, hence based on experiment. The majority of research physicists do experiments and make measurements. This course is meant as an introduction to modern experimental techniques.

In this course you will:

- apply the theory you have learned in the real (experimental) world;
- learn how to use various types of hardware, instrumentation, and software;
- learn basic statistics, error analysis, and determination of statistical and systematic errors;
- perform the best possible (i.e. the most precise and accurate) experiment within the constraints of the available resources (equipment, time, etc.) - just like in real research!

2. General Information:

Prerequisite: exposure to Modern Physics at the P330 level. Please consult the instructor if you have not taken this course.

Weekly lecture: M, 13:00-13:50, room 5. This lecture will cover (at an introductory and practical level) basic electronics, error analysis and statistics as well as essential elements of the laboratory physics and apparatus. If possible, a brief introduction to the use of MatLab for graphing and fitting of data will also be given. The **course schedule**

http://www-hep.phys.unm.edu/∼gold/phys307L/schedule.html

will be continuously updated.

Lab: M/W 14:00-16:50 rooms 116, 135. You nominally sign up for one of the two sessions. You are expected to show up *well-prepared* for the lab so that you should be able to complete the data collection for most the experiments in *one afternoon session.*

Perform the experiments with a partner, but keep your own lab notebook, do your own data analysis and write your own lab reports.

Except for the oscilloscope experiment we have only one set-up per experiment. Therefore you have to sign-up (with the TA or instructor) for an experiment the week before starting

it. Please keep in mind the **schedule**– it is your responsibility to complete the experiments on time!

3. Preparation for each Experiment:

The key to this course is to read and study the write-up (including reference material) *before* coming to the laboratory. (It will be obvious to the instructor when you haven't done this!) You may want to look at the apparatus of your next experiment in the week before actually doing it. Remember that you have limited time to spend for the performance of an experiment - do *not* spend this valuable time on preparations which should be done prior to coming into the lab.

4. Lab notebook

Data and observations must be recorded in a lab notebook: *The notebook must be bound and have numbered pages. Pages are not to be torn out; any pages that have a line drawn through will be ignored. The first page will be an index for your experiments 1-10. Each experiment must begin on a new page and be labeled by its number, date started, and lab partner. All raw data must appear in the notebook, as well as a description of the apparatus, observations, calculations and answers to questions regardless of whether a formal write-up is being done for this experiment. This log will be examined periodically and it has to be handed in together with the final lab report at the end of the semester.*

5. Guidelines for writing lab reports:

The lab report is an exercise in critical thinking and scientific writing, as well as usage of the English language. Lab reports must be typed. *No handwritten reports will be accepted* . When relevant, hand-drawn sketches of the experimental apparatus are acceptable.

#1 Abstract:

A concise (short paragraph) statement of the objective of the experiment, the results (including errors and accepted values if relevant) and the conclusion. Should include one or both of the following sentences:

"We have measured $q = (xx \pm yy)x10^z$ [unit] in [excellent, good, fair, poor] agreement of the accepted value v [unit]".

"Our experimental test of the hypothesis h yields a value of [chisq/degree of freedom], in agreement with the hypothesis at a confidence level of xx %".

#2 Introduction:

Explain the goals of the experiment. What is the scientific reason for doing the experiment?

#3 Method:

Briefly describe the apparatus and procedure. This should not be a repeat or summary of the lab manual, but rather a reflection of your understanding of what the important components are and how they work. Imagine that you were designing the experiment. For example, how would you design the Helmholtz coils?

#4 Calibrations:

Explain what calibrations are necessary. Discuss how calibrations were done. Display calibration data in a table. Describe and include any fits that were done to obtain calibration constants. Include an estimate of the systematic error, for example from the error on the fit to a slope.

#5 Data:

Briefly describe how the data was taken, including choice of data points. Present the raw data in a well organized **table or tables.** Derive and discuss any **formulas** used in applying calibrations and calculating derived quantities from your data. Present calibrated and derived data in a table or tables.

#6 Analysis and Results:

Describe any analysis (calculations of averages, graphs, fits, etc.) done to obtain your final results for parameters measured and/or hypotheses tested (e.g., de Broglie). Discuss in detail your calculations of **statistical and systematic errors.** Include a list of systematic errors considered and discuss how each was estimated.

#7 Conclusions:

Compare your results with expected values and/or discuss how well hypotheses were verified. Answer all questions in the lab manual or additional questions asked by the instructor. What is the major source of systematic error that you have considered? If necessary, conjecture on additional systematics that you did not have time to investigate. Speculate on the cause of any discrepancies, and suggest further experimentation that might resolve such discrepancies.

5. List of Experiments:

The following 10 experiments are to be done this semester[1]

- The oscilloscope
- e/m Ratio for Electrons (dark)
- Electron Diffraction (very dark, and works marginally)
- Balmer Series (dark)
- Planck's Constant (dark)
- Excitation Levels of Neon
- Electron Spin Resonance
- Poisson Statistics (MCA)
- Mass of the Electron (MCA)
- Speed of Light (MCA)

Important Notes: The oscilloscope experiment must be done first. It is recommended that the next four experiments which are less challenging be done next. (They require a dark room and are set up in room 135.) The last three use a computer interfaced multi-channel (pulse-height) analyzer (MCA). Take time to read the technical information on this instrument and to familiarize yourself with its operation. The Poisson statistics and electron mass are easist to do sequentially as they use the same equipment.

It is recommended that you do some quick data analysis while you're still taking data, i.e. using some of your measured numbers calculate a couple final results. This way you can check right away whether your results are more or less as expected.

[1]The five underlined exeriments are to be written up as formal lab reports.

6. Requirements/Grade:

Complete all 10 experiments, which should not take you more than about 12-13 afternoons. We like to emphasize quality over quantity. This pace allows you to take additional data on any given experiment if your analysis reveals problems with your initial data set. You will formally write up only 5 of the 10 experiments. The grade will be based primarily on the five lab reports (underlined in the above list). Also important is the completeness of your lab book, In addition, general performance in the lab will be considered. There will be no midterm, but there will be a comprehensive final exam, in which you will be expected to demonstrate understanding and successful completion of all 10 experiments undertaken. More details on the final exam will be given later.

Experiment 1

The Oscilloscope

1.1 Preface

This simple experiment will help you gain familiarity with one of the most useful and most widely used instruments in any physics lab, the oscilloscope. In addition, you will compare the oscilloscope with the digital multimeter (DMM).

1.2 Review of Basic Oscilloscope Functions

1.2.1 Basic Structure

Despite its apparent complexity, the oscilloscope, in its most frequent application, may simply be considered as a voltmeter which visually displays the input voltage signal as a curve in time. Visual representation of the signal is provided by means of a cathode-ray tube (CRT) and two pairs of deflecting electrode plates which control the vertical and horizontal movement of the CRT electron beam. When a signal appears at the input, it is first amplified, then split in two. One part is applied to the vertical-deflection plates, while the other is used to trigger a generator which applies a linear ramp voltage to the horizontal-deflection plates. This latter voltage causes the beam to be swept horizontally across the screen at a constant speed. Since the beam is now also being deflected vertically in proportion to the input signal, a curve representing the waveform of the signal in time is produced. This is the simplest and most important operation mode of the oscilloscope. Examples of further applications are given later.

1.2.2 Bandwidth and Risetime

One of the most important operating characteristics of the oscilloscope is the bandwidth of the vertical amplifier. This parameter essentially governs how fast a signal can be

accepted and correctly displayed by the oscilloscope without distortion. This is especially important for signals from detectors such as photomultipliers which can emit pulses of nanosecond risetime. Because of the finite bandwidth of the amplifier, the oscilloscope has an intrinsic risetime of its own, i.e. a signal with a perfectly vertical rising edge (0 risetime) will be displayed as a signal with a finite risetime (t_{osc}). A rough relation between the bandwidth and this risetime is given by the formula $t_{osc}[ns] = 350/f_{3db}[MHz]$, where f_{3db} is the bandwidth of the oscilloscope in Megahertz. The risetime displayed for a signal with a risetime t_{pulse} will thus be a combination of the risetime of the pulse and the oscilloscope risetime. An approximate formula for t_{disp} is given by $t^2_{disp} = t^2_{pulse} + t^2_{osc}$. A 3 ns risetime pulse on a 100 MHz oscilloscope ($\rightarrow$ 3.5 ns risetime) will thus be displayed as a pulse with a 4.6 ns risetime. Similarly, if a 10 ns risetime is measured on the same oscilloscope, the true risetime of the signal is $t_{pulse} = 9.4$ ns.

1.2.3 Controls and Operating Modes

Input Coupling

As in any good voltmeter, the input impedance of the oscilloscope is very high (make sure you understand why!), usually $1M\Omega$, in parallel with a small capacitance on the order of 10-20 pF. For fast signal viewing from 50Ω cables, some oscilloscopes also provide a switch which allows selection of a 50Ω input impedance so as to obviate cable termination. Otherwise this termination can easily be achieved with a BNC T and a 50Ω terminator - make sure you know how this is done. On most oscilloscopes two (sometimes more) inputs are available allowing the simultaneous display of several signals. Depending on how triggering is performed, this allows a visual comparison of two or more signals. At each input, the type of coupling may be selected:

AC - In this mode any constant dc level is suppressed and only nonzero ac frequencies are displayed.
DC - dc constant levels, as well as ac frequencies are displayed. Thus varying signals superimposed onto a constant dc level may be seen.
GND - The input signal is directly shunted to ground.

Vertical and Horizontal Sensitivity

VERTICAL SENSITIVITY - This controls the vertical scale. On most oscilloscopes a vernier control is available which allows a continuous adjustment between the indicated markings. Note that these markings are only valid when the vernier is in the *calibrated* position!
TIME - This determines the speed at which the beam is swept across the screen and thus the horizontal scale. Again, the indicated settings are only valid in the *calibrated*

position.

DELAYED SWEEP - In this mode the time sweep is made after a certain delay time determined by the delay setting dial.

EXTERNAL X - When in this position, the time base generator is disconnected allowing the horizontal deflection of the beam to be controlled by an external voltage applied at the EXT-X or channel-2 input.

Triggering(Synchronization)

Triggering or synchronization is the most important adjustment to be made when using the oscilloscope. As we have seen, the horizontal sweep of the oscilloscope is activated only when there is a triggering signal satisfying certain conditions. This triggering signal may be the input signal itself or some other external signal, depending on the mode selected. The conditions for a trigger include the slope of the signal and its amplitude. In this manner a precise point on the signal may be selected for the beginning of the sweep. For a repetitive signal such as a sine wave, for example, this produces a steady trace on the display screen, always starting at the same point on the signal.

Signal Source

INTERNAL - Triggering is done by the input signal itself as outlined above. This is the normal mode of operation.

EXTERNAL - Triggering is made by an externally applied signal at the EXT. Trig. input.

LINE - Triggering is made on the ac line voltage.

Trigger Conditions

SLOPE - Selects the slope of the signal on which triggering should be made. Normally, positive signals are triggered on the positive slope and negative signals on the negative slope.

LEVEL or THRESHOLD - This defines the voltage level at which triggering of the sweep begins. Signals not reaching this minimum level are therefore not displayed. For most beginners, failure to obtain a trace is usually due to setting this level incorrectly.

Trigger Modes

NORMAL - In this mode no sweep is made unless a triggering signal satisfying the desired conditions is present. At all other times the screen remains blank.

AUTO - A continuous sweep is performed even if no signal is present at the input. This is useful for finding the trace and adjusting its position on the screen. When a signal is present, synchronization is as in the normal mode.

SINGLE SWEEP - Only one single sweep is made.

EXTERNAL or X-INPUT - In this position the internal ramp generator is disconnected and the horizontal movement of the beam is controlled by the voltage at the X-input.

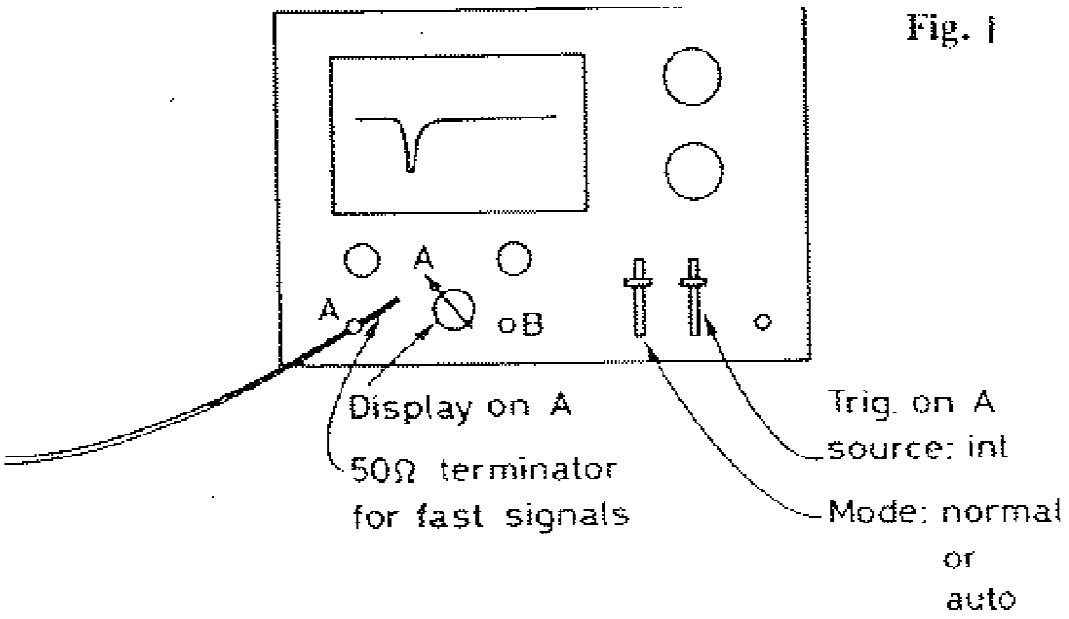

Figure 1.1: Normal signal viewing

Display Modes

CHANNEL 1 - Displays channel 1 only.
CHANNEL 2 - Displays channel 2 only.
ALTERNATE - Displays channels 1 and 2 on alternate sweeps, i.e. one *full* sweep is made alternatively for each channel. This mode is useful for comparing the relation between two signals.
CHOP - In this mode the display is alternated between channels 1 and 2 *during* a sweep. This is usually done at a high frequency on the order of 500 kHz. The two signals are thus "*chopped*" in appearance.
ADD - The signals in channels 1 and 2 are added and displayed.

1.2.4 Applications and Examples

Signal Viewing

Figure 1.1 shows the scheme for normal signal viewing. If no signal is observed, check the following (not necessarily in the order listed!)
1) Check slope and trigger level.
2) Check that the trigger is on internal (or external, if that is what you are using).
3) Is the trace positioned on the screen? Put on *Auto* (if not already) and position trace with the horizontal and vertical position knobs. If there is still no trace, check the

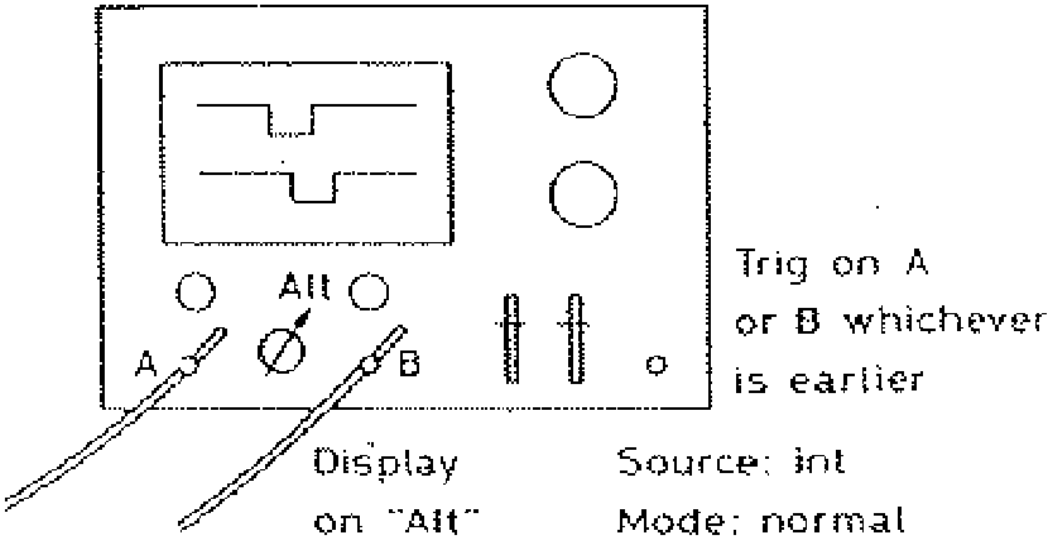

Figure 1.2: setting a coincidence

intensity.
4) Check the horizontal and vertical scales. Are they about the right order of magnitude for the signal you are observing?
5) Check that the input is not on OFF or GND.
6) Are you sure of your input signal? Try one that you know exists.

Comparison of Signals

Signals may be compared in time and amplitude using the setup in Fig. 1.2. The oscilloscope sweep is triggered by either A or B according to the selection on the trigger source. With the display on *Alternate*, the relation in time of the second signal can be seen. This is the usual method for setting coincidences.

If the oscilloscope is not equipped with two channels an alternate scheme is to use the external trigger, shown in Fig. 1.3.

A second example of signal comparison is checking the threshold of a discriminator or setting the levels of a Single Channel Analyzer (SCA). This is shown in Fig. 1.4. The output of the SCA or discriminator is used to trigger the scope for viewing the linear signal. Note that a delay must be added in order to take into account the processing time of the SCA or discriminator. Quite
obviously only those linear signals which pass through the discriminator will be displayed since only these signals will have a trigger. In this way a certain amplitude may be selected

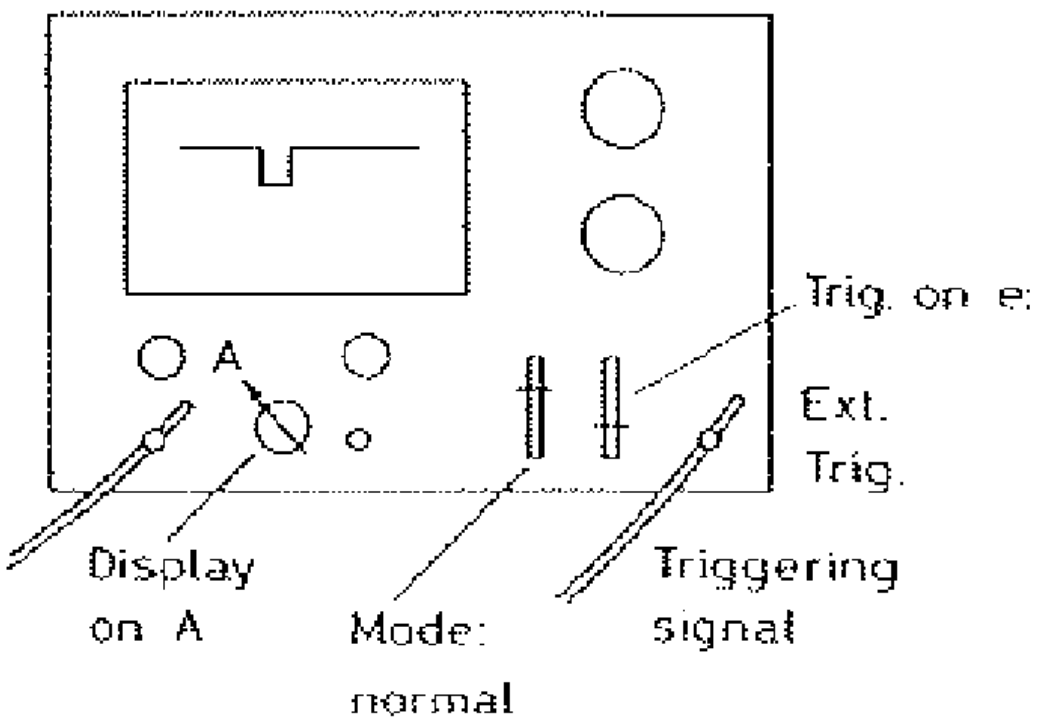

Figure 1.3: using the external trigger

or the level of the discriminator checked with respect to the noise.

1.3 Procedure

Review Ohm's law, Kirchhoff's two laws, and simple circuit analysis. You will need to be thoroughly familiar with those topics. In class we will also discuss the idea of complex impedance for AC circuits – resistance (R) and reactance (X): $Z(\omega) = R + iX(\omega)$. In this formalism, one can apply Kirchoff's laws to AC circuits with capacitors and inductors just for DC circuits with resistors. The current and voltage are now frequency dependent (the real part of complex V,I). Pure capacitive elements contribute a reactance to the circuit $X = 1/(i\omega C)$, and pure inductive elements a reactance $X = i\omega L$.

You will be using the Heathkit ET-1000 Circuit Design Trainer from the 308 lab of next semester as a signal generator and a power supply. Familiarize yourself with its layout and its options. Also make sure that any potential switch on the scope probe is in the $\times 1$ position.

1. Start by examining a low DC voltage (say +5 V) on the scope. Then examine sine

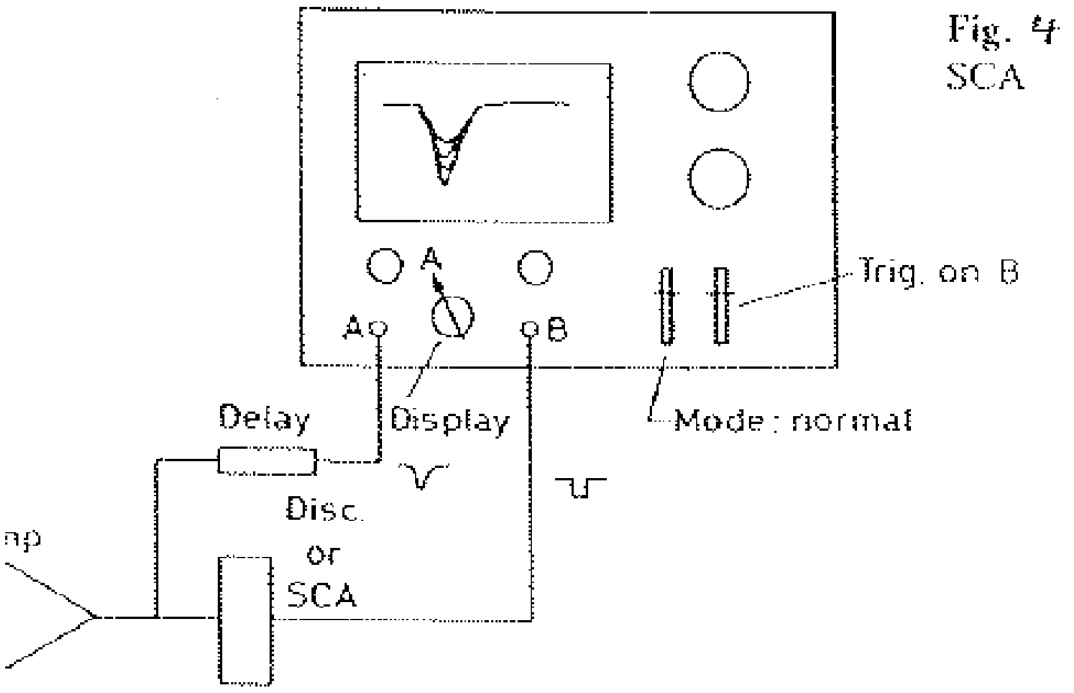

Figure 1.4: setting the levels of a discriminator (SCA)

and triangular waves of different frequencies, and compare the measured frequency with the dial setting on the Heath Trainer. Always compare your measured result with your expectation.

2. Compare (for relatively low frequencies, ≈ 100 Hz) the sine wave on the scope with the DMM reading of the same sine wave. Why are the two measurements different, i.e. what is actually measured in the two instruments? For the scope measurements is there any noticeable difference between using AC and DC coupling?

3. Study the difference between AC and DC coupling by looking at a sine wave from our Wavetek Function Generator. Make sure that the DC offset is initially set to zero. Now vary the DC offset on the Function Generator and carefully observe the difference on the scope between AC and DC coupling. Note how with AC coupling the scope display is independent of the DC offset of the input signal, whereas under DC coupling you can move the sine wave up/down the scope display by varying the DC offset. Make sure you understand the implications of using AC/DC coupling and how one can disentangle AC and DC components of a signal or waveform.

4. Take a low voltage DC power supply and with the scope examine and measure its AC "ripple", i.e. the (hopefully small!) AC component sitting on top of the DC.

5. Build a voltage divider from two 10KΩ resistors.

6. Derive an expression for V_{out} as a function of V_{in}. Use V_{in} around 20V and 10k for the two resistors.

7. With a DMM measure the actual values of R_1, R_2, V_{in}, V_{out}, and the current I. Compare V_{out} and I with your calculated expectations and comment.

8. Now for a quantitative comparison of the input impedances of DMM (typically 10MΩ) and scope (typically 1MΩ). Measure V_{out} also with the scope, compare with the DMM reading, and comment.

9. Now change R_2 in such a way that you would expect a difference in V_{out} between scope and DMM readings. Compare both readings with the expected V_{out}, and explain the differences.

10. Build an AC circuit by replacing in the voltage divider $R_1 \rightarrow Z_1 = 1/(i\omega C)$ and $Z_2 = R$. What is the characteristic frequency of the circuit? Plot the circuit gain and phase as a function of frequency. (I suggest using MATLAB for the plotting.) Now choosing appropriate values for C and R measure the gain and phase shift with your scope and a waveform generator. Does it agree with your calculation? If time permits, repeat with $Z_1 = R$ and $Z_2 = i\omega L$.

1.4 References

[1] Melissinos and Napolitano, Ch. 3.

Experiment 2

The Ratio e/m for Electrons

2.1 Objective

Study the effects of electric and magnetic fields on a charged particle and measure the charge-to-mass ratio (e/m) of the electron.

2.2 Theory

In 1897 J.J. Thomson first measured the charge-to-mass ratio (e/m) of the electron. His experiment involved analyzing the electron's motion in an electric and magnetic field. Some time later R.A. Millikan determined the charge of the electron and resolved this ratio using an electric field alone. It was Thompson's hypothesis of the electron's existence, and its charge-to-mass ratio, that lead to the concept of the first atomic particle.

Helmholtz coils give us a simple solution for the value of the magnetic field along the axis of symmetry. For coils of N wires each carrying current I, having radius R show that the field along the symmetry axis x is given by,

$$B = \frac{\mu R^2 N I}{(R^2 + x^2)^{\frac{3}{2}}}. \tag{2.1}$$

In the Helmholtz configuration, $x = R/2$, The permeability of free space $\mu = 4\pi \times 10^{-7} \frac{weber}{amp-meter}$. In our apparatus $N = 130$ and $R = .15$ meters, therefore

$$B = (7.8 \times 10^{-4} \frac{weber}{amp - meter^2}) \times I. \tag{2.2}$$

By measuring V,I, and the radius of curvature r we can detetermine the ratio e/m.

2.3 Procedure

Fig. 2.1 shows the apparatus. The e/m tube is filled with helium at a pressure of $\sim 10^{-2}$mm Hg. Connect a regulated 6-9 Vdc supply rated at 2 A to the Helmholtz coil jacks. Be sure to observe the color-coded polarity on all input jacks. You will need to connect an ammeter in series between the supply and the coil jacks so that you can measure the current to 1% or better accuracy. A wire wound potentiometer control to the right of the coil jacks on the panel serves to adjust the current in the coils.

Now connect a 6.3 V (ac or dc, but do *not* exceed 6.3 V!) supply rated at 1.5 A to the heater jacks of the electron gun at the right side of the base panel. Besides powering the heating element, this supply also powers the small scale lamps on the coil brackets.

Lastly connect a high voltage source of 150-300 Vdc rated at 40 mA to the Electrode jacks of the electron gun. The high voltage applied to the anode of the gun accelerates the electrons boiled off from the cathode to form the necessary electron beam. The value of this voltage determines the average velocity of the electrons in the beam and appears in the final expression for the ratio of e/m. Regardless of the metering on your high voltage supply, the accelerating voltage must be measured with an accurate dc voltmeter connected at the jacks labelled Voltmeter on the base panel.

Key to Figure 2.1	
E	Envelope to vacuum tube
G	Electron Gun
F	Focusing element of gun
Z	Heater or filament of gun within cathode
A	Anode of gun
S	Electron Beam
H	Helmholtz Coils
B	Space of magnetic field
M	Mirror scale
W	Lamps to measure r
All Others	Various connectors as labelled

Turn the *Current Adjust* control to zero and set the switch on the panel to the e/m position. Nothing should be connected to the jacks labelled *Deflection Plates* at this time. Turn on the *Heater* supply and allow the electron gun filament to heat up for two minutes. At the end of this time apply a 200 Vdc potential from the high voltage supply to the *Electrodes* for the initial value of accelerating voltage.

With the accelerating voltage on, you should be able to see the violet hue of the electron beam projecting horizontally from the electron gun. For proper viewing of the beam this experiment should be conducted in a darkened room or in subdued lighting

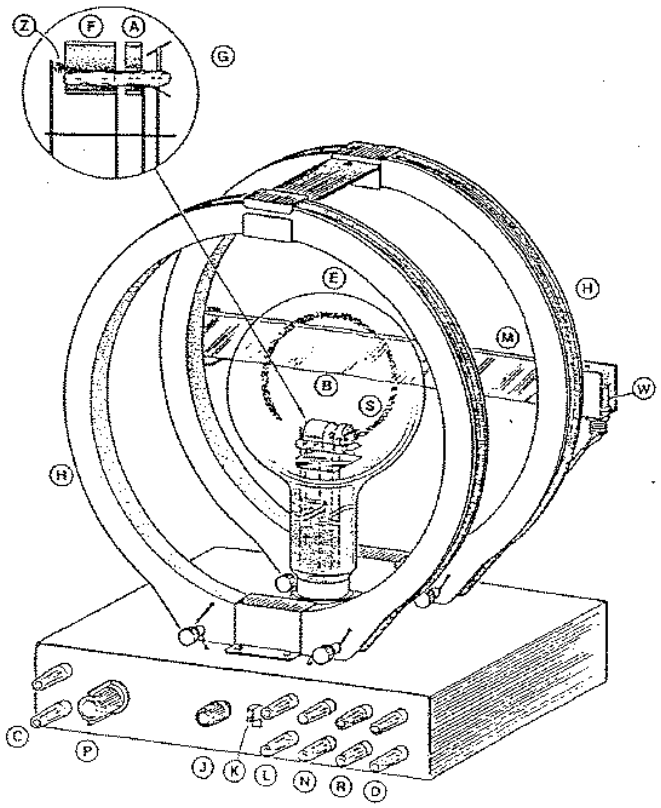

Figure 2.1: Charge-to-Mass Ratio Apparatus.

using a black cloth hood to mask the tube and to backdrop the beam. Turn on the coil current and increase the *Current Adjust* control from zero to a current value that bends the beam around into a complete circle on itself. It may be necessary to rotate the tube socket until the end of the curving beam strikes between the two wire leads supplying the heating filament on the left side of the electron gun. This brings the beam and gun into

an exact parallel position with the plane of the coils.

2.4 Data

Three data variables are necessary to make a determination of the ratio e/m. They are the accelerating voltage, the coil current, and the radius of the beam curvature. Each of these variables must be measured as accurately as is possible in order that e/m come close to the accepted value of $1.76 \times 10^{11} \frac{coul.}{kg}$. However, the electron beam radius involves by far the largest error because the beam is enclosed in a glass envelope forcing a sighting measurement to be made at a distance which is fraught with parallax error. To overcome this defect, an anti-parallax scale is mounted and illuminated by two small lamps on the back of the coil. The technique for measuring the beam radius is to move your head in order to align the electron beam with the reflection of the beam that you see on the mirrored scale. Each side of the beam loop may have a slightly different radius of curvature. Therefore, take a mean of the two radii for the value of r.

For about ten different combinations of accelerating voltage V and coil current I record the corresponding value of the radius r. Calculate e/m and its error.

In addition, take enough data point to be able to do the following. Plot r vs. I^{-1} at const. V, and determine e/m from a linear least squares fit. Do the same via plotting r^2 vs. V at const. I.

You now have three results for e/m. Compare the three including their errors with the accepted value.

Note: The greatest source of systematic error in this experiment is the velocity of the electrons, v_e. First, the non-uniformity of the accelerating field caused by the hole in the anode causes v_e to be slightly less than its theoretical value. Second, collisions with the helium atoms in the tube further rob the electrons of their velocity. Since e/m is proportional to $1/r^2$, and r is proportional to v_e, experimental values for e/m will be greatly affected by these two effects. To minimize this error you can try to measure radii to the *outside* of the beam path. To minimize the relative effect of collisions, keep the accelerating voltage as high as possible (above ∼250 V tends to give best results). On the other hand, if the voltage is too high, the radius measurement will be distorted by the curvature of the glass at the edge of the tube. Best results are typically obtained for radii of less than ∼5 cm. Your experimental values for e/m *will* be higher than theoretical, due to the fact that both sources of error mentioned cause the radius to be measured as smaller than it should be.

Also go through the qualitative experiments suggested next.

2.5 Qualitative Experiments

You can qualitatively demonstrate the vector effects of an electric and magnetic field on a charged particle with the e/m apparatus as predicted by the Lorentz force law.

With the electron beam on and the Helmholtz coils operating, rotate the glass envelope and observe the resulting spiral path of the beam in the magnetic field. How does the Lorentz vector expression account for this spiraling? Turn the coil current down to zero and then switch the polarity of the coil leads to reverse the current direction which will in turn reverse the magnetic vector. Turn the coil current on again and observe the deflection of the electrons.

An applied electric field will also deflect the electron beam. A pair of skewed plates at the right side of the electron gun produces an electric field around the emerging electron beam when a voltage is applied. To show the electric field deflection, connect in parallel the voltage leads from the *Electrode* jacks to the jacks labelled $Deflection\ Plates$. Switch on the accelerating voltage supply and set the central switch to the $Electrical\ Deflection$ position. There should be no current in the coils in this case. Note how the beam deflection varies with the voltage value. If the polarity of the plates is in the same sense as the color-coded jacks, can you tell what sign the charge is in the beam? Turn down the voltage to zero and reverse the polarity of the $Deflection\ Plate\ Jacks$. In which direction is the beam deflected now? Explain. Observe what happens when the beam bends and hits the deflection plates.

In retrospect, J.J. Thomson originally determined the charge to mass ratio of the electron by first deflecting an electron beam with an electric field, and then compensating this deflection with a opposing magnetic field deflection. You can reenact this procedure here qualitatively. First deflect the electron beam using the electrical deflection plates (reverse the polarity sense of the jacks). Turn on the current to the Helmholtz coils and adjust the current until the deflection of the magnetic field cancels the deflection of the electric field. This is the substance of the historic Thomson experiment which we cannot reproduce here in a quantitative way due to the uncertainty of the electric field value between the deflection plates.

2.6 Questions

1. Why do we see the electron beam at all?

2. We ignored the Earth's magnetic field in our procedure. How much error does this introduce into this experiment? (see http://www.ngdc.noaa.gov/seg/geomag/)

3. Suppose that protons were emitted in the vacuum tube instead of electrons. How would this effect the experiment?

4. Show that if the magnetic field is held constant, the time t required for an electron to make a complete circle in your e/m tube and return to the anode is independent of the accelerating voltage by deriving an expression for this time. The reciprocal $f = \frac{1}{t}$ is called the electron's cyclotron frequency.

5. Would a relativistic correction for the electron's momentum be appreciable for the present experiment?

Experiment 3

Electron Diffraction

3.1 Objectives

- Electrons as waves.
- Study and verification of the de Broglie hypothesis $\lambda = h/p$.
- Measurement of the spacing of diffracting planes in graphite.

3.2 Theory

In a bold and daring hypothesis in his 1924 doctoral dissertation Louis de Broglie reasoned that if electromagnetic radiation can be interpreted as *both* particles (Photoelectric Effect, Compton Scattering) and waves (diffraction), then perhaps the electron, which had traditionally been interpreted as a particle, could also have a wave interpretation. De Broglie hypothesized that *all particles* have a wave behavior with a universal relationship between the wavelength and momentum given by $\lambda = h/p$. This expression is called the de Broglie relationship and the wavelength is called the de Broglie wavelength. The momentum in this relationship is the momentum that is conserved in collisions, i.e. the relativistic momentum. The de Broglie relationship holds for all particles. Note that it is identical to the one for photons ($E = h\nu$).

Diffraction phenomena represent clear evidence for wave properties. *How can an electron be both wave and particle?*

In this experiment you will investigate the diffraction of electrons passing through a thin layer of graphite (carbon), which acts as a diffraction grating. It was Max von Laue, who in 1912 suggested (in connection with x-ray studies) that the basic granularity of matter at the atomic level might provide a suitable grating. Bragg, using the cubic system of NaCl, first calculated the inter-atomic spacings and showed them to be of the

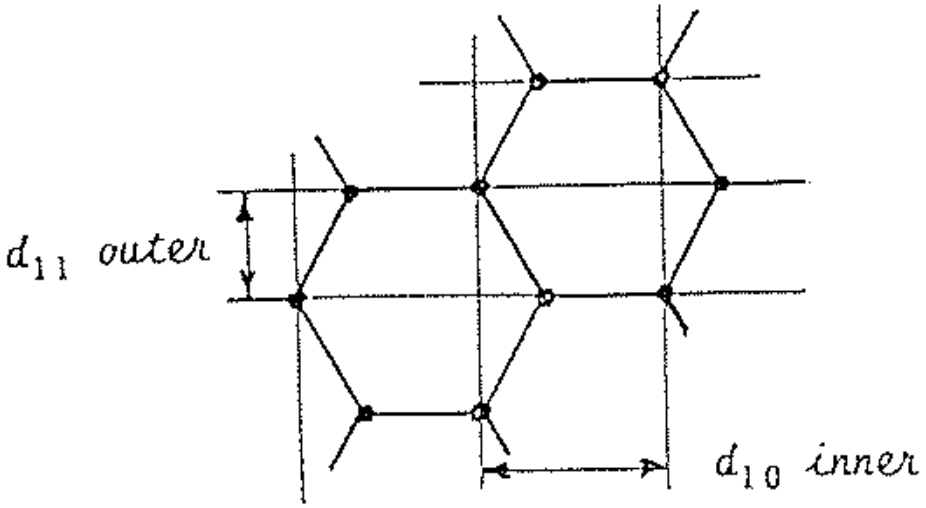

Figure 3.1: Structure of Graphite

right order for x-rays. Fig. 3.1 shows the hexagonal structure of graphite with the two characteristic spacings of 0.123 and 0.213 nm.

3.3 Apparatus

Our electron diffraction tube, see Fig. 3.2, comprises a 'gun' which emits a narrow, converging beam of electrons within an evacuated clear glass bulb on the front surface of which is deposited a luminescent screen. Across the exit aperture of the gun lies a micro-mesh nickel grid, onto which a *very* thin layer (only a few molecular layers!) of graphite has been deposited.
The electron beam penetrates through this graphite target to become diffracted into two rings corresponding to the separation of the carbon atoms of 0.123 and 0.213 nm. The diffraction pattern appears as rings due to the polycrystalline nature of graphite. The source of the electron beam is an indirectly-heated oxide-coated cathode.

3.4 Important Precautions

Due to its extreme thinness the graphite can easily be punctured by current overload. Such current overload causes the graphite target to become overheated and to glow dull

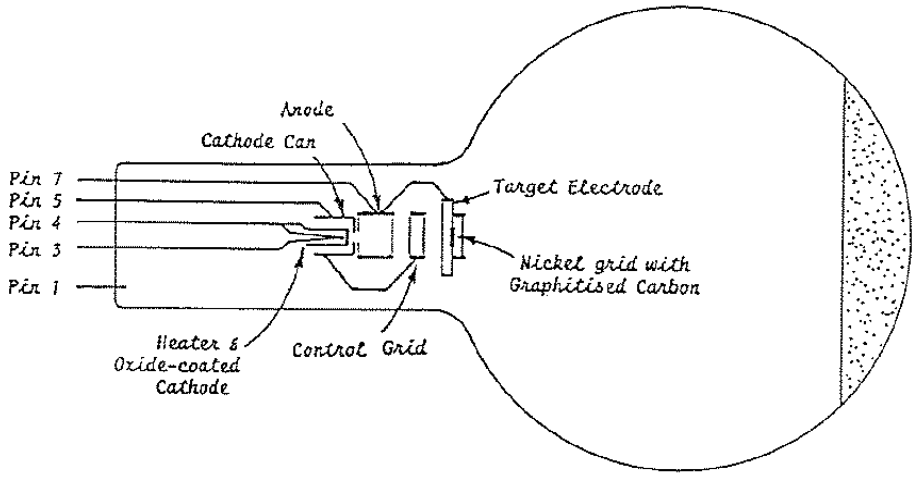

Figure 3.2: Schematic of the Electron Diffraction Tube

red. It is therefore important to monitor the anode current and to keep it below 0.25 mA at all times. Use a handheld digital multimeter. In actuality you will likely find that the current tends to stay well below this value, typically a few μA (micro-Amps). It is also good practice to inspect the target periodically during an experiment.

The 33k resistor R in Fig. 3.3 is incorporated into the filament protection circuit of the stand to provide 'negative auto-bias' and so reduce the likelihood of damage to the target due to accidental abuse. The total emitted current passes through R. Therefore an increase in current causes the cathode-can to become more negatively biased, thereby reducing the emitted current.

3.5 Experimental Procedure

Connect the tube into the circuit shown in Fig. 3.3 **but ignore** V_B. Both heater supply and HV are obtained from the 813 KeV power unit. The HV should be connected to the "+" and "−" HV connections to get the full voltage which is read on the top-scale of the KeV unit's meter. Be sure the high voltage slider is at zero before switching on the unit. Switching on the unit (in back) will also switch on the heater. **IMPORTANT:** Switch on the heater supply (V_F), and wait one minute for the cathode temperature to stabilize before applying the HV (anode voltage V_A).

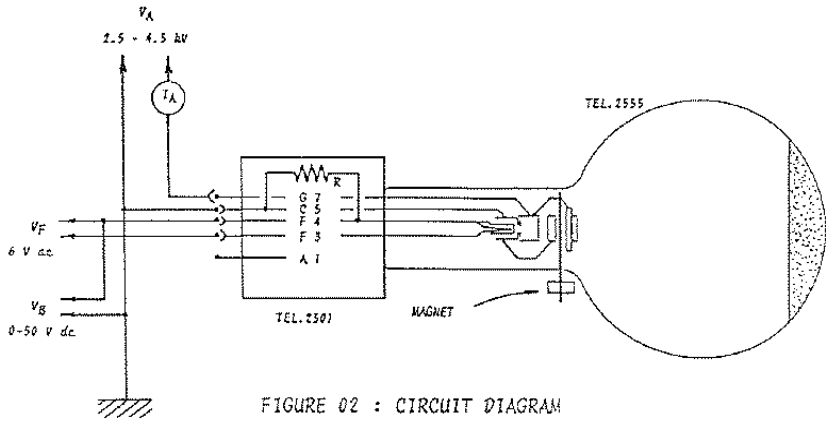

Figure 3.3: Circuit Diagram

3.6 Data Taking and Analysis

The tube is old and rings are faint, so do the best you can. Be sure the room is very dark. The rings are quite distinct at the full 5 kV, but get very hard to see as you go down in voltage. Try to go as low as 2.5 kV. Take at least 10 different data points, measuring the diameter of the two rings with the calipers. You can adjust the position of the spot by using the little magnet on the neck of the tube. You want the rings centered so you can do the correction for the curvature of the tube-face. Do the geometry and correct for the curvature (and thickness?) of the glass (see Figure 3.4). The length L in Figure 3.4 is controlled during production of the tube to be 13.0 ± 0.2 cm.

The kinetic energy and momentum of the electrons are of course related to the accelerating potential. From Fig. 3.4 we also know that $D = 2L\tan\theta$, where D is the *extrapolated* diameter. Show that by using the de Broglie relation, the lattice spacing d is related to the accelerating voltage V_A approximately by,

$$d = \frac{4\pi L\hbar c}{D\sqrt{2eV_A mc^2}} \tag{3.1}$$

Plot D as a function of $V_A^{-1/2}$ for all your data and indicate the estimated error in D as vertical error bars. The straight lines you should get verify the theory and substantiate de Broglie's hypothesis. Also calculate the two values for d from your data (no need to make the above approximation!), and compare with the accepted values of 0.123 and 0.213 nm.

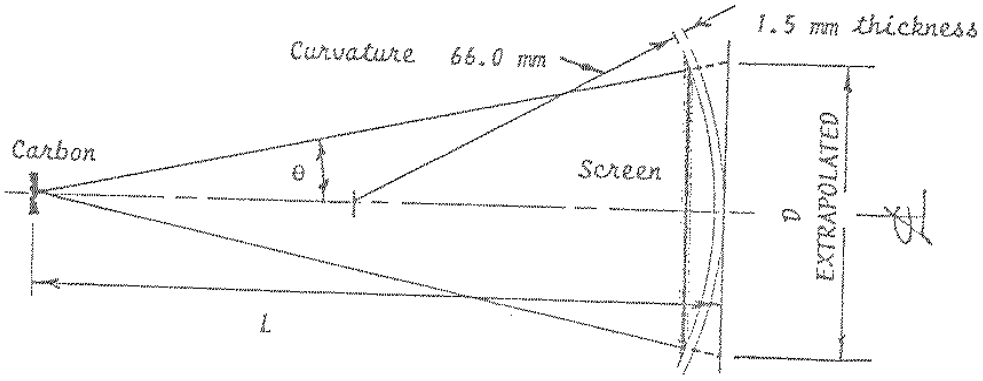

Figure 3.4: Curvature and glass thickness of the electron diffraction tube. The length $L = 13.0 \pm 0.2$ cm.

3.7 References

Any good Modern Physics textbook.

Experiment 4

Balmer Series

4.1 Objectives

In this experiment we will observe the Balmer Series of Hydrogen and Deuterium.

- Review basic atomic physics.
- Calibrate an optical spectrometer using the known mercury spectrum.
- Study the Balmer Series in the hydrogen spectrum.
- Determine the Rydberg constant for hydrogen.
- Compare hydrogen with deuterium

4.2 Apparatus

The instrument used in this laboratory is a so-called "constant-deviation" spectrometer. Fig. 4.1 shows the composite prism used in this device and the optical path for an incident ray. It may be seen that the angle of incidence and the angle of exit can remain fixed for all wavelengths by an appropriate rotation of the prism. This has obvious advantages for positioning and alignment of source and detector. All that is required for the spectral analysis of light is to rotate the prism relative to the incident light keeping the incident ray and the axis of the analyzing telescope fixed at a 90 deg angle. The rotation of the prism is calibrated with a known source (Hg in our case), and an interpolation between the known lines is used for the final calibration.

Our spectrometer may be old, but it is nevertheless a quality instrument which must be handled carefully. To adjust the spectrometer, first bring the cross-hairs into sharp focus by sliding the ocular in or out to suit your vision. Next bring the slit into sharp

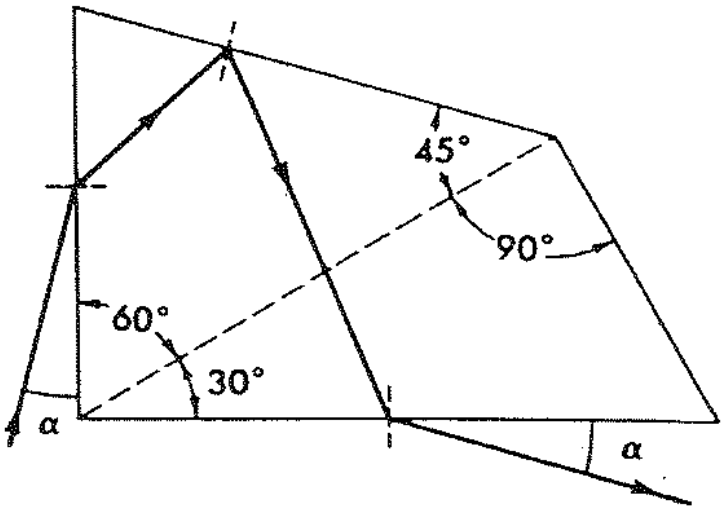

Figure 4.1: A Pellin-Broca constant-deviation prism. The prism acts as a spectrometer because it has a wave-length dependent index of refraction

focus by turning the large knurled ring near the center of the viewing telescope. When the instrument is properly adjusted, the cross-hairs and the slit will be in sharp focus and there will be no parallax between them.

4.3 Calibration of the Spectrometer

Turn on the mercury tube and let it warm up for a few minutes. With the spectrometer slit wide ($\frac{1}{2}$ to 1 mm) find a line of the mercury spectrum. Now narrow the slit until the mercury line becomes sharp and narrow. In practice the narrower the slit, the better is the resolution of the instrument. However, narrowing the slit also causes loss of intensity. In almost all optical equipment there is a trade off between resolution and intensity. The optical scientist must decide, within the limitations of his/her instrument, how to compromise intensity and resolution requirements.

Locate all of the mercury lines that you can. You should see all of the lines listed below. In addition, you may see other faint lines from mercury, from impurities, or from more complicated molecular behavior.

404.7 nm	(deep violet very hard to see!!)
435.8 nm	violet
skip	(very weak blue-green)
546.1 nm	green
577.0 nm	yellow
579.0 nm	yellow
690.75 nm	red

When you are turning the screw drive which rotates the prism, note the positions on the dial which correspond to the mercury lines listed above. **Important:** turn the screw in one direction only to avoid error in gear back lash (the gears do not mesh exactly and there are dead spots when you reverse the direction). Use your data and the known values to calibrate your instrument.

4.4 The Hydrogen Spectrum

Observe the spectrum of hydrogen. You should see at least four and possibly five lines. Show your raw and your corrected (using the above calibration) data. The wavelengths which you observe can be fitted by an expression of the form of equation 4.1.

$$\frac{1}{\lambda} = R\left(\frac{1}{2^2} - \frac{1}{n^2}\right),\ n = 3, 4, 5, ... \tag{4.1}$$

R is the Rydberg constant, and n is the principle quantum number. Use the above equation to find the value for R. You must correctly identify each wavelength with the right quantum number in order to get R as a constant. You should get four or five evaluations of R.

Expression 4.1 above was discovered empirically in 1885 by a Swiss high school teacher named Balmer for whom this spectral series is named. Although the original equation in

a slightly different form was good guess work by Balmer, it remained for both Rydberg and Ritz to suggest independently in the 1890's that equation 4.1 might be modified to be

$$\frac{1}{\lambda} = R\left(\frac{1}{m^2} - \frac{1}{n^2}\right),\ m = 1, 2, 3, \ldots\ n = 2, 3, 4, \ldots\ n > m \tag{4.2}$$

giving rise to the possibility of the existence of other spectral series which were subsequently observed. Equation 4.2 is also basic to the Ritz combination principle. If we convert the hydrogen emission wavelengths to frequencies, we find that certain pairs of frequencies added together give other frequencies which appear in the spectrum.

The value of the Rydberg constant, R ($= \mu e^4/8\epsilon_0^2 ch^3, \mu$ = reduced mass), was explained theoretically only after the Bohr model (1913) and the comprehensive development of Quantum Mechanics in the 1920's. Quantum theory owes much to experiments of the type performed with the constant deviation spectrometer.

Also measure the Balmer spectrum for deuterium. Why would you expect it to be different from hydrogen? In addition, test the resolving power of your instrument by observing the doublet splitting of the famous yellow Na lines (λ = 589.0 nm and λ = 589.6 nm). Describe as quantitatively as possible whether you could resolve these two lines or not.

4.5 Analysis

What is your value of the Rydberg constant and its standard deviation? Compare your results with the accepted value for hydrogen: $R = 1.0967758 \times 10^7\ m^{-1}$. In your report discuss briefly the atomic/quantum physics underlying the hydrogen spectrum.

Calculate the expected difference between hydrogen and deuterium, for the Rydberg constant and for the wavelength of the H_α line. Compare your hydrogen and deuterium results. Could you measure any difference, and, in particular, could you even expect to see any difference based on your Na result?

4.6 References

[1] Melissinos and Napolitano, Chapters 1,5,6.

Experiment 5

Planck's Constant

5.1 Introduction

The emission and absorption of light was an early subject for investigation by the German physicist Max Planck. As he attempted to formulate a theory to explain the spectral distribution of emitted light based on a classical wave model, he ran into considerable difficulty. Classical theory (Rayleigh-Jeans Law) predicted that the amount of light emitted from a black body would increase dramatically as the wavelength decreased, whereas experiment showed that it approached zero. This discrepancy became known as the ultraviolet catastrophe.

Experimental data for the radiation of light by a hot, glowing body also showed that the maximum intensity of emitted light departed dramatically from the classically predicted values (Wien's Law). In order to reconcile theory with laboratory results, Planck was forced to develop a new model for light called the quantum model. In this model, light is emitted in small, discrete bundles of energy or quanta, later called photons.

The relationship between the classical and quantum theories for the emission and absorption of light can be investigated with our apparatus. In combination with a mercury vapor light source an accurate determination of the ratio h/e and thus of h, Planck's constant, is possible. This constant has turned out to be one of the most important fundamental constants in all of modern physics.

5.2 Background Theory

5.2.1 Planck's Quantum Theory

By the late 1800's many physicists thought they had explained all the main principles of the universe and discovered all the natural laws. But as scientists continued working, inconsistencies that couldn't easily be explained began showing up in some areas of study.

In 1901 Planck published his law of radiation. In it he stated that an oscillator, or any similar physical system, has a *discrete* set of possible energy values or levels; energies between these values never occur. He went on to state that the emission and absorption of radiation is associated with transitions or jumps between two energy levels. The energy lost or gained by the oscillator is emitted or absorbed as a quantum of radiant energy, the magnitude of which is expressed by the equation $E = h\nu$, where E equals the radiant energy, ν is the frequency of the radiation, and h is a fundamental constant of nature, later known as Planck's constant.

Planck's constant was found to have significance beyond relating the frequency and energy of light, and became a cornerstone of the quantum mechanical view of the atomic and subatomic world. In 1918 Planck was awarded the Nobel prize for introducing the quantum theory of light.

5.2.2 The Photoelectric Effect

In the photoelectric effect, light strikes a material, causing electrons to be emitted. The classical wave model predicted that as the intensity of incident light was increased, the amplitude and thus the energy of the wave would increase. This would then cause more energetic photoelectrons to be emitted. The new quantum theory, however, predicted that higher frequency light would produce higher energy photoelectrons, independent of intensity, while increased intensity would only increase the number of electrons emitted (or the photoelectric current). In the early 1900's several investigators found that the kinetic energy of the photoelectrons was dependent on the wavelength, or frequency, and independent of intensity, while the magnitude of the photoelectric current, or number of electrons was dependent on the intensity as predicted by the quantum model. Einstein applied Planck's theory and explained the photoelectric effect in terms of the quantum model using his famous equation, for which he received the Nobel prize in 1921:

$$E = h\nu = KE_{max} + W_0 \tag{5.1}$$

where KE_{max} is the maximum kinetic energy of the emitted photoelectrons, and W_0 is the energy needed to remove them from the surface of the material (the work function). E is the energy supplied by the quantum of light known as a photon.

5.2.3 The h/e Experiment

A photon with energy $h\nu$ is incident upon an electron in the cathode of a vacuum tube. The electron uses a minimum W_0 of its energy to escape the cathode, leaving it with a maximum energy of KE_{max} in the form of kinetic energy. Normally the emitted electrons reach the anode of the tube, and can be measured as a photoelectric current. However, by

applying a reverse potential V between the anode and cathode, the photoelectric current can be stopped. KE_{max} can be determined by measuring the minimum reverse potential needed to stop the photoelectrons and reduce the photoelectric current to zero. In our experiment the stopping potential is measured directly, rather than by monitoring the photoelectric current, see later. Relating kinetic energy to stopping potential V gives a linear relation between V and the frequency ν. Plotting V vs ν allows the extraction of the constants h and W_0 from a least squares fit.

5.3 Equipment and Setup

Fig. 5.1 shows the setup using a mercury vapor light source and the h/e apparatus. Apart from the equipment shown in Fig. 5.1 only a digital voltmeter is required. Before proceeding check the two battery voltages. Minimum values are indicated on the h/e apparatus. Note that the unit can also be powered using a dual ± 9 V power supply.

The grating is blazed to produce the brightest spectrum on one side only. During your experiment you may need to turn the lens/grating assembly around in order to have the brightest spectrum on a convenient side of your lab table.

Turn on the light source and allow it to warm up for five minutes. Check the alignment of the light source and the aperture by looking at the light shining on the back of the lens/grating assembly. If necessary, adjust the back plate of the light aperture assembly by loosening the two retaining screws and sliding the aperture plate left or right until the light shines directly on the center of the lens/grating assembly.

Connect a digital voltmeter (DVM) to the OUTPUT terminals of the h/e apparatus.

Set the h/e apparatus directly in front of the light source. By sliding the lens/grating assembly back and forth on its support rods, focus the light onto the white reflective mask of the h/e apparatus (Fig. 5.2).

Roll the light shield of the apparatus out of the way to reveal the white photodiode mask inside the apparatus. Rotate the h/e apparatus until the image of the aperture is centered on the window in the photodiode mask. Then tighten the thumbscrew on the base support rod to hold the apparatus in place.

Slide the lens/grating assembly back and forth on its support rods, until you achieve the sharpest possible image of the aperture on the window in the photodiode mask. Tighten the thumbscrew on the lens/grating assembly and replace the light shield.

Turn the power switch ON. Rotate the h/e apparatus about the pin of the coupling bar assembly until one of the colored maxima in the first order shines directly on the slot in the white reflective mask. Rotate the h/e apparatus on its support base so that the same spectral maximum that falls on the opening in the white reflective mask also falls on the window in the photodiode mask. The white reflective mask on the h/e apparatus is made of a special fluorescent material. This allows you to see the ultraviolet line as a

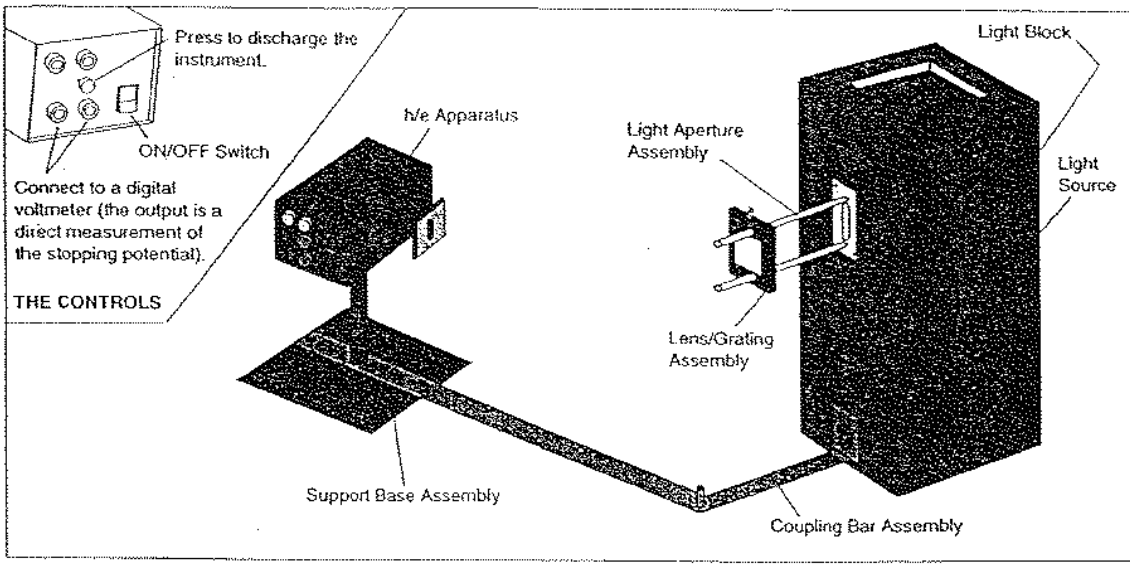

Figure 5.1: Equipment setup using a mercury vapor light source and the h/e apparatus.

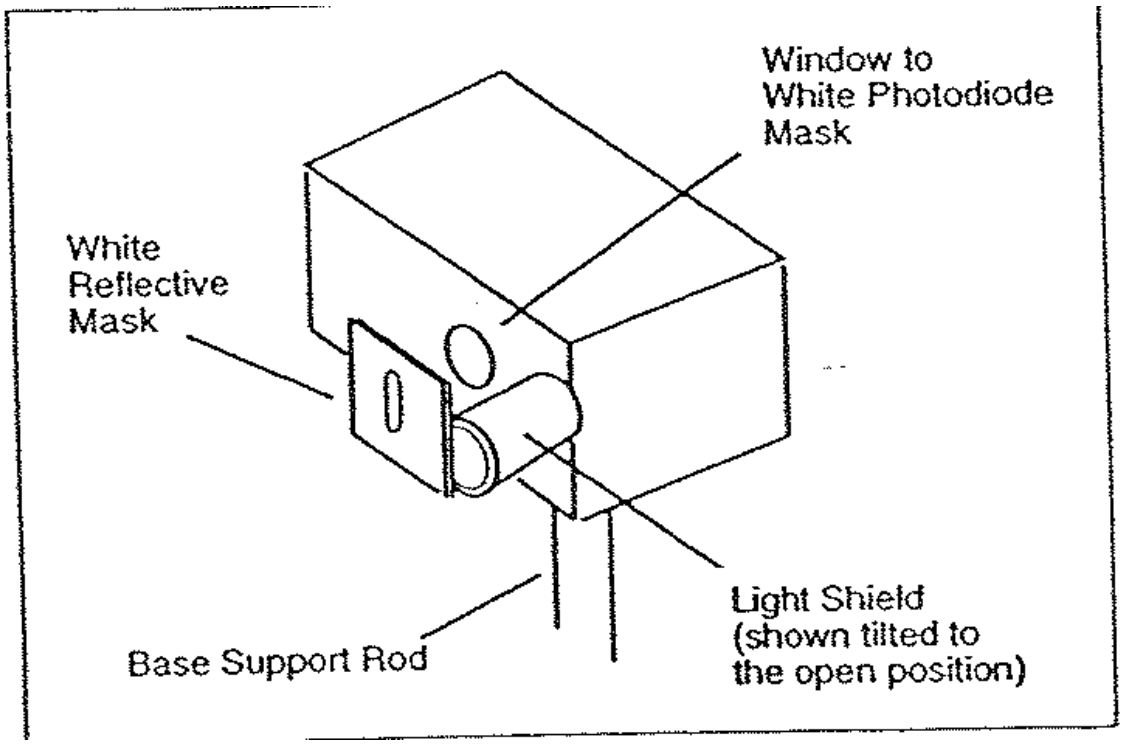

Figure 5.2: h/e Light Shield

blue line, and it also makes the violet line appear more blue. You can see the actual colors of the light if you hold a piece of white non-fluorescent material in front of the mask. The palm of your hand works in a pinch, although it fluoresces enough that the UV line will still be visible.
→ Important: when making measurements it is important that *only one* color falls on the photodiode window. There must be *no* overlap from adjacent spectral maxima.

Press the PUSH TO ZERO button on the side panel of the h/e apparatus to discharge any accumulated potential in the unit's electronics. This will assure the apparatus records only the potential of the light you are measuring. Note that the output voltage will drift with the absence of light on the photodiode.

Read the output voltage on your DVM. It is a direct measure of the stopping potential for the photoelectrons. See the Technical Information section at the end of this writeup for an explanation. For some apparatus, the stopping potential will temporarily read high and then drop down to the actual stopping potential voltage.

5.3.1 Using the Filters

The h/e apparatus includes three filters: one green and one yellow, plus a variable transmission filter. The filter frames have magnetic strips and mount to the outside of the white reflective mask of the h/e apparatus. Use the green and yellow filters when you're using the green and yellow spectral lines. These filters limit higher frequencies of light from entering the h/e apparatus. This prevents ambient room light from interfering with the lower energy yellow and green light and masking the true results. It also blocks the higher frequency UV light from the higher order spectra which may overlap with lower orders of yellow and green, see Fig. 5.3. In general you should make sure that room light does not interfere with your results, i.e. test by switching off the room lights.

The variable transmission filter consists of computer-generated patterns of dots and lines that vary the intensity (not the frequency) of the incident light. The relative transmission percentages are 100%, 80%, 60%, 40%, and 20%.

5.4 Experiment 1: The Photon Theory of Light

According to the photon theory of light, the maximum kinetic energy, KE_{max}, of photoelectrons depends only on the frequency of the incident light, and is independent of the intensity. Thus the higher the frequency of the light, the greater its energy. In contrast, the classical wave model of light predicted that KE_{max} would depend on light intensity, i.e. the brighter the light, the greater its energy.

Both of these assertions will be investigated here.

5.4.1 Procedure

Part A

Set up the equipment, check (and adjust if necessary) focus and alignment as described earlier. Connect your DVM. Adjust the apparatus so that only one of the spectral colors falls upon the
opening of the photodiode mask. If you select the green or yellow line, use the corresponding filter. Place the variable transmission filter in front of the white reflective mask (and over the colored filter, if one is used) so that the light passes through the 100% section and onto the photodiode. Record the DVM reading.

Press and release the instrument discharge button, and observe how much time is required to return to the recorded voltage.

Move the variable transmission filter to the next section, record the new DVM reading, and the time to recharge after the discharge button has been pressed and released. Repeat these steps for all five sections of the filter. Important: for consistent results you want to measure the recharge time to reach the *same* voltage for each of the five intensities.

Repeat the entire procedure using a second color from the spectrum.

Part B

You can easily see five colors in the mercury spectrum. Adjust the apparatus so that only one of the yellow bands falls upon the photodiode, and use the yellow filter. Record the DVM voltage. Repeat the process for each color. Be sure to use the green filter when measuring the green line.

5.4.2 Analysis

Plot your charging time results.

Describe the effect that passing different amounts of the same colored light through the variable transmission filter has on the stopping potential and thus on the maximum energy of the photoelectrons, as well as the charging time after pressing the discharge button.

Describe the effect that different colors of light had on the stopping potential and thus on the maximum energy of the photoelectrons.

Defend whether this experiment supports a wave or a quantum/photon model of light based on your lab results.

Explain why there is a slight drop in the measured stopping potential as the light intensity is decreased.

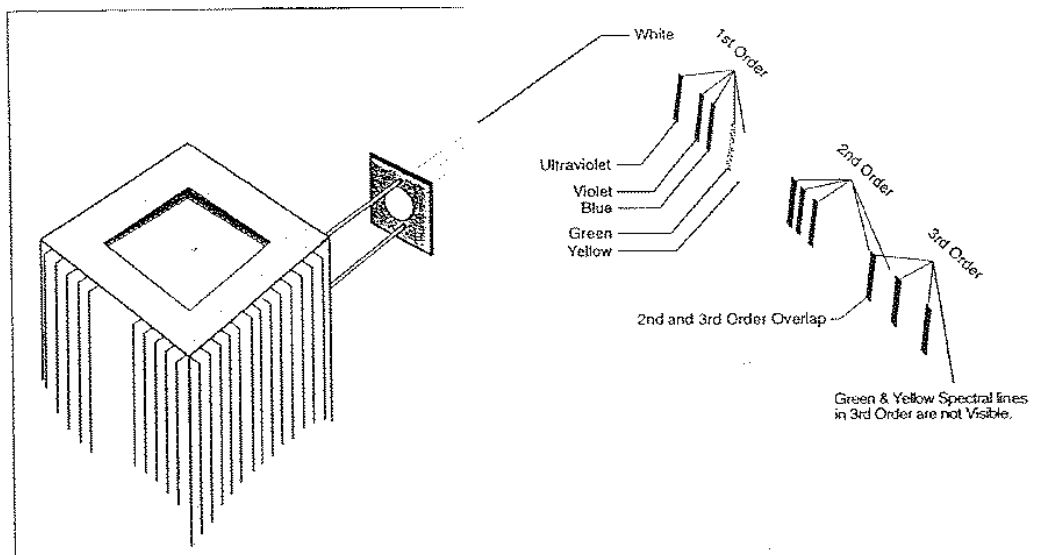

All values except wavelength for yellow line are from *Handbook of Chemistry and Physics, 46th ed.* The wavelength of the yellow was determined experimentally using a 600 line/mm grating.

➢ **NOTE:** The yellow line is actually a doublet with wavelengths of 578 and 580mm.

Color	Frequency (Hz)	Wavelength (nm)
Yellow	5.18672E+14	578
Green	5.48996E+14	546.074
Blue	6.87858E+14	435.835
Violet	7.40858E+14	404.656
Ultraviolet	8.20264E+14	365.483

Figure 5.3: The expected three orders of light gradients you should see.

5.5 Experiment 2: Determination of h

According to the quantum/photon model of light, the energy of light is directly proportional to its frequency. With careful experimentation the constant of proportionality, Planck's constant h, can be determined.

5.5.1 Procedure

Make sure focus and alignment are still ok. For each color in the first order measure and record the stopping potential (don't forget the yellow and green filters). Repeat these five measurements to test for reproducibility.

Move to the second order and repeat the above process, i.e. take two sets of readings.

5.5.2 Analysis

Plot all your results. Perform four linear least squares fits to your four data sets, and determine h and W_0 for each fit. Then calculate your final results (incl. errors!) for h and W_0 as a weighted average. Compare with the accepted value of h, and comment on the quality of your result.

5.6 Technical Information on the h/e Apparatus

In the h/e apparatus, monochromatic light falls on the cathode plate of a vacuum photodiode tube that has a low work function, W_0. Photoelectrons ejected from the cathode collect on the anode.

The photodiode tube and its associated electronics have a small capacitance which becomes charged by the photoelectric current. When the potential on this capacitance reaches the stopping potential of the photoelectrons, the current decreases to zero, and the anode-to-cathode voltage stabilizes. This final voltage between the anode and cathode is therefore the stopping potential.

To let you measure the stopping potential, the anode is connected to a built-in amplifier with an ultrahigh input impedance ($> 10^{13}\Omega$), and the output from this amplifier is connected to the output jacks. This high impedance, unity gain ($V_{out}/V_{in} = 1$) amplifier lets you measure the stopping potential with a DVM. Note that while the impedance of this amplifier is very high, it is not infinite, and some charge will leak off. Thus charging the apparatus is analogous to filling a bath tub with different water flow rates while the drain is partly open.

Due to the very high input impedance, once the capacitor has been charged from the photodiode current it takes a long time to discharge this potential through some leakage. Therefore a shorting switch ("Push to zero") enables the user to quickly bleed

off the charge. However, the op-amp output will not stay at zero volts after the switch is released since the op-amp input is floating.

Due to variances in the assembly process, each apparatus has a slightly different capacitance. When the zero switch is released, the internal capacitance along with the user's body capacitance coupled through the switch is enough to make the output voltage jump and/or oscillate. Once photoelectrons charge the anode, the input voltage will stabilize.

Experiment 6

Excitation and Ionization Energies of Neon

6.1 Theory

The essence of this experiment is the demonstration of energy quantization of atoms, Ne in this case. This is achieved via inelastic e^- scattering off Ne atoms. As such it is closely related to the original Franck-Hertz experiment (1914), which showed that an electron must have a certain minimum energy to make an inelastic collision with an atom. We now interpret that minimum energy as the energy of an excited state of the atom. It is strongly advised to read up on the Franck-Hertz experiment.

From a collision standpoint, free electrons colliding with orbiting electrons need to have at least the minimum energy required to excite the bound electrons to higher quantum levels. This experiment involves collecting these electrons after their atomic collisions, and determining the separate excitation energy levels that are available. The theory is quite simple. If an electron collides with a bound electron, and has sufficient energy to "move" the bound electron up into new orbits (or even ionize the atom), then the energy absorbed by the atom is lost to the free electron. This is an inelastic collision, and the free electron will slow down appreciably. In particular, it can now easily be captured by an anode positioned near the beam. As a function of the electron accelerating potential, V_A, the number of electrons captured will increase rapidly near the energy levels of the atomic gas in the tube. These peaks in current will signal the energy levels of the atom.

The enclosed paper by N. Taylor *et al.* gives more details and background information on this type of experiments as well as on the level scheme of Neon.

6.2 Apparatus

- Hertz Critical Potentials tube filled with neon
- Tube stand
- Picoamplifier and Alarmed Meter
- Power Supply and Digital Multimeter

Figs. 6.1 and 6.2 show schematically the tube and circuit diagram. The tube comprises a cathode ray gun which projects a divergent beam of electrons into a clear glass tube containing Neon gas at low pressure. Located inside the bulb is a wire ring collector so positioned that it cannot receive electrons directly from the source of the beam. The ring is connected to a shielded cable terminating in a BNC plug. The source of the beam is a tungsten hairpin filament connected to pins 3 and 4, and housed within a cathode can which is connected to pin 5. The anode cylinder of the gun has an external connection to pin 1. The inside surface of the glass bulb is coated with a transparent conducting layer. This coating is insulated from the wire ring but connected internally to the anode cylinder.

6.3 Objectives

1. Get the hardware to work successfully! This is not completely trivial since you are dealing with a somehat delicate instrument capable of measuring collector currents in the pA range. Any movement close to the glass bulb during scanning of the accelerating voltage should be avoided as it is liable to seriously distort your results.
2. Identify as many energy levels of neon as you can resolve, and determine their excitation energies in eV.
3. Find the ionization energy (in eV) of neon.
4. Measure the energy resolution (FWHM) of the first peak, and any others that you can, or at least give an upper limit if that peak consists of several levels.

6.4 Method

- Set up the apparatus as shown in Fig. 6.2. For the filament voltage V_F use an HP 6213A 12V DC power supply (or similar) capable of delivering $\sim$ 1 A. Important: Do *not* let V_F exceed 2.5 V! Make sure that you zero the alarmed meter at the range

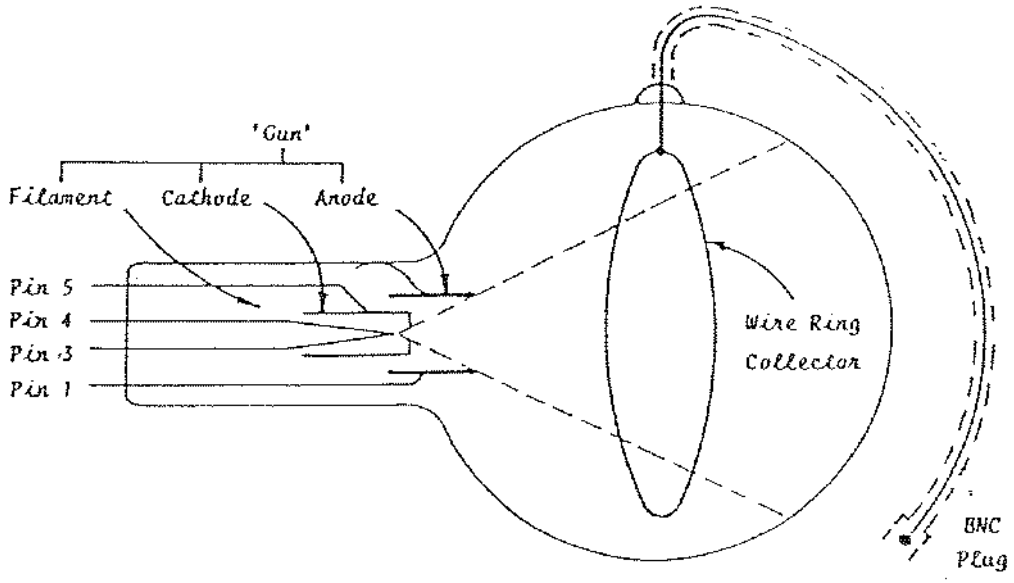
'Gun'
Filament
Cathode
Anode
Pin 5
Pin 4
Pin 3
Pin 1
Wire Ring
Collector
BNC
Plug

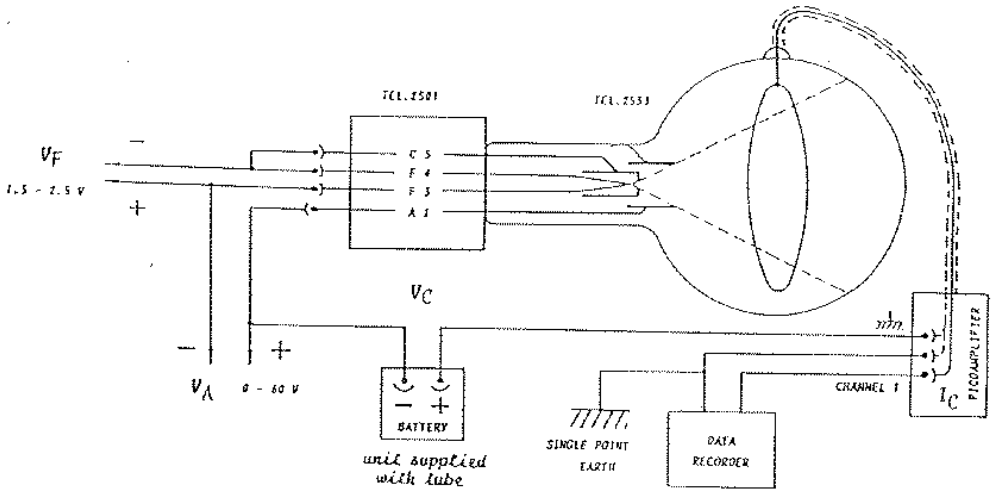

Figure 6.2: Circuit Diagram. For the Data Recorder we use the so-called Alarmed Meter.

setting that you actually end up using. If, for any reason, you decide to play with the range setting you must zero the alarm readings again. You may decide to use a DVM instead of the alarm, and the readings on it will not need to be readjusted. This tube is capable of stable collection currents at constant accelerating voltages, however it is also easily disturbed. If your setup doesn't achieve this stability, examine it for good connection everywhere and disturb the whole table as little as possible while taking your data.

- Vary the accelerating (Anode) voltage V_A and record the collector current I_C. Start with a coarse scan to verify that your results are qualitatively similar to typical results shown in Fig. 6.3. Then do a finer scan to cover the peak regions with sufficient data points. For comparison take data for two different filament voltages V_F. Higher V_F tend to give better peak-to-valley results, i.e. the excitation energy peaks tend to show up more prominently. But remember to *not* exceed 2.5 V for V_F!

- Reverse the potential of the collector ring, and find the ionization potential of neon. Consult Fig. 6.4 for a typical result.

- Check your answers for excitation energies and ionization energy against known values $before$ dismantling the equipment. The ionization energy of Neon is 21.56 eV, and known excitation energies can be found in the paper by N.Taylor *et al.*

6.5 Analysis

Summarize your results, and compare them with known values. What is the electron configuration of the dominant structures that you found? Fig. 6.3 in the enclosed paper by N. Taylor *et al.* will be helpful in this regard. Your peak positions and your ionization energy will likely have a (hopefully more or less constant) offset relative to the known values - how do you explain this?

6.6 References

[1] Melissinos and Napolitano, Chapter 1.
[2] Appendix :"Energy Levels in helium...", Am J. Phys Vol 49 No 3, March 1981.

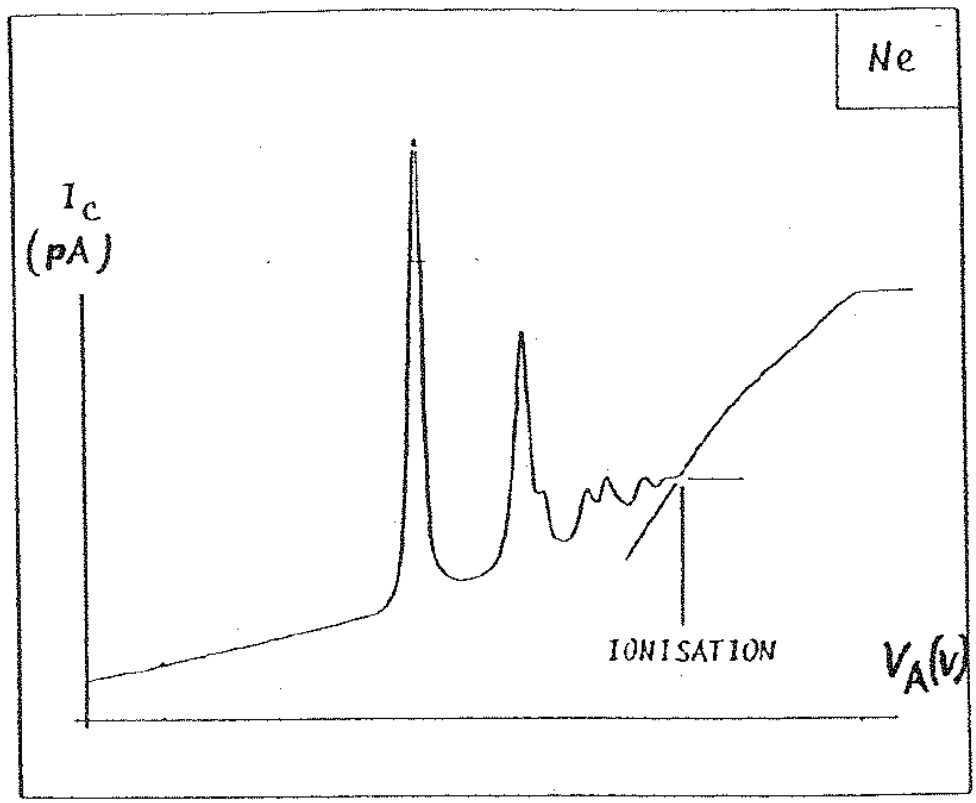

Figure 6.3: Typical excitation energy spectrum for Neon measured with this type of apparatus.

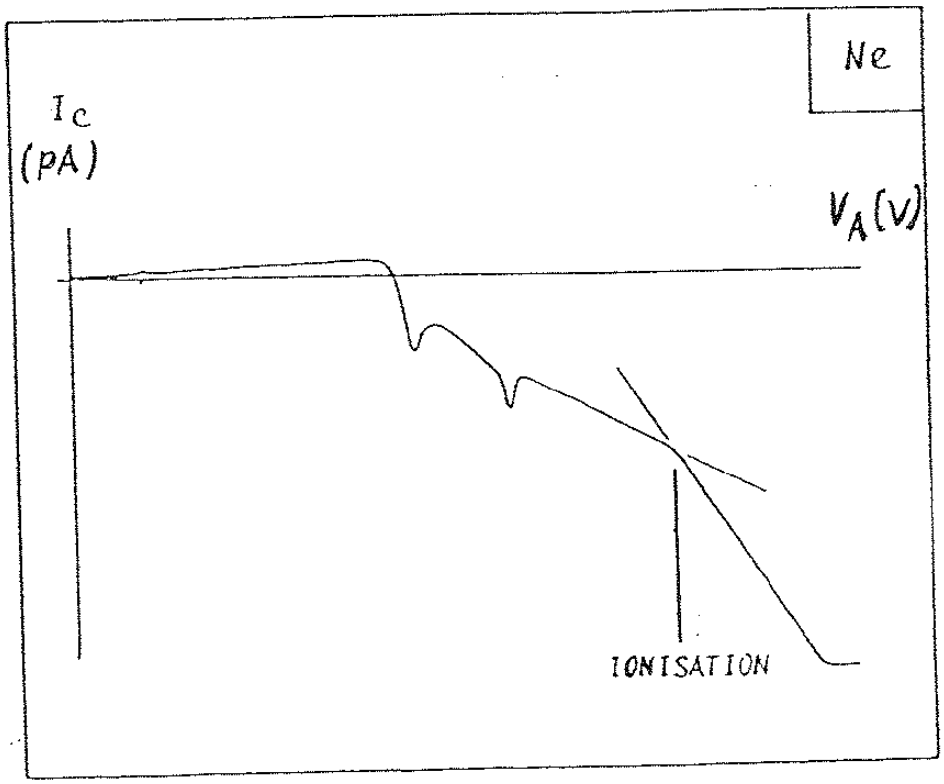

Figure 6.4: Onset of ionization in case of reversed collector bias.

Experiment 7

Electron Spin Resonance (ESR)

7.1 Introduction

Using ESR (Electron Spin Resonance, also known as Electron Paramagnetic Resonance) you will be measuring one of the best known quantities in all of physics, the famous g_s-factor of the electron. This will be achieved by looking for the "spin-flip" transition of a free (unpaired) electron exposed to a magnetic field.

7.1.1 ESR in Theory

The basic setup for ESR is shown in Fig. 7.1. A test sample is placed in a uniform magnetic field. The sample is also wrapped within a coil that is connected to an RF (radio frequency) oscillator. The smaller magnetic field induced in the coil by the oscillator is at right angles to the uniform magnetic field.

Consider, for the moment, a single electron within the test sample. The electron has an intrinsic (not related to any orbital motion!) magnetic dipole moment $\vec{\mu}_s$ that is related to its intrinsic angular momentum, or spin, by the vector equation:

$$\vec{\mu}_s = -g_s \mu_B \vec{S}/\hbar \tag{7.1}$$

where:

g_s = a constant characteristic of the electron, its intrinsic g-factor

μ_B = the Bohr magneton = $e\hbar/2m_e = 5.788 \times 10^{-9} eV/G$

$\vec{S}$ = the spin of the electron

$\hbar$ = Planck's constant/2π = 6.582×10^{-16} eV-sec, or $\hbar c = 197.3$ eV-nm.

The magnetic dipole moment of this electron interacts with the uniform magnetic field, $E = -\vec{\mu}_s \cdot \vec{B}$. Due to its quantum nature, the electron can orient its spin in one

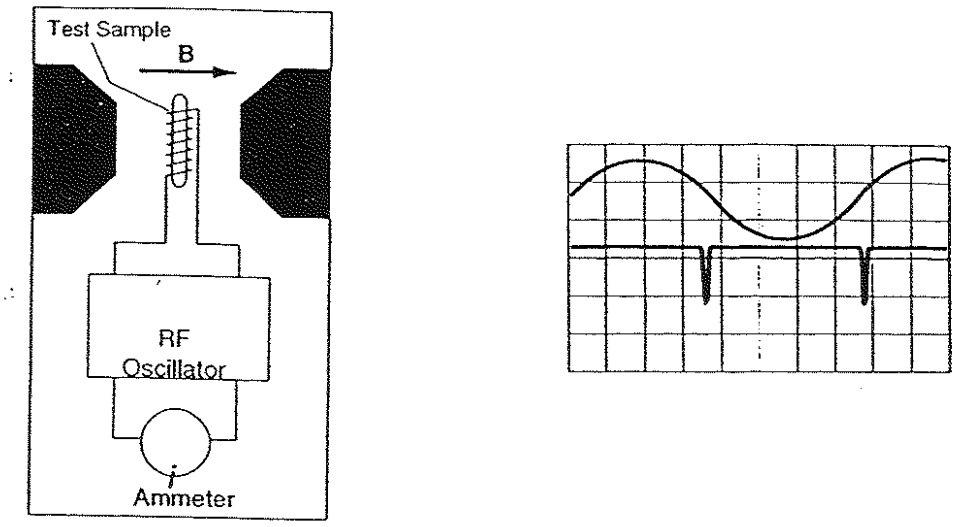

Figure 7.1: ESR diagram (left), scope display (right)

of only two ways ("space quantization"), spin up or spin down, with energies equal to $E_0 \pm g_s \mu_B B/2$; where E_0 is the energy of the electron before the magnetic field was applied. In the language of Quantum Mechanics, the energy degeneracy has been lifted by the B field, i.e. the energy level has been split. The energy difference between these two possible orientations is equal to $g_s \mu_B B$.

Resonance occurs when the RF oscillator is tuned to a frequency ν, such that the photon energy, $h\nu$, is equal to the difference between the two possible energy states of the electron. Electrons in the lower energy state can then absorb a photon and jump to the higher energy state. This absorption of energy affects the permeability of the test sample, which affects the inductance of the coil and thereby the oscillations of the RF oscillator. The result is an observable change in the current flowing through the oscillator. The condition for resonance, therefore, is:

$$h\nu = g_s \mu_B B \quad (2)$$

7.1.2 ESR in Practice

For an electron with only two energy states, in a magnetic field of a given magnitude, it would be necessary to set the RF frequency with considerable accuracy in order to observe resonance. In practice, this difficulty is solved by varying the magnitude of the B field about some constant value. With our apparatus, this is done by supplying a small AC current, superimposed on a larger DC current, to a pair of Helmholtz coils. The result is a B field that varies sinusoidally about a constant value.

If the RF frequency is such that equation (2) is satisfied at some point between the minimum and maximum values of the sinusoidally varying B field, then resonance will occur twice during each cycle of the field. Resonance is normally observed using a dual trace oscilloscope. The oscilloscope traces, during resonance, appear as in Figure 7.1 (right) . The upper trace is a measure of the current going to the Helmholtz coils, which is proportional to the B field. The lower trace shows the envelope of the voltage across the RF oscillator, which dips sharply each time the B field passes through the resonance point.

7.1.3 ESR in Research

In actual ESR research the situation is significantly more complicated than is implied above. With multiple unpaired electrons, finite orbital angular momenta, and shared molecular orbitals the energy level splittings become quite complex. However, the details of the analysis of such systems provide significant insight into the inner structure of the molecules.

The test sample included with our apparatus, DPPH (Diphenyl-Picryl-Hydrazyl, see Fig. 7.2),
is a particularly simple substance for ESR measurements. It has a total orbital angular momentum of zero, and only one unpaired electron. Therefore, for a given value of the external B field, it has only a single resonant frequency. This makes it possible to investigate some of the basic ESR principles without (or before) getting into the more complex world of ESR analysis.

7.2 The ESR Apparatus

7.2.1 The Probe Unit

The ESR Probe Unit (see Fig. 7.3) is the heart of the ESR apparatus. It contains an RF oscillator with a built-in signal amplifier, and 1000:1 frequency divider. The frequency divider allows the RF frequency, which is in the MHz range, to be measured with a standard kHz frequency meter. The frequency and amplitude of the RF signal can be

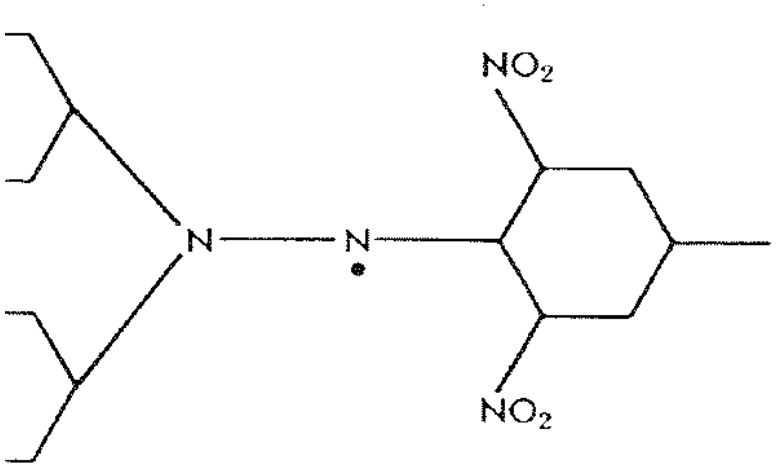

Figure 7.2: Chemical structure of DPPH, $(C_6H_5)_2N - NC_6H_2(NO_2)_3$.

controlled using the knobs shown in the Figure. The range of frequencies provided by the oscillator depends on which RF probe is being used (see Fig. 4). This is because the inductance of the probe determines, in part, the inductance of the oscillator circuit.

The Probe Unit is connected to the ESR Adapter (see Fig. 7.4), which in turn provides the connections to the necessary power supply, frequency meter, and oscilloscope. The Probe Unit requires $\pm 12\ V$, and the frequency output for a digital counter is a TTL signal.

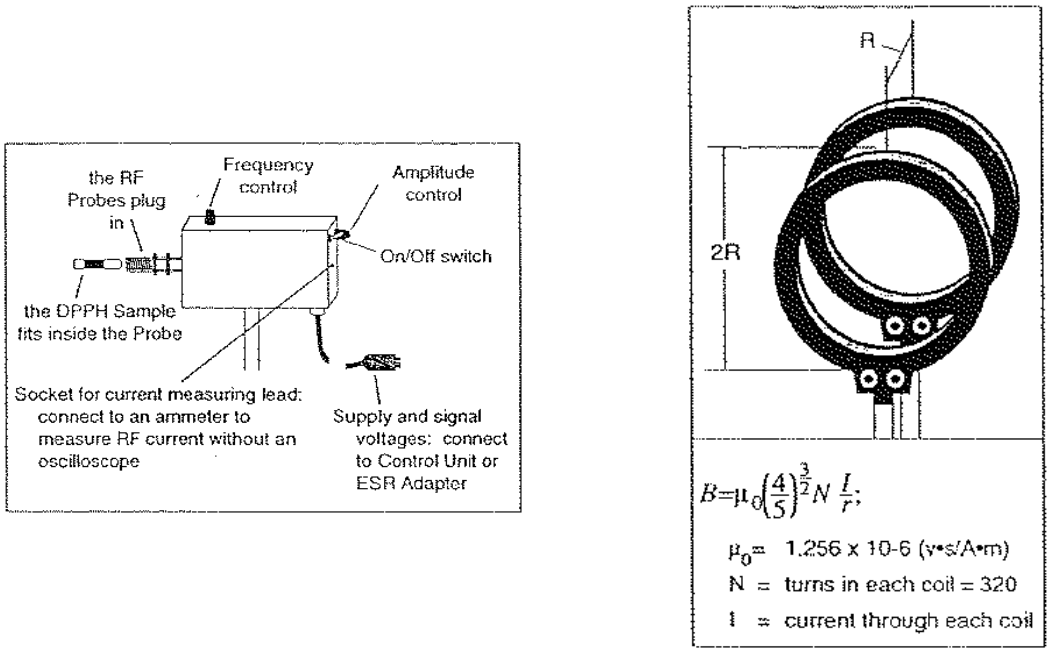

Figure 7.3: ESR probe unit (left) and Helmholtz coils (right)

7.2.2 Helmholtz Coils

The Helmholtz coils provide a highly uniform magnetic field in which to place the sample material for the ESR measurement. They should be connected in parallel and placed so that the separation between them is equal to the radius (see Fig. 7.3). Their diameter is 13.5 cm, and it turns out that the correct separation is achieved by positioning them essentially flush against the ESR Probe Unit. Make sure the two coils are as parallel as possible. When all this is the case, the B field in the central region between the two coils is highly uniform, and is given in Fig. 7.3. You should be able to derive the expression for B yourself, starting with the Biot-Savart law. It can also be found in most introductory physics textbooks.

→ IMPORTANT: The current to *each* of the coils should never exceed 2A, i.e. the total current should never exceed 4A!

7.3 Basic ESR Setup

7.3.1 Required Equipment

In addition to the Probe Unit, the ESR Adapter, and the Helmholtz coils, you will need the following additional equipment: Frequency Meter, DC Power Supply (10V, 3-4A), Power supplies providing ±12 VDC to the ESR Adapter, a Variac plus a 6.3 V transformer to provide approx. 2 VAC, DC Ammeter, Oscilloscope, a 1000 μF capacitor, and our home-made phase shifter box.

Figures 7.4 and 7.5 show the setup and the required connections. Please be careful not to short out anything! The +12 V draws considerably more current than the -12 V, make sure your power supply doesn't limit the current too much.

7.3.2 Setup

Connect the Helmholtz coils in parallel (A to A, Z to Z, see Fig. 7.4) and position them appropriately.
Connect the power supplies, ammeter, oscilloscope, and circuit components to the Helmholtz coils as shown in Figures 7.4 and 7.5. Do not terminate the scope in 50 Ω.
Circuit Explanation:

The Helmholtz coils require a small AC current superimposed on a larger DC current. This is supplied by the Variac/small transformer and DC power supply, respectively. They are connected in parallel, with the 1000 μF capacitor isolating the AC from the DC to prevent wave distortion. Because of the inductance of the Helmholtz coils, the current in the coils is out of phase with the voltage that is observed on the oscilloscope. To correct this, a 100 $k\Omega$ variable resistor and a 0.1

μF capacitor are used to shift the phase of the voltage that is displayed on the oscilloscope, see Fig. 7.5. This allows the experimenter to adjust the phase between the oscilloscope traces, so that the AC current to the Helmholtz coils and the ESR resonance pulses appear symmetrical, which in reality they are.

Turn on the power supplies. Adjust the DC to approximately 1 A and the AC to about 2 V. Channel 1 of the oscilloscope will show the current to the Helmholtz coils, except for the phase shift caused by the induction of the coils. The trace should be a simple sine wave. If you switch channel 1 to DC coupling, it should show an AC voltage superimposed on a DC voltage.

Insert the medium-sized RF probe into the Probe Unit, and turn on the Probe Unit. Make sure the two green LEDs on the side of the ESR Adapter are on. Adjust the frequency to about 50 MHz (50 kHz on your frequency meter) and the amplitude to a

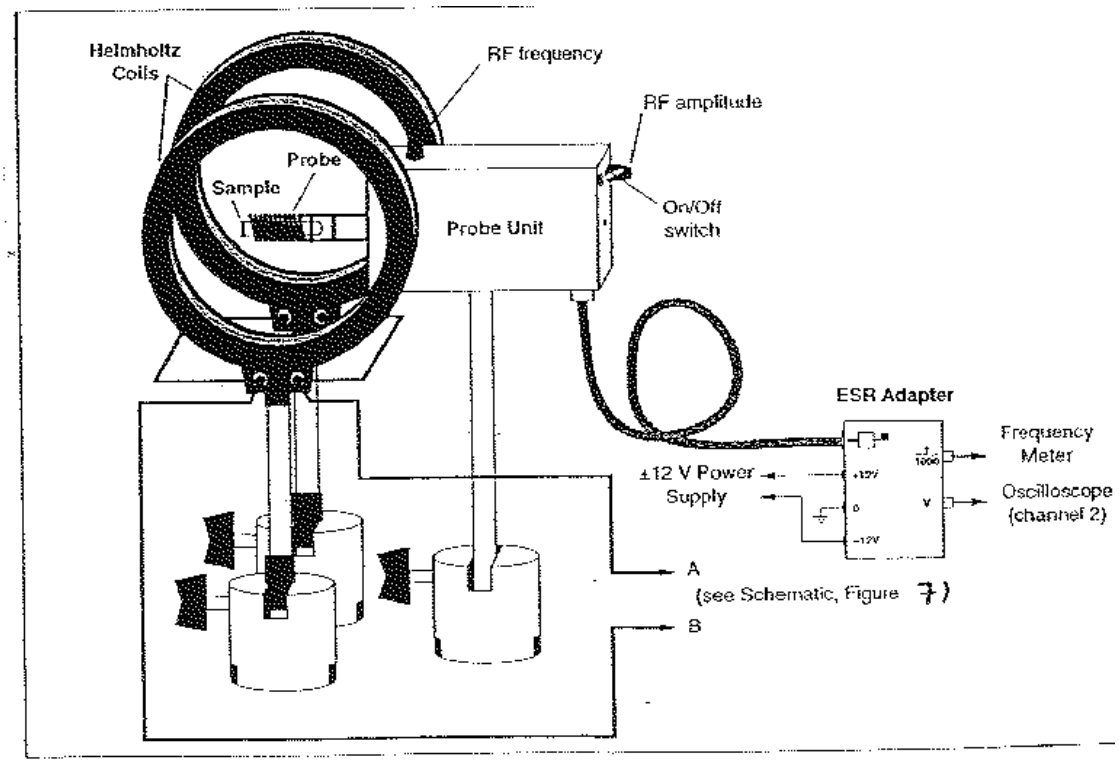

Figure 7.4: ESR setup

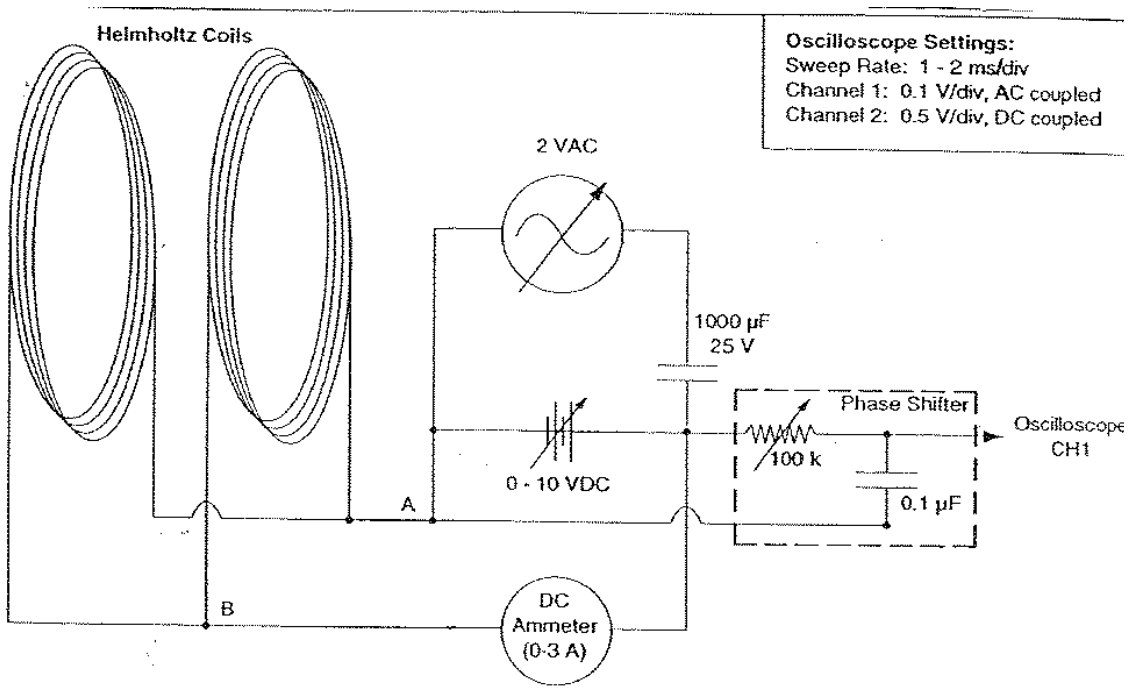

Figure 7.5: Schematic for Helmholtz coil connections

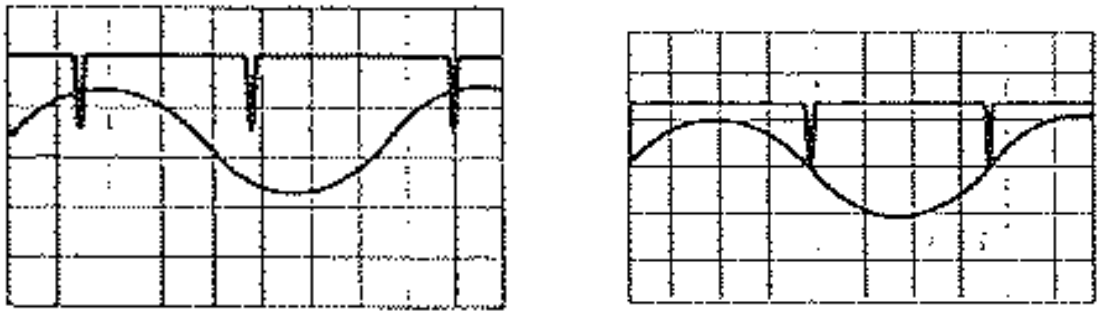

Figure 7.6: Scope displays

midrange value. Then insert the test sample into the RF probe and place the probe and sample in the center of the Helmholtz coils, with the Helmholtz coil axis perpendicular to the sample. The oscilloscope traces should now appear as in Figure 7.6. If you don't see the resonance pulses, slowly vary the DC current to the Helmholtz coils, or vary the RF frequency, until you do.
Note: do not limit the voltage on the coils d.c. power supply, keep this limit relatively high and only adjust the current to the coils (otherwise the a.c. sine wave may get distorted).

7.4 Taking ESR Data

Adjust the phase shifter so that the resonance pulses are symmetric with respect to the oscilloscope trace that shows the current to the Helmholtz coils. Refine the adjustment of the DC current until the resonance pulses occur when the AC component of the current to the Helmholtz coils is zero.
To do this:

a. Make sure that channel 1 is AC coupled.
b. Using the scope controls, ground the input to channel 1, zero the trace, and then unground the input.
c. Adjust the DC current. As you do, notice how the resonance pulses move closer together or farther apart. Adjust the DC current, and the phase shifter if necessary, until the pulses occur just when the AC current to the Helmholtz coils is zero. This is most accurately accomplished if you adjust the vertical position of channel 2 so that the bottom of the resonance pulses are just at the zero level of channel 1.

After these adjustments, the scope traces should appear as in Fig. 7.6. Everything is set for making ESR measurements. Since the current has been adjusted so that the resonance pulses occur when the AC current to the coils is zero, the current to the Helmholtz coils at resonance is just the DC value indicated by the ammeter.

Measure the RF frequency and the DC current. Then vary the current and find the new resonance frequency, or the other way around. For each of the three RF probes take at least five different data points, covering as large a frequency range as possible. In order of decreasing number of turns the three RF probes cover approximate frequency ranges of 13-30 MHz, 30-75 MHz, and 75-130 MHz, respectively.

7.5 Analysis

Calculate g_s for each data point, then mean, σ, σ_{mean} and compare with the accepted value. You should also determine g_s from a linear least squares fit. Comment on your results relative to the accepted value.

What systematic error do you think results from the fact that the ESR Probe Unit (metal!) protrudes into the region between the Helmholtz coils? Explain whether your results show evidence for such a systematic effect.

7.6 References

[1] Melissinos and Napolitano, Chapter 7.

Experiment 8

Poisson Statistics

8.1 Preface

This simple experiment will help you gain familiarity with the second most important statistical distribution in physics, the Poisson distribution. It describes the results of experiments where one counts events that occur at random, but at a definite average rate (example: radioactive decays). It is of paramount importance in all of atomic, and, in particular, subatomic physics.

8.2 Method

You will use the same setup as for the electron rest mass experiment. No source will be needed as you will simply measure the background count rate in our NaI detector. In addition, you will use our multichannel analyzer (MCA) in *multichannel scaling* mode (MCS) instead of pulse height analysis mode (PHA). In MCS function, the MCA no longer acts as a pulse height selector, but as a multichannel scaler with each channel acting as an independent scaler. At the start of operation, the MCA counts the incident pulse signals (regardless of amplitude) for a certain *dwell time*, and stores this number in the first channel. It then jumps to the next channel and counts for another dwell time period, after which it jumps to the next channel and so on. In MCS mode, therefore, the channels represent bins in time. Typical dwell times will be in the milliseconds range.

Suggested starting values:

HV of 1000V for the NaI, minimum gain (both fine and coarse) for the preamp/amp/discriminator (PAD) module, no radioactive source.

MCA setup: To put the MCA into MCS mode, we need to connect two pins on the MCA

input connector. This is done with a "hydra" break-out cable. Find a break-out cable, and connect the cable labeled MCS/REJ to the one labeled SCA. With the **computer off**, attach the break-out connector to the MCA card.

Setup the software with 256 channels. (Note: this means the computer will effectively perform this simple counting experiment 256 times for you!), MCS mode of operation with 1 pass. Make sure sync is set to internal and presets on (or the number of passes doesn't work correctly). And now the important part: adjust the dwell time such that the average count rate per channel is around 1-2 counts. Save the resulting spectrum as an ASCII file to a floppy. Repeat this procedure for two other dwell times such that the average count rate per channel is around 5 counts and around 10 counts, respectively.

8.3 Analysis

Plot your three resulting distributions (with MATLAB). Notice the significant asymmetry of the distribution for the lowest average count rate (Poisson at work!). Calculate mean and standard deviation in each case. How closely do your results follow the expectation for Poisson distributions, i.e. that the standard deviation is equal to the square root of the mean? Also notice how your highest average count rate case is rather symmetric, i.e. already for an average count rate of around 10 the Poisson distribution is virtually indistinguishable from a Gaussian.

Compare your three count rate distributions with the expected Poisson distributions graphically (with statistical error bars), and calculate the chisquare per degree of freedom. For the highest average count rate case, repeat with a Gaussian distribution.

8.4 References

[1] Melissinos and Napolitano, Chapter 10.

Experiment 9

Mass of the Electron

9.1 Objective

To determine the rest mass of the electron, m_e, via γ-ray interactions (mainly Compton scattering and photoeffect) in a NaI scintillation detector. Based on the enclosed article by Mudhole and Umakantha, you will perform this experiment as outlined there.

9.2 Theory

You must become familiar with γ-ray interactions in matter, the Sodium Iodide (NaI) detector including the Photomultiplier Tube (PMT), and the Multichannel Analyzer (MCA). See the enclosed handout (mainly from ref.1). Our MCA is actually a PC with an internal MCA card (called PCA3). It digitizes pulses in the range (0-10)V and with risetimes from (0.5-30)μs.

9.3 Procedure

Warning! Check the polarity of the high voltage for the PMT, and do not exceed the maximum HV, which should be indicated on the NaI detector. If in doubt, ask before turning on the HV!

The PMT output needs to be connected to the MCA via a preamp/amplifier module. Check the signals at various places with an oscilloscope. For instance, the raw anode output of the PMT should be a negative pulse (why?). The preamp/amp module will then integrate, amplify, and shape this pulse into a positive (or bipolar with positive leading part) pulse with significantly longer rise time than the raw anode pulse. This amplification and shaping is required for the pulse to become 'digestible' to the MCA.

Also observe the PMT output as you change the HV (gain of the PMT increases with increasing HV - make sure you understand why).

Record the spectra from several γ-sources to familiarize yourself with the physics and the hardware. If the backscatter peak is weak try to enhance it by positioning some material appropriately. Use the photopeaks for calibration, i.e., channel number versus energy deposited. This relationship should be highly linear. Do a linear least squares fit. Good sources for the calibration are ^{22}Na, ^{137}Cs, and ^{60}Co, resulting in a total of 5 photopeaks. Please make sure your lab report contains copies of all your spectra. The most useful sources, based on their longevity, are (with their half-life and most abundant E_γ):
^{137}Cs ($\tau_{1/2}$= 30.2 years; 0.662 MeV)
^{60}Co ($\tau_{1/2}$= 5.3 years; 1.17 MeV, 1.33 MeV)
^{22}Na ($\tau_{1/2}$= 2.6 years; 0.511 MeV, 1.275 MeV)
^{133}Ba ($\tau_{1/2}$= 10.5 years; 0.356 MeV)
Note that in case of ^{22}Na and ^{60}Co you might also see the sum peak at higher energies. Look for it and make sure you understand what is happening there. If you take data long enough with your detector close to a wall (no Pb bricks as shielding and no sources around!) you will likely see a peak at 1.46 Mev from ^{40}K in concrete, a well-known background line in concrete buildings. Identify this peak in a background spectrum.

Also determine the resolution (FWHM) in % using your ^{137}Cs photopeak. Typical numbers for NaI detectors are 5%-10%. Another useful exercise is to take data for a certain amount of time with a weak source, then remove the source, and take data for the same amount of time with the MCA in subtract mode, i.e. performing a background subtraction.

Using your calibration determine the Compton edge and the backscatter peak (both in keV) for as many sources as possible. Then calculate m_e incl. error(in keV). It is important to collect as many data points for m_e as possible, at least four each from the Compton edge and from the backscatter peak. If, for example, you can't use the Compton edge from a particular source, try to still use the backscatter peak. An example for this is ^{60}Co - why can't you use the Compton edge in this case? For sources with two γ lines accumulate enough statistics so that you can use the sum peak and its Compton edge. In addition, take a long-enough background spectrum so that you can use the ^{40}K line, mentioned above.

Do your results from the Compton edges indicate whether the half-height point is really the best measure of the Compton edge?

Is there any systematic difference in your results between the accuracy obtained for m_e using the Compton edges vs. using the backscatter peaks? If yes, can you think of a

reason why?

Why do the backscatter events show up in a *peak*, i.e. why are they not distributed over a much wider energy range?

9.4 References

[1] Melissinos and Napolitano, Chapter 8.
[2] Appendix: "Determination of the rest-mass energy of the electron...", Am J. Phys Vol 45 No 11, Nov. 1977.
[3] Appendix : Interaction of Electrons and Photons with Matter
[5] G.F. Knoll, Radiation Detection and Measurement, 2nd ed., 1989, Wiley.
[6] W.R. Leo, Techniques for Nuclear and Particle Physics Experiments, 2nd ed., 1994, Springer.

Experiment 10

The Speed of Light c

10.1 Introduction

In this experiment you will measure the speed of light, c. This is one of the most fundamental constants in physics, and at the same time the fastest quantity you'll ever measure! By using short pulses of light and a high speed detector you will determine c with good accuracy (few %) in a *direct* time-of-flight (TOF) measurement over distances of only one to two meters.

10.2 Apparatus

Warning! This experiment uses a photomultiplier tube (PMT) that will be ruined if exposed to ambient light when at operating voltages. Please be careful - the PMT must never be exposed to any bright light source while its high voltage is turned on. Permanent damage will result!

A schematic of the set-up is shown in Fig. 10.1. The circuit in Fig. 10.2 sends out short (few nanosecond) light pulses via a green LED (light emitting diode) at frequencies around $f \sim 10kHz$. This frequency is determined by the external dc power supply (150 to 200 Vdc, please do not exceed 200 V!). These light pulses are detected with a PMT which requires negative high voltage in the range of 1800 to 2400 V.

This high voltage is applied to the photomultiplier tube (PMT). The photocathode has a thin layer of a photosensitive substance, typically antimony-cesium alloys. The photocathode will emit a number of electrons proportional to the intensity of light that it receives. These photoelectrons are accelerated by the potential applied between the cathode and the first of a series of electrodes called dynodes. A typical PMT will contain ten to fourteen dynodes. The first dynode is maintained at a positive potential with

respect to the photocathode. Each subsequent dynode is kept at about the same potential difference with respect to the preceding one. The electrons that are emitted from the photocathode are attracted to the first dynode and acquire enough kinetic energy to free additional electrons as they collide with the dynode (secondary emission). This charge multiplication process occurs at each dynode. After the last dynode stage, the electrons are collected at the anode of the tube. The output of the PMT is
therefore a negative current pulse. Our PMT actually has negative HV applied to the photocathode while the anode is grounded. However, this does not change the basic physics of the device.

A pulse from the LED pulser labelled 'start' in Fig. 10.2 and the anode (not dynode!) pulse from the PMT (with some time delay cable) are sent to the start and stop input of a time-to-amplitude (TAC) converter, respectively. The TAC generates an output voltage pulse whose amplitude is proportional to the start-stop time difference, as long as this time difference is within the range selected by a front panel knob. The TAC output is analyzed by a Multichannel Analyzer (MCA), the basic function of which is described at the end of this handout.

This experiment contains an important source of a systematic error which, if not very carefully corrected for, could easily ruin your results quite dramatically. The phenomenon is known as 'time walk', and it plays an important role in high resolution timing experiments in nuclear and particle physics. The principle is shown in Fig. 10.3. If a device (like our TAC) triggers at a fixed voltage or discriminator level, its triggering time will occur later for smaller pulses than for larger pulses, even if the maximum pulse amplitude is reached at the same time. We are assuming here that the pulse rise time remains constant, i.e. is independent of pulse amplitude. In our application this time walk occurs because the PMT signal increases in amplitude as the LED assembly is moved closer to the PMT. Explain why this is the case.

In order to compensate for this PMT amplitude change we have polarizers mounted in front of the LED and the PMT. By rotating the PMT relative to the LED assembly you can change the amount of light hitting the photocathode thereby keeping the output amplitude constant. **NOTE:** it is extremely important for good results to take *all* data points at one and the same PMT amplitude.

10.3 Procedure

1. Familiarize yourself with the hardware. Note that the TAC has a threshold of -250 mV and requires a $\Delta t > 2$ nsec.

2. With a HV of around 1800 to 2000 V for the PMT, the anode amplitude should be

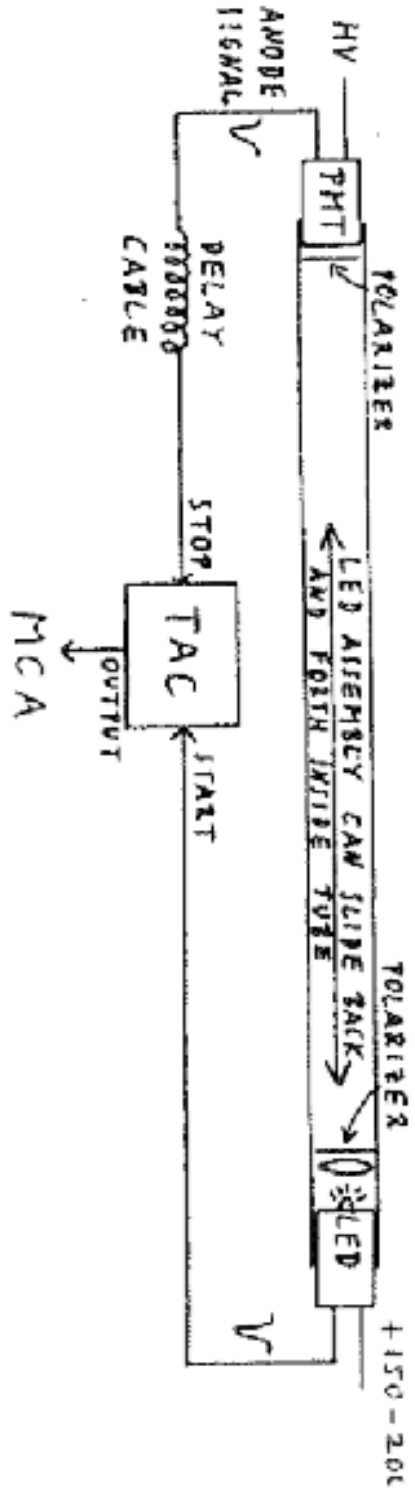

Figure 10.1: Schematic of Speed of Light Apparatus.

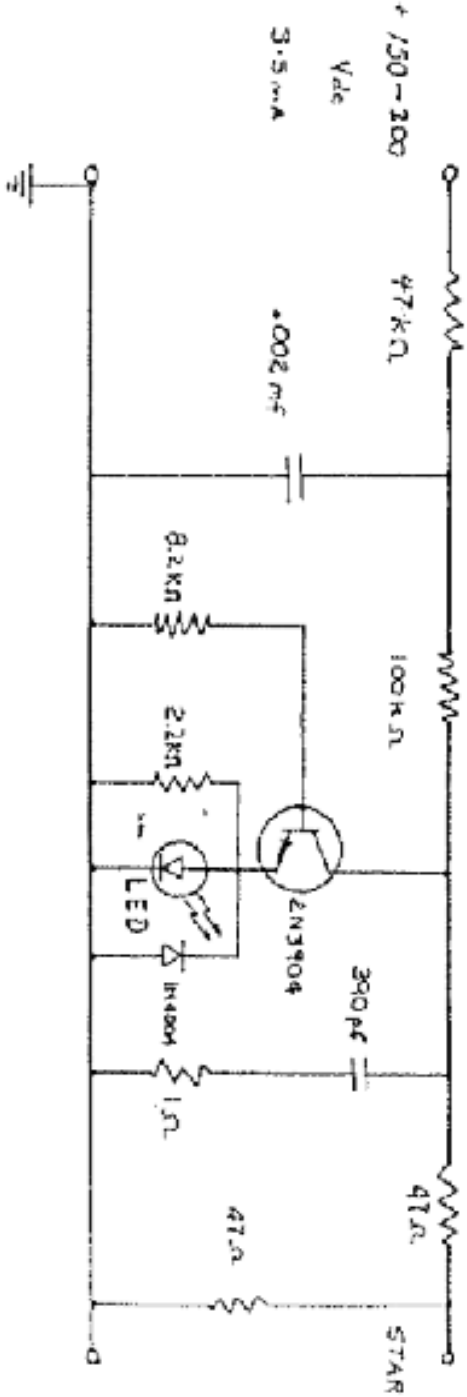

Figure 10.2: Speed of Light LED-pulsing Circuit.

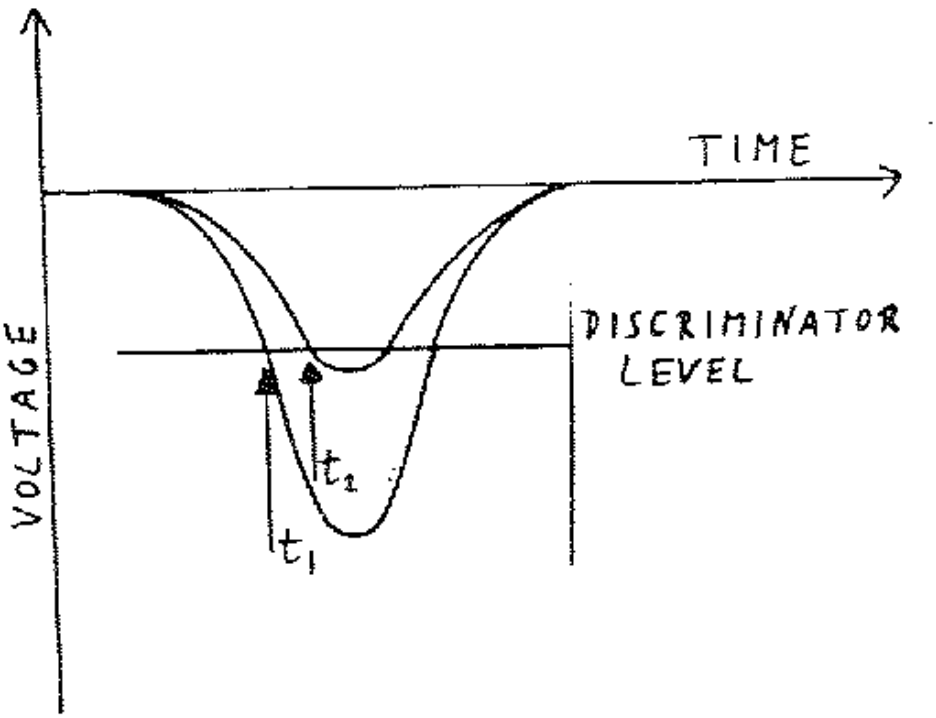

Figure 10.3: Illustration of 'time walk'.

several volts (into 50Ω), even at large distances between LED and PMT. If this is not the case, you need to adjust the relative alignment of LED/lens assembly and PMT. The polarizer should be set for maximum amplitude at the largest distances.

3. Using the oscilloscope, look at both start and stop signals for the TAC simultaneously, and make sure there is sufficient delay between them. Then take some data.

4. Calibrate your system, i.e. by inserting several different cables of known delay, or using a delay box, determine the number of picoseconds per channel. Your time resolution (Full Width at Half Maximum or FWHM of your peak) should be better than 1 ns. Think about this remarkable fact in terms of the distance that light travels in 1 ns! Measure and report your time resolution. In addition, check the linearity of your calibration.

5. Measure the systematic uncertainty due to the time walk. First, estimate the precision to which you can hold the amplitude constant (the uncertainty in the amplitude). Find a way to *measure* the systematic uncertainty on the value of c due to this uncertainty in amplitude. For your measurements, choose a value for the amplitude that will minimize the systematic uncertainty.

6. Take the following data:

   - Measure several times over a short ($\sim 25\ cm$) change in distance and compare the results, including error, with data taken over a *much* larger change in distance ($\sim\ 150\ cm$). Which set of data would you expect to give better results, and why?
   - Take data at successively larger (or smaller, depending upon where you start) distances and determine c and its error from a least squares fit to your x versus t curve. For a comparison take a few data points without the time walk correction, and determine c from those.
   - Summarize and compare your results (incl. their errors) for c from an overall mean, from your linear least squares fit, and also from your data taken without the time walk correction. What conclusions do you draw?

7. By using error propagation show that the relative error in c is dominated by the time resolution σ_t, and not by the position resolution σ_x.

8. If you are using the PCA3 software as part of your MCA system, CTRL+F2 will erase all data. If you happen to press F2 without holding down CTRL, CTRL+F2 will *not* work until F2 is pressed a second time.

10.4 References

[1] Melissinos and Napolitano
[2] Canberra Model 2044 Time Analyzer manual (available in the lab).
[3] W.R. Leo, Techniques for Nuclear and Particle Physics Experiments, 2nd ed., 1994, Springer.

Appendix A

General References

Note that many of these are available in the lab. Also, see hyperlinks in the class web page (e.g. table of isotopes).

Statistics and Data Analysis

1. "Data Analysis for Physical Science Students:, Lous Lyons (my personal favoite)
2. "Data Reduction and Error Analysis for the Physicsl Sciences", P. Bevington, D. Robinson (updated classic)

Experimental Methods

1. "Experiments in Modern Physics", Melissinos and Napolitano, 2nd ed., 2003, Academic Press.
2. G.F. Knoll, Radiation Detection and Measurement, 2nd ed., 1989, Wiley.
3. W.R. Leo, Techniques for Nuclear and Particle Physics Experiments, 2nd ed., 1994, Springer.
4. Technical notes are available for all experimental hardware.

Physics

1. "Optics", Hecht and Zajac, Addison Wesley Publishing Company; 3rd edition (August 1997).
2. "Electricity and Magnetism, Berkeley Physics Series Vol II", E. Purcell, McGraw-Hill Science/Engineering/Math; 2 edition (August 1, 1984)
3. any recent modern physics book
4. Melissinos (op. cit.)

Appendix B

Tables

1. PHYSICAL CONSTANTS

Table 1.1. Reviewed 2005 by P.J. Mohr and B.N. Taylor (NIST). Based mainly on the "CODATA Recommended Values of the Fundamental Physical Constants: 2002" by P.J. Mohr and B.N. Taylor, Rev. Mod. Phys. **77**, 1 (2005). The last group of constants (beginning with the Fermi coupling constant) comes from the Particle Data Group. The figures in parentheses after the values give the 1-standard-deviation uncertainties in the last digits; the corresponding fractional uncertainties in parts per 10^9 (ppb) are given in the last column. This set of constants (aside from the last group) is recommended for international use by CODATA (the Committee on Data for Science and Technology). The full 2002 CODATA set of constants may be found at `http://physics.nist.gov/constants`

Quantity	Symbol, equation	Value	Uncertainty (ppb)
speed of light in vacuum	c	299 792 458 m s^{-1}	exact*
Planck constant	h	$6.626\ 0693(11)\times10^{-34}$ J s	170
Planck constant, reduced	$\hbar \equiv h/2\pi$	$1.054\ 571\ 68(18)\times10^{-34}$ J s	170
		$= 6.582\ 119\ 15(56)\times10^{-22}$ MeV s	85
electron charge magnitude	e	$1.602\ 176\ 53(14)\times10^{-19}$ C $= 4.803\ 204\ 41(41)\times10^{-10}$ esu	85, 85
conversion constant	$\hbar c$	197.326 968(17) MeV fm	85
conversion constant	$(\hbar c)^2$	0.389 379 323(67) GeV^2 mbarn	170
electron mass	m_e	0.510 998 918(44) MeV/c^2 $= 9.109\ 3826(16)\times10^{-31}$ kg	86, 170
proton mass	m_p	938.272 029(80) MeV/c^2 $= 1.672\ 621\ 71(29)\times10^{-27}$ kg	86, 170
		$= 1.007\ 276\ 466\ 88(13)$ u $= 1836.152\ 672\ 61(85)\ m_e$	0.13, 0.46
deuteron mass	m_d	1875.612 82(16) MeV/c^2	86
unified atomic mass unit (u)	(mass ^{12}C atom)/12 = (1 g)/(N_A mol)	931.494 043(80) MeV/c^2 $= 1.660\ 538\ 86(28)\times10^{-27}$ kg	86, 170
permittivity of free space	$\epsilon_0 = 1/\mu_0 c^2$	$8.854\ 187\ 817\ \ldots\ \times10^{-12}$ F m^{-1}	exact
permeability of free space	μ_0	$4\pi \times 10^{-7}$ N A^{-2} $= 12.566\ 370\ 614\ \ldots\ \times10^{-7}$ N A^{-2}	exact
fine-structure constant	$\alpha = e^2/4\pi\epsilon_0\hbar c$	$7.297\ 352\ 568(24)\times10^{-3} = 1/137.035\ 999\ 11(46)^\dagger$	3.3, 3.3
classical electron radius	$r_e = e^2/4\pi\epsilon_0 m_e c^2$	$2.817\ 940\ 325(28)\times10^{-15}$ m	10
(e^- Compton wavelength)/2π	$\lambda\!\!\!^{-}_e = \hbar/m_e c = r_e\alpha^{-1}$	$3.861\ 592\ 678(26)\times10^{-13}$ m	6.7
Bohr radius ($m_{\rm nucleus} = \infty$)	$a_\infty = 4\pi\epsilon_0\hbar^2/m_e e^2 = r_e\alpha^{-2}$	$0.529\ 177\ 2108(18)\times10^{-10}$ m	3.3
wavelength of 1 eV/c particle	hc/(1 eV)	$1.239\ 841\ 91(11)\times10^{-6}$ m	85
Rydberg energy	$hcR_\infty = m_e e^4/2(4\pi\epsilon_0)^2\hbar^2 = m_e c^2\alpha^2/2$	13.605 6923(12) eV	85
Thomson cross section	$\sigma_T = 8\pi r_e^2/3$	0.665 245 873(13) barn	20
Bohr magneton	$\mu_B = e\hbar/2m_e$	$5.788\ 381\ 804(39)\times10^{-11}$ MeV T^{-1}	6.7
nuclear magneton	$\mu_N = e\hbar/2m_p$	$3.152\ 451\ 259(21)\times10^{-14}$ MeV T^{-1}	6.7
electron cyclotron freq./field	$\omega^e_{\rm cycl}/B = e/m_e$	$1.758\ 820\ 12(15)\times10^{11}$ rad s^{-1} T^{-1}	86
proton cyclotron freq./field	$\omega^p_{\rm cycl}/B = e/m_p$	$9.578\ 833\ 76(82)\times10^{7}$ rad s^{-1} T^{-1}	86
gravitational constant‡	G_N	$6.6742(10)\times10^{-11}$ m^3 kg^{-1} s^{-2}	1.5×10^5
		$= 6.7087(10)\times10^{-39}\ \hbar c$ $(\text{GeV}/c^2)^{-2}$	1.5×10^5
standard gravitational accel.	g_n	9.806 65 m s^{-2}	exact
Avogadro constant	N_A	$6.022\ 1415(10)\times10^{23}$ mol^{-1}	170
Boltzmann constant	k	$1.380\ 6505(24)\times10^{-23}$ J K^{-1}	1800
		$= 8.617\ 343(15)\times10^{-5}$ eV K^{-1}	1800
molar volume, ideal gas at STP	$N_A k$(273.15 K)/(101 325 Pa)	$22.413\ 996(39)\times10^{-3}$ m^3 mol^{-1}	1700
Wien displacement law constant	$b = \lambda_{\rm max}T$	$2.897\ 7685(51)\times10^{-3}$ m K	1700
Stefan-Boltzmann constant	$\sigma = \pi^2 k^4/60\hbar^3 c^2$	$5.670\ 400(40)\times10^{-8}$ W m^{-2} K^{-4}	7000
Fermi coupling constant**	$G_F/(\hbar c)^3$	$1.166\ 37(1)\times10^{-5}$ GeV^{-2}	9000
weak-mixing angle	$\sin^2\widehat{\theta}(M_Z)$ ($\overline{\rm MS}$)	0.23122(15)††	6.5×10^5
$W^\pm$ boson mass	m_W	80.403(29) GeV/c^2	3.6×10^5
Z^0 boson mass	m_Z	91.1876(21) GeV/c^2	2.3×10^4
strong coupling constant	$\alpha_s(m_Z)$	0.1176(20)	1.7×10^7

$\pi = 3.141\ 592\ 653\ 589\ 793\ 238$ e $= 2.718\ 281\ 828\ 459\ 045\ 235$ $\gamma = 0.577\ 215\ 664\ 901\ 532\ 861$

1 in $\equiv 0.0254$ m 1 G $\equiv 10^{-4}$ T 1 eV $= 1.602\ 176\ 53(14)\times10^{-19}$ J kT at 300 K $= [38.681\ 684(68)]^{-1}$ eV

1 Å $\equiv 0.1$ nm 1 dyne $\equiv 10^{-5}$ N 1 eV/$c^2 = 1.782\ 661\ 81(15)\times10^{-36}$ kg 0 °C $\equiv 273.15$ K

1 barn $\equiv 10^{-28}$ m^2 1 erg $\equiv 10^{-7}$ J $2.997\ 924\ 58\times10^9$ esu $= 1$ C 1 atmosphere $\equiv 760$ Torr $\equiv 101\ 325$ Pa

* The meter is the length of the path traveled by light in vacuum during a time interval of 1/299 792 458 of a second.
† At $Q^2 = 0$. At $Q^2 \approx m_W^2$ the value is $\sim 1/128$.
‡ Absolute lab measurements of G_N have been made only on scales of about 1 cm to 1 m.
** See the discussion in Sec. 10, "Electroweak model and constraints on new physics."
†† The corresponding $\sin^2\theta$ for the effective angle is 0.23152(14).

Table 4.1. Revised 2005 by C.G. Wohl (LBNL) and D.E. Groom (LBNL). Adapted from the Commission on Atomic Weights and Isotopic Abundances, "Atomic Weights of the Elements 1999," Pure and Applied Chemistry **73**, 667 (2001), and G. Audi, A.H. Wapstra, and C. Thibault, Nucl. Phys. **A729**, 337 (2003). The atomic number (top left) is the number of protons in the nucleus. The atomic mass (bottom) is weighted by isotopic abundances in the Earth's surface. Atomic masses are relative to the mass of ^{12}C, defined to be exactly 12 unified atomic mass units (u) (approx. g/mole). Relative isotopic abundances often vary considerably, both in natural and commercial samples; this is reflected in the number of significant figures given. A number in parentheses is the atomic mass of the longest-lived known isotope of that element—no stable isotope exists. The exceptions are Th, Pa, and U, which do have characteristic terrestrial compositions. As of early 2006 element 112 has not been assigned a name, and there are no confirmed elements with Z > 112.

PERIODIC TABLE OF THE ELEMENTS

1 IA												13 IIIA	14 IVA	15 VA	16 VIA	17 VIIA	18 VIIIA
1 H Hydrogen 1.00794	2 IIA																2 He Helium 4.002602
3 Li Lithium 6.941	4 Be Beryllium 9.012182											5 B Boron 10.811	6 C Carbon 12.0107	7 N Nitrogen 14.0067	8 O Oxygen 15.9994	9 F Fluorine 18.9984032	10 Ne Neon 20.1797
11 Na Sodium 22.989770	12 Mg Magnesium 24.3050	3 IIIB	4 IVB	5 VB	6 VIB	7 VIIB	8	9 VIII	10	11 IB	12 IIB	13 Al Aluminum 26.981538	14 Si Silicon 28.0855	15 P Phosph. 30.973761	16 S Sulfur 32.065	17 Cl Chlorine 35.453	18 Ar Argon 39.948
19 K Potassium 39.0983	20 Ca Calcium 40.078	21 Sc Scandium 44.955910	22 Ti Titanium 47.867	23 V Vanadium 50.9415	24 Cr Chromium 51.9961	25 Mn Manganese 54.938049	26 Fe Iron 55.845	27 Co Cobalt 58.933200	28 Ni Nickel 58.6934	29 Cu Copper 63.546	30 Zn Zinc 65.39	31 Ga Gallium 69.723	32 Ge German. 72.64	33 As Arsenic 74.92160	34 Se Selenium 78.96	35 Br Bromine 79.904	36 Kr Krypton 83.80
37 Rb Rubidium 85.4678	38 Sr Strontium 87.62	39 Y Yttrium 88.90585	40 Zr Zirconium 91.224	41 Nb Niobium 92.90638	42 Mo Molybd. 95.94	43 Tc Technet. (97.907216)	44 Ru Ruthen. 101.07	45 Rh Rhodium 102.90550	46 Pd Palladium 106.42	47 Ag Silver 107.8682	48 Cd Cadmium 112.411	49 In Indium 114.818	50 Sn Tin 118.710	51 Sb Antimony 121.760	52 Te Tellurium 127.60	53 I Iodine 126.90447	54 Xe Xenon 131.293
55 Cs Cesium 132.90545	56 Ba Barium 137.327	57–71 Lantha-nides	72 Hf Hafnium 178.49	73 Ta Tantalum 180.9479	74 W Tungsten 183.84	75 Re Rhenium 186.207	76 Os Osmium 190.23	77 Ir Iridium 192.217	78 Pt Platinum 195.078	79 Au Gold 196.96655	80 Hg Mercury 200.59	81 Tl Thallium 204.3833	82 Pb Lead 207.2	83 Bi Bismuth 208.98038	84 Po Polonium (208.982430)	85 At Astatine (209.987148)	86 Rn Radon (222.017578)
87 Fr Francium (223.019736)	88 Ra Radium (226.025410)	89–103 Actinides	104 Rf Rutherford. (261.10877)	105 Db Dubnium (262.1141)	106 Sg Seaborg. (263.1221)	107 Bh Bohrium (262.1246)	108 Hs Hassium (277.1498)	109 Mt Meitner. (268.1387)	110 Ds Darmstadt. (271.1461)	111 Rg Roentgen. (272.1536)	112 (277.1639)						

Lanthanide series	57 La Lanthan. 138.9055	58 Ce Cerium 140.116	59 Pr Praseodym. 140.90765	60 Nd Neodym. 144.24	61 Pm Prometh. (144.912749)	62 Sm Samarium 150.36	63 Eu Europium 151.964	64 Gd Gadolin. 157.25	65 Tb Terbium 158.92534	66 Dy Dyspros. 162.50	67 Ho Holmium 164.93032	68 Er Erbium 167.259	69 Tm Thulium 168.93421	70 Yb Ytterbium 173.04	71 Lu Lutetium 174.967
Actinide series	89 Ac Actinium (227.027752)	90 Th Thorium 232.038055	91 Pa Protactin. 231.035884	92 U Uranium 238.02891	93 Np Neptunium (237.048173)	94 Pu Plutonium (244.064204)	95 Am Americ. (243.061381)	96 Cm Curium (247.070354)	97 Bk Berkelium (247.070307)	98 Cf Californ. (251.079587)	99 Es Einstein. (252.08298)	100 Fm Fermium (257.085105)	101 Md Mendelev. (258.098431)	102 No Nobelium (259.1010)	103 Lr Lawrenc. (262.1096)

5. ELECTRONIC STRUCTURE OF THE ELEMENTS

Table 5.1. Reviewed 2005 by C.G. Wohl (LBNL). The electronic configurations and the ionization energies are from the NIST database, "Ground Levels and Ionization Energies for the Neutral Atoms," W.C. Martin, A. Musgrove, S. Kotochigova, and J.E. Sansonetti (2003), `http://physics.nist.gov` (select "Physical Reference Data"). The electron configuration for, say, iron indicates an argon electronic core (see argon) plus six $3d$ electrons and two $4s$ electrons. The ionization energy is the least energy necessary to remove to infinity one electron from an atom of the element.

	Element		Electron configuration ($3d^5$ = five $3d$ electrons, *etc.*)						Ground state $^{2S+1}L_J$	Ionization energy (eV)
1	H	Hydrogen	$1s$						$^2S_{1/2}$	13.5984
2	He	Helium	$1s^2$						$^1S_0$	24.5874
3	Li	Lithium	(He) $2s$						$^2S_{1/2}$	5.3917
4	Be	Beryllium	(He) $2s^2$						$^1S_0$	9.3227
5	B	Boron	(He) $2s^2$	$2p$					$^2P_{1/2}$	8.2980
6	C	Carbon	(He) $2s^2$	$2p^2$					$^3P_0$	11.2603
7	N	Nitrogen	(He) $2s^2$	$2p^3$					$^4S_{3/2}$	14.5341
8	O	Oxygen	(He) $2s^2$	$2p^4$					$^3P_2$	13.6181
9	F	Fluorine	(He) $2s^2$	$2p^5$					$^2P_{3/2}$	17.4228
10	Ne	Neon	(He) $2s^2$	$2p^6$					$^1S_0$	21.5645
11	Na	Sodium	(Ne) $3s$						$^2S_{1/2}$	5.1391
12	Mg	Magnesium	(Ne) $3s^2$						$^1S_0$	7.6462
13	Al	Aluminum	(Ne) $3s^2$	$3p$					$^2P_{1/2}$	5.9858
14	Si	Silicon	(Ne) $3s^2$	$3p^2$					$^3P_0$	8.1517
15	P	Phosphorus	(Ne) $3s^2$	$3p^3$					$^4S_{3/2}$	10.4867
16	S	Sulfur	(Ne) $3s^2$	$3p^4$					$^3P_2$	10.3600
17	Cl	Chlorine	(Ne) $3s^2$	$3p^5$					$^2P_{3/2}$	12.9676
18	Ar	Argon	(Ne) $3s^2$	$3p^6$					$^1S_0$	15.7596
19	K	Potassium	(Ar)	$4s$					$^2S_{1/2}$	4.3407
20	Ca	Calcium	(Ar)	$4s^2$					$^1S_0$	6.1132
21	Sc	Scandium	(Ar) $3d$	$4s^2$		Transition elements			$^2D_{3/2}$	6.5615
22	Ti	Titanium	(Ar) $3d^2$	$4s^2$					$^3F_2$	6.8281
23	V	Vanadium	(Ar) $3d^3$	$4s^2$					$^4F_{3/2}$	6.7462
24	Cr	Chromium	(Ar) $3d^5$	$4s$					$^7S_3$	6.7665
25	Mn	Manganese	(Ar) $3d^5$	$4s^2$					$^6S_{5/2}$	7.4340
26	Fe	Iron	(Ar) $3d^6$	$4s^2$					$^5D_4$	7.9024
27	Co	Cobalt	(Ar) $3d^7$	$4s^2$					$^4F_{9/2}$	7.8810
28	Ni	Nickel	(Ar) $3d^8$	$4s^2$					$^3F_4$	7.6398
29	Cu	Copper	(Ar) $3d^{10}$	$4s$					$^2S_{1/2}$	7.7264
30	Zn	Zinc	(Ar) $3d^{10}$	$4s^2$					$^1S_0$	9.3942
31	Ga	Gallium	(Ar) $3d^{10}$	$4s^2$	$4p$				$^2P_{1/2}$	5.9993
32	Ge	Germanium	(Ar) $3d^{10}$	$4s^2$	$4p^2$				$^3P_0$	7.8994
33	As	Arsenic	(Ar) $3d^{10}$	$4s^2$	$4p^3$				$^4S_{3/2}$	9.7886
34	Se	Selenium	(Ar) $3d^{10}$	$4s^2$	$4p^4$				$^3P_2$	9.7524
35	Br	Bromine	(Ar) $3d^{10}$	$4s^2$	$4p^5$				$^2P_{3/2}$	11.8138
36	Kr	Krypton	(Ar) $3d^{10}$	$4s^2$	$4p^6$				$^1S_0$	13.9996
37	Rb	Rubidium	(Kr)	$5s$					$^2S_{1/2}$	4.1771
38	Sr	Strontium	(Kr)	$5s^2$					$^1S_0$	5.6949
39	Y	Yttrium	(Kr) $4d$	$5s^2$		Transition elements			$^2D_{3/2}$	6.2173
40	Zr	Zirconium	(Kr) $4d^2$	$5s^2$					$^3F_2$	6.6339
41	Nb	Niobium	(Kr) $4d^4$	$5s$					$^6D_{1/2}$	6.7589
42	Mo	Molybdenum	(Kr) $4d^5$	$5s$					$^7S_3$	7.0924
43	Tc	Technetium	(Kr) $4d^5$	$5s^2$					$^6S_{5/2}$	7.28
44	Ru	Ruthenium	(Kr) $4d^7$	$5s$					$^5F_5$	7.3605
45	Rh	Rhodium	(Kr) $4d^8$	$5s$					$^4F_{9/2}$	7.4589
46	Pd	Palladium	(Kr) $4d^{10}$						$^1S_0$	8.3369
47	Ag	Silver	(Kr) $4d^{10}$	$5s$					$^2S_{1/2}$	7.5762
48	Cd	Cadmium	(Kr) $4d^{10}$	$5s^2$					$^1S_0$	8.9938

49	In	Indium	(Kr) $4d^{10}5s^2$	$5p$		$^2P_{1/2}$	5.7864
50	Sn	Tin	(Kr) $4d^{10}5s^2$	$5p^2$		$^3P_0$	7.3439
51	Sb	Antimony	(Kr) $4d^{10}5s^2$	$5p^3$		$^4S_{3/2}$	8.6084
52	Te	Tellurium	(Kr) $4d^{10}5s^2$	$5p^4$		$^3P_2$	9.0096
53	I	Iodine	(Kr) $4d^{10}5s^2$	$5p^5$		$^2P_{3/2}$	10.4513
54	Xe	Xenon	(Kr) $4d^{10}5s^2$	$5p^6$		$^1S_0$	12.1298
55	Cs	Cesium	(Xe)	$6s$		$^2S_{1/2}$	3.8939
56	Ba	Barium	(Xe)	$6s^2$		$^1S_0$	5.2117
57	La	Lanthanum	(Xe) $5d$	$6s^2$		$^2D_{3/2}$	5.5769
58	Ce	Cerium	(Xe) $4f$ $5d$	$6s^2$		$^1G_4$	5.5387
59	Pr	Praseodymium	(Xe) $4f^3$	$6s^2$		$^4I_{9/2}$	5.473
60	Nd	Neodymium	(Xe) $4f^4$	$6s^2$		$^5I_4$	5.5250
61	Pm	Promethium	(Xe) $4f^5$	$6s^2$		$^6H_{5/2}$	5.582
62	Sm	Samarium	(Xe) $4f^6$	$6s^2$		$^7F_0$	5.6437
63	Eu	Europium	(Xe) $4f^7$	$6s^2$		$^8S_{7/2}$	5.6704
64	Gd	Gadolinium	(Xe) $4f^7$ $5d$	$6s^2$		$^9D_2$	6.1498
65	Tb	Terbium	(Xe) $4f^9$	$6s^2$		$^6H_{15/2}$	5.8638
66	Dy	Dysprosium	(Xe) $4f^{10}$	$6s^2$		$^5I_8$	5.9389
67	Ho	Holmium	(Xe) $4f^{11}$	$6s^2$		$^4I_{15/2}$	6.0215
68	Er	Erbium	(Xe) $4f^{12}$	$6s^2$		$^3H_6$	6.1077
69	Tm	Thulium	(Xe) $4f^{13}$	$6s^2$		$^2F_{7/2}$	6.1843
70	Yb	Ytterbium	(Xe) $4f^{14}$	$6s^2$		$^1S_0$	6.2542
71	Lu	Lutetium	(Xe) $4f^{14}5d$	$6s^2$		$^2D_{3/2}$	5.4259
72	Hf	Hafnium	(Xe) $4f^{14}5d^2$	$6s^2$		$^3F_2$	6.8251
73	Ta	Tantalum	(Xe) $4f^{14}5d^3$	$6s^2$		$^4F_{3/2}$	7.5496
74	W	Tungsten	(Xe) $4f^{14}5d^4$	$6s^2$		$^5D_0$	7.8640
75	Re	Rhenium	(Xe) $4f^{14}5d^5$	$6s^2$		$^6S_{5/2}$	7.8335
76	Os	Osmium	(Xe) $4f^{14}5d^6$	$6s^2$		$^5D_4$	8.4382
77	Ir	Iridium	(Xe) $4f^{14}5d^7$	$6s^2$		$^4F_{9/2}$	8.9670
78	Pt	Platinum	(Xe) $4f^{14}5d^9$	$6s$		$^3D_3$	8.9588
79	Au	Gold	(Xe) $4f^{14}5d^{10}6s$			$2S_{1/2}$	9.2255
80	Hg	Mercury	(Xe) $4f^{14}5d^{10}6s^2$			$^1S_0$	10.4375
81	Tl	Thallium	(Xe) $4f^{14}5d^{10}6s^2$	$6p$		$^2P_{1/2}$	6.1082
82	Pb	Lead	(Xe) $4f^{14}5d^{10}6s^2$	$6p^2$		$^3P_0$	7.4167
83	Bi	Bismuth	(Xe) $4f^{14}5d^{10}6s^2$	$6p^3$		$^4S_{3/2}$	7.2855
84	Po	Polonium	(Xe) $4f^{14}5d^{10}6s^2$	$6p^4$		$^3P_2$	8.414
85	At	Astatine	(Xe) $4f^{14}5d^{10}6s^2$	$6p^5$		$^2P_{3/2}$	
86	Rn	Radon	(Xe) $4f^{14}5d^{10}6s^2$	$6p^6$		$^1S_0$	10.7485
87	Fr	Francium	(Rn)	$7s$		$^2S_{1/2}$	4.0727
88	Ra	Radium	(Rn)	$7s^2$		$^1S_0$	5.2784
89	Ac	Actinium	(Rn) $6d$	$7s^2$		$^2D_{3/2}$	5.17
90	Th	Thorium	(Rn) $6d^2$	$7s^2$		$^3F_2$	6.3067
91	Pa	Protactinium	(Rn)$5f^2$ $6d$	$7s^2$		$^4K_{11/2}$*	5.89
92	U	Uranium	(Rn)$5f^3$ $6d$	$7s^2$		$^5L_6$*	6.1941
93	Np	Neptunium	(Rn)$5f^4$ $6d$	$7s^2$		$^6L_{11/2}$*	6.2657
94	Pu	Plutonium	(Rn)$5f^6$	$7s^2$		$^7F_0$	6.0260
95	Am	Americium	(Rn)$5f^7$	$7s^2$		$^8S_{7/2}$	5.9738
96	Cm	Curium	(Rn)$5f^7$ $6d$	$7s^2$		$^9D_2$	5.9914
97	Bk	Berkelium	(Rn)$5f^9$	$7s^2$		$^6H_{15/2}$	6.1979
98	Cf	Californium	(Rn)$5f^{10}$	$7s^2$		$^5I_8$	6.2817
99	Es	Einsteinium	(Rn)$5f^{11}$	$7s^2$		$^4I_{15/2}$	6.42
100	Fm	Fermium	(Rn)$5f^{12}$	$7s^2$		$^3H_6$	6.50
101	Md	Mendelevium	(Rn)$5f^{13}$	$7s^2$		$^2F_{7/2}$	6.58
102	No	Nobelium	(Rn)$5f^{14}$	$7s^2$		$^1S_0$	6.65
103	Lr	Lawrencium	(Rn)$5f^{14}$	$7s^2$ $7p$?		$^2P_{1/2}$?	4.9?
104	Rf	Rutherfordium	(Rn)$5f^{14}6d^2$	$7s^2$?		$^3F_2$?	6.0?

Lanthanides

Transition elements

Actinides

* The usual LS coupling scheme does not apply for these three elements. See the introductory note to the NIST table from which this table is taken.

6. ATOMIC AND NUCLEAR PROPERTIES OF MATERIALS

Table 6.1. Revised May 2002 by D.E. Groom (LBNL). Gases are evaluated at 20°C and 1 atm (in parentheses) or at STP [square brackets]. Densities and refractive indices without parentheses or brackets are for solids or liquids, or are for cryogenic liquids at the indicated boiling point (BP) at 1 atm. Refractive indices are evaluated at the sodium D line. Data for compounds and mixtures are from Refs. 1 and 2. Futher materials and properties are given in Ref. 3 and at `http://pdg.lbl.gov/AtomicNuclearProperties`.

Material	Z	A	$\langle Z/A\rangle$	Nuclear [a] collision length λ_T {g/cm^2}	Nuclear [a] interaction length λ_I {g/cm^2}	$dE/dx\|_{\rm min}$ [b] $\left\{\frac{\rm MeV}{\rm g/cm^2}\right\}$	Radiation length [c] X_0 {g/cm^2}	{cm}	Density {g/cm^3} ({g/ℓ} for gas)	Liquid boiling point at 1 atm(K)	Refractive index n ($(n-1)\times10^6$ for gas)
H_2 gas	1	1.00794	0.99212	43.3	50.8	(4.103)	61.28 [d]	(731000)	(0.0838)[0.0899]		[139.2]
H_2 liquid	1	1.00794	0.99212	43.3	50.8	4.034	61.28 [d]	866	0.0708	20.39	1.112
D_2	1	2.0140	0.49652	45.7	54.7	(2.052)	122.4	724	0.169[0.179]	23.65	1.128 [138]
He	2	4.002602	0.49968	49.9	65.1	(1.937)	94.32	756	0.1249[0.1786]	4.224	1.024 [34.9]
Li	3	6.941	0.43221	54.6	73.4	1.639	82.76	155	0.534		—
Be	4	9.012182	0.44384	55.8	75.2	1.594	65.19	35.28	1.848		—
C	6	12.011	0.49954	60.2	86.3	1.745	42.70	18.8	2.265 [e]		—
N_2	7	14.00674	0.49976	61.4	87.8	(1.825)	37.99	47.1	0.8073[1.250]	77.36	1.205 [298]
O_2	8	15.9994	0.50002	63.2	91.0	(1.801)	34.24	30.0	1.141[1.428]	90.18	1.22 [296]
F_2	9	18.9984032	0.47372	65.5	95.3	(1.675)	32.93	21.85	1.507[1.696]	85.24	[195]
Ne	10	20.1797	0.49555	66.1	96.6	(1.724)	28.94	24.0	1.204[0.9005]	27.09	1.092 [67.1]
Al	13	26.981539	0.48181	70.6	106.4	1.615	24.01	8.9	2.70		—
Si	14	28.0855	0.49848	70.6	106.0	1.664	21.82	9.36	2.33		3.95
Ar	18	39.948	0.45059	76.4	117.2	(1.519)	19.55	14.0	1.396[1.782]	87.28	1.233 [283]
Ti	22	47.867	0.45948	79.9	124.9	1.476	16.17	3.56	4.54		—
Fe	26	55.845	0.46556	82.8	131.9	1.451	13.84	1.76	7.87		—
Cu	29	63.546	0.45636	85.6	134.9	1.403	12.86	1.43	8.96		—
Ge	32	72.61	0.44071	88.3	140.5	1.371	12.25	2.30	5.323		—
Sn	50	118.710	0.42120	100.2	163	1.264	8.82	1.21	7.31		—
Xe	54	131.29	0.41130	102.8	169	(1.255)	8.48	2.87	2.953[5.858]	165.1	[701]
W	74	183.84	0.40250	110.3	185	1.145	6.76	0.35	19.3		—
Pt	78	195.08	0.39984	113.3	189.7	1.129	6.54	0.305	21.45		—
Pb	82	207.2	0.39575	116.2	194	1.123	6.37	0.56	11.35		—
U	92	238.0289	0.38651	117.0	199	1.082	6.00	≈0.32	≈18.95		—
Air, (20°C, 1 atm.), [STP]			0.49919	62.0	90.0	(1.815)	36.66	[30420]	(1.205)[1.2931]	78.8	(273) [293]
H_2O			0.55509	60.1	83.6	1.991	36.08	36.1	1.00	373.15	1.33
CO_2 gas			0.49989	62.4	89.7	(1.819)	36.2	[18310]	[1.977]		[410]
CO_2 solid (dry ice)			0.49989	62.4	89.7	1.787	36.2	23.2	1.563	sublimes	—
Shielding concrete [f]			0.50274	67.4	99.9	1.711	26.7	10.7	2.5		—
SiO_2 (fused quartz)			0.49926	66.5	97.4	1.699	27.05	12.3	2.20 [g]		1.458
Dimethyl ether, $(CH_3)_2O$			0.54778	59.4	82.9	—	38.89	—	—	248.7	—
Methane, CH_4			0.62333	54.8	73.4	(2.417)	46.22	[64850]	0.4224[0.717]	111.7	[444]
Ethane, C_2H_6			0.59861	55.8	75.7	(2.304)	45.47	[34035]	0.509(1.356) [h]	184.5	(1.038) [h]
Propane, C_3H_8			0.58962	56.2	76.5	(2.262)	45.20	—	(1.879)	231.1	—
Isobutane, $(CH_3)_2CHCH_3$			0.58496	56.4	77.0	(2.239)	45.07	[16930]	[2.67]	261.42	[1900]
Octane, liquid, $CH_3(CH_2)_6CH_3$			0.57778	56.7	77.7	2.123	44.86	63.8	0.703	398.8	1.397
Paraffin wax, $CH_3(CH_2)_{n\approx23}CH_3$			0.57275	56.9	78.2	2.087	44.71	48.1	0.93		—
Nylon, type 6 [i]			0.54790	58.5	81.5	1.974	41.84	36.7	1.14		—
Polycarbonate (Lexan) [j]			0.52697	59.5	83.9	1.886	41.46	34.6	1.20		—
Polyethylene terephthlate (Mylar) [k]			0.52037	60.2	85.7	1.848	39.95	28.7	1.39		—
Polyethylene [l]			0.57034	57.0	78.4	2.076	44.64	≈47.9	0.92–0.95		—
Polyimide film (Kapton) [m]			0.51264	60.3	85.8	1.820	40.56	28.6	1.42		—
Lucite, Plexiglas [n]			0.53937	59.3	83.0	1.929	40.49	≈34.4	1.16–1.20		≈1.49
Polystyrene, scintillator [o]			0.53768	58.5	81.9	1.936	43.72	42.4	1.032		1.581
Polytetrafluoroethylene (Teflon) [p]			0.47992	64.2	93.0	1.671	34.84	15.8	2.20		—
Polyvinyltolulene, scintillator [q]			0.54155	58.3	81.5	1.956	43.83	42.5	1.032		—
Aluminum oxide (Al_2O_3)			0.49038	67.0	98.9	1.647	27.94	7.04	3.97		1.761
Barium fluoride (BaF_2)			0.42207	92.0	145	1.303	9.91	2.05	4.89		1.56
Bismuth germanate (BGO) [r]			0.42065	98.2	157	1.251	7.97	1.12	7.1		2.15
Cesium iodide (CsI)			0.41569	102	167	1.243	8.39	1.85	4.53		1.80
Lithium fluoride (LiF)			0.46262	62.2	88.2	1.614	39.25	14.91	2.632		1.392
Sodium fluoride (NaF)			0.47632	66.9	98.3	1.69	29.87	11.68	2.558		1.336
Sodium iodide (NaI)			0.42697	94.6	151	1.305	9.49	2.59	3.67		1.775
Silica Aerogel [s]			0.50093	66.3	96.9	1.740	27.25	136@ρ=0.2	0.04–0.6		1.0+0.21ρ
NEMA G10 plate [t]				62.6	90.2	1.87	33.0	19.4	1.7		—

Material	Dielectric constant ($\kappa = \epsilon/\epsilon_0$) () is ($\kappa$–1)×$10^6$ for gas	Young's modulus [10^6 psi]	Coeff. of thermal expansion [10^{-6}cm/cm-°C]	Specific heat [cal/g-°C]	Electrical resistivity [$\mu\Omega$cm(@°C)]	Thermal conductivity [cal/cm-°C-sec]
H_2	(253.9)	—	—	—	—	—
He	(64)	—	—	—	—	—
Li	—	—	56	0.86	8.55(0°)	0.17
Be	—	37	12.4	0.436	5.885(0°)	0.38
C	—	0.7	0.6–4.3	0.165	1375(0°)	0.057
N_2	(548.5)	—	—	—	—	—
O_2	(495)	—	—	—	—	—
Ne	(127)	—	—	—	—	—
Al	—	10	23.9	0.215	2.65(20°)	0.53
Si	11.9	16	2.8–7.3	0.162	—	0.20
Ar	(517)	—	—	—	—	—
Ti	—	16.8	8.5	0.126	50(0°)	—
Fe	—	28.5	11.7	0.11	9.71(20°)	0.18
Cu	—	16	16.5	0.092	1.67(20°)	0.94
Ge	16.0	—	5.75	0.073	—	0.14
Sn	—	6	20	0.052	11.5(20°)	0.16
Xe	—	—	—	—	—	—
W	—	50	4.4	0.032	5.5(20°)	0.48
Pt	—	21	8.9	0.032	9.83(0°)	0.17
Pb	—	2.6	29.3	0.038	20.65(20°)	0.083
U	—	—	36.1	0.028	29(20°)	0.064

1. R.M. Sternheimer, M.J. Berger, and S.M. Seltzer, Atomic Data and Nuclear Data Tables **30**, 261–271 (1984).
2. S.M. Seltzer and M.J. Berger, Int. J. Appl. Radiat. **33**, 1189–1218 (1982).
3. D.E. Groom, N.V. Mokhov, and S.I. Striganov, "Muon stopping-power and range tables," Atomic Data and Nuclear Data Tables **78**, 183–356 (2001).
4. S.M. Seltzer and M.J. Berger, Int. J. Appl. Radiat. **35**, 665 (1984) & `http://physics.nist.gov/PhysRefData/Star/Text/contents.html`.

a. σ_T, λ_T and λ_I are energy dependent. Values quoted apply to high energy range, where energy dependence is weak. Mean free path between collisions (λ_T) or inelastic interactions (λ_I), calculated from $\lambda^{-1} = N_A \sum w_j \sigma_j / A_j$, where N is Avogadro's number and w_j is the weight fraction of the jth element in the element, compound, or mixture. $\sigma_{\rm total}$ at 80–240 GeV for neutrons ($\approx \sigma$ for protons) from Murthy *et al.*, Nucl. Phys. **B92**, 269 (1975). This scales approximately as $A^{0.77}$. $\sigma_{\rm inelastic} = \sigma_{\rm total} - \sigma_{\rm elastic} - \sigma_{\rm quasielastic}$; for neutrons at 60–375 GeV from Roberts *et al.*, Nucl. Phys. **B159**, 56 (1979). For protons and other particles, see Carroll *et al.*, Phys. Lett. **80B**, 319 (1979); note that $\sigma_I(p) \approx \sigma_I(n)$. σ_I scales approximately as $A^{0.71}$.

b. For minimum-ionizing muons (results are very slightly different for other particles). Minimum dE/dx from Ref. 3, using density effect correction coefficients from Ref. 1. For electrons and positrons see Ref. 4. Ionization energy loss is discussed in Sec. 27.

c. From Y.S. Tsai, Rev. Mod. Phys. **46**, 815 (1974); X_0 data for all elements up to uranium are given. Corrections for molecular binding applied for H_2 and D_2. For atomic H, $X_0 = 63.05$ g/cm^2.

d. For molecular hydrogen (deuterium). For atomic H, $X_0 = 63.047$ g cm^{-2}.

e. For pure graphite; industrial graphite density may vary 2.1–2.3 g/cm^3.

f. Standard shielding blocks, typical composition O_2 52%, Si 32.5%, Ca 6%, Na 1.5%, Fe 2%, Al 4%, plus reinforcing iron bars. The attenuation length, $\ell = 115 \pm 5$ g/cm^2, is also valid for earth (typical $\rho = 2.15$), from CERN–LRL–RHEL Shielding exp., UCRL–17841 (1968).

g. For typical fused quartz. The specific gravity of crystalline quartz is 2.64.

h. Solid ethane density at −60°C; gaseous refractive index at 0°C, 546 mm pressure.

i. Nylon, Type 6, $(NH(CH_2)_5CO)_n$

j. Polycarbonate (Lexan), $(C_{16}H_{14}O_3)_n$

k. Polyethylene terephthlate, monomer $C_5H_4O_2$

l. Polyethylene, monomer CH_2 =CH_2

m. Polymide film (Kapton), $(C_{22}H_{10}N_2O_5)_n$

n. Polymethylmethacralate, monomer CH_2 =$C(CH_3)CO_2CH_3$

o. Polystyrene, monomer C_6H_5CH=CH_2

p. Teflon, monomer CF_2 =CF_2

q. Polyvinyltolulene, monomer 2-$CH_3C_6H_4CH$=CH_2

r. Bismuth germanate (BGO), $(Bi_2O_3)_2(GeO_2)_3$

s. 97% SiO_2 + 3% H_2O by weight; see A. R. Buzykaev *et al.*, Nucl. Instrum. Methods **A433**, 396 (1999). Aerogel in the density range 0.04–0.06 g/cm^3 has been used in Čerenkov counters, but aerogel with higher and lower densities has been produced. ρ = density in g/cm^3.

t. G10-plate, typically 60% SiO_2 and 40% epoxy.

Appendix C

"Energy Levels in helium...", Am J. Phys Vol 49 No 3, March 1981

Energy levels in helium and neon atoms by an electron-impact method

N. Taylor, K. D. Bartle, and D. Mills
Department of Physical Chemistry, University of Leeds, Leeds LS2 9JT, England

D. S. Beard
Teltron Limited, 32/36 Telford Way, London W3, England
(Received 7 February 1980; accepted 20 May 1980)

Electronic energy levels in noble gas atoms may be determined with a simple teaching apparatus incorporating a resonance potentials tube in which the electron beam intensity is held constant. The resulting spectra are little inferior to those obtained by more elaborate electron-impact methods and complement optical emission spectra. Singlet–triplet energy differences may be resolved, and the spectra of helium and neon may be used to illustrate the applicability of Russell–Saunders and other, "intermediate," coupling schemes.

I. INTRODUCTION

Determination of the ionization potentials of rare gases using commercial gas-filled thermionic tubes[1] is a familiar experiment in many teaching laboratories. However, the characteristics of certain of these are often difficult to interpret and in any case seldom yield information about electronically excited states before ionization. In this article we describe an electron-impact method using a resonance potentials tube which, with an associated voltage-scanning and emission-stabilizing unit, enables both ionization potentials and the energies of various electronic levels to be determined. The experiment thus complements conventional studies of emission spectra by spectroscopic methods since the optical selection rules are now relaxed. The results obtained compare favorably with those from more advanced methods such as the use of sulphur hexafluoride to scavenge the low-energy electrons or high-resolution electron-energy-loss spectrometry.

II. ELECTRON IMPACT METHOD USING RESONANCE POTENTIALS TUBES

The construction of the resonance potentials tube[2] is shown schematically in Fig. 1. The simple diode electron gun is contained in a sidearm and allows electrons at a kinetic energy determined by the anode potential to be passed as a divergent beam across the cell containing a gas at low pressure to be collected at a conducting coating held at the same potential as the anode. A ring electrode within the cell is positioned so as to avoid collection directly from the incident beam, but when biased with a small positive potential (1.5 V) with respect to the anode the ring can collect electrons which have imparted most of their energy to gas atoms on impact. The enhanced sensitivity to electrons of low energy gives large ring electrode currents only when the energy of the incident beam matches that of an electronic transition in the gas atoms, and a spectrum of *resonance* or *critical* potentials is thus obtained on scanning a range of anode potential. In this mode the approach to ionization is indicated by a progressively increasing ring current with anode potential as many more transitions become possible. Reverting to a small negative ring potential enables ionization to be observed more directly from the onset of ion collection.

The control unit carries out the following functions:

(a) The electron beam intensity is maintained at a constant level irrespective of anode potential. This emission stabilization is important in obtaining good resolution from the commercially available tubes.

(b) The anode potential may be "ramped" as a linear variation with time within the range 10–30 V or may be adjusted to hold at some fixed value.

(c) The ring electrode currents are monitored with a simple solid state electrometer and the output used to drive a potentiometric recorder.

A circuit diagram is available on request from the authors.

III. OPTICAL SPECTRA AND SELECTION RULES

The spectra of most small and medium size atoms are in accord with Russell–Saunders LS coupling in which the electrostatic interactions are dominant over spin-orbit terms in determining the major separations of the energy levels. L and S are "good" quantum numbers at this extreme and term symbols generated from the various values of L and S serve as a simple and convenient way of identifying the energy levels and hence the spectral lines. The selection rules now include $\Delta L = 0, \pm 1$ ($L = L' = 0$ not allowed) and $\Delta S = 0$ to supplement the more general cases $\Delta J = 0, \pm 1$ ($J = J' = 0$ not allowed) and $\Delta l = \pm 1$ (the Laporte rule) which forbids transitions between states of the same "parity," i.e., either both even (Σl_i = even integer) or both odd (Σl_i = odd integer). When spin (own) orbit coupling is small, secondary splitting arises according to a given pattern which depends on atomic number Z. For $Z \leq 4$ the split levels have decreasing energy with increasing J and for $Z > 4$ the order tends more and more to be reversed. One outcome is the Landé interval rule, which states that the energy interval between pairs of adjacent levels is proportional to the J value of the upper level of each pair, but deviations from this occur because of neglect of spin-other-orbit and spin–spin magnetic interactions. Helium gives one of many possible examples of the characteristic energy level pattern determined by LS coupling (see Table I); the fine splitting of the 2^3P states, for example, due to the magnetic terms are in this case less than 1 cm^{-1} and are not in accord with the interval rule.

 0002-9505/81/030265-04$00.50

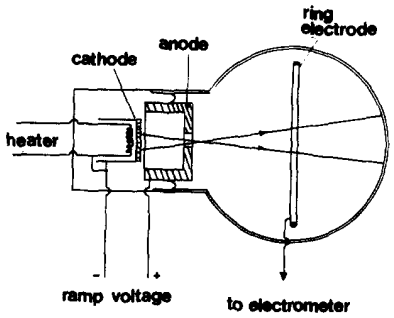

Fig. 1. Resonance-potentials tube.

Although often used, LS term symbols for atoms in which the electron interactions are grossly distorted from those described above have more limited usefulness in that levels have major separations due to other than electrostatic terms and the sense of "order" can be lost. In addition, selection rules, intensity relationships, etc. derived at the LS extreme are not now applicable. Two major factors disturb LS coupling as a useful representation. For "not too highly excited states" the spin (with own) orbit energies increase more rapidly with atomic number Z than the electrostatic terms such that they are dominant at high Z. At this situation the interaction energy depends primarily on the spin-orbit terms of the "core" of unexcited electrons and somewhat less so on the spin-orbit term of the excited or "optical" electron. This $J_c j_2$ or $j_1 j_2$ coupling,[3] when pure, thus neglects the electrostatic terms between the core and optical electron that at the LS extreme contributed to the separation of the levels. The levels thus appear for a given configuration as two widely spaced pairs and in, say, a p^5np configuration where J_c and j_2 can both take values of $\frac{3}{2}$ and $\frac{1}{2}$ have designations $\{\frac{3}{2}, \frac{1}{2}\}$ $(J = 1,2)$, $\{\frac{3}{2}, \frac{3}{2}\}$ $(J = 0,1,2,3)$, (widely separated from) $\{\frac{1}{2}, \frac{1}{2}\}$ $(J = 0,1)$ and $\{\frac{1}{2}, \frac{3}{2}\}$ $(J = 1,2)$ in order of ascending energy. J_c and j_2 (at this limit) are "good" quantum numbers and selection rules now include $\Delta j_2 = 0, \pm 1$ ($j_2 = j_2' = 0$ not allowed) and $\Delta J_c = 0$. The second feature disturbing LS coupling occurs when excitation is large. In this case the spin-orbit term of the optical electron diminishes most rapidly with increasing n and thus can become negligible compared with the coupling of the orbital angular momenta of optical electron and core. The combinations of J_c and l_2 (optical electron) yield a good quantum number K, and levels thus appear as closely spaced pairs dependent on S_2 for the final splitting. This form of pair coupling has wide applicability and is termed $J_c l_2$, or occasionally jK, coupling. Among the heavier rare gases the $2p^5 3p$ configuration of neon involves relatively large electrostatic but small spin-orbit terms and thus follows the general pattern of LS coupling whereas $2p^5 4p$, $5p$, $6p$ configurations, etc. are more akin to the $J_c l_2$ pair coupling scheme.[4] Likewise as Z increases, pair coupling becomes more suitable for all configurations. The selection of a suitable term representation for a given case is best determined by a comparison of the calculated relative splittings in a given configuration with those experimentally determined. Here the relative contributions of the various electron interaction terms are assessed within some framework of approximations. The most suitable type of term symbol is that reflecting most closely those conditions. Likewise, relative line intensities, g factors, etc. may be compared with experimentally determined values to confirm the scheme. Using this approach Cowan and Andrew[5] suggest for the $2p^5 3p$ configuration of neon that a scheme based on Ls coupling is perhaps most applicable. In this further example of pair coupling the ll interactions are dominant, with the spin-orbit term of the core the other major contribution. Despite this, $J_c l_2$ representations are most commonly used for neon and many other atoms and we shall follow this convention in the discussion of our results and in Table II.

Selection rules for transitions caused by electron impact are expected to differ greatly from those applicable to interaction with photons since the incident electron has spin thus relaxing spin conservation ($\Delta S = 0$); the parity restrictions are also relaxed since these are applicable only when electric dipole radiation is involved. Essentially we shall determine the significance of such changes from a comparison with the optical spectra.

IV. RESULTS AND DISCUSSION

Helium

Figure 2 [curve (a)] illustrates a typical recorder trace of resonance potentials for a tube filled with helium; curve (b) is the corresponding current due to He^+ ion collection when the ring electrode is biased negatively. The voltage axis in these cases has been "corrected" by assuming the literature value[6] of 24.58 V for the first ionization potential. The resonance potentials correspond to transitions from the ground state 1^1S to the levels indicated. These energies may be compared with values obtained spectroscopically (Table I).

Although the precision is lower, the technique gives results comparable with optical methods. However, the observations of transitions from the ground state and of the many optically forbidden transitions are particularly useful additions to the complementary optical procedure. Thus we

Table I. Energy levels and resonance potentials of helium. Transition to levels marked * from the ground state are forbidden by optical selection rules.[a]

Observed resonance potentials		Electron energy levels from optical spectroscopy LS		
(eV)	(cm^{-1})	term symbol	(eV)	(cm^{-1})
19.85	160000	$*2^3S_1$	19.819	159850
20.70	167000	$*2^1S_0$	20.615	166270
		$*2^3P_{2,1,0}$	20.963	169080
		2^1P_1	21.218	171130
22.90	185000	$*3^3S_1$	22.718	183230
		$*3^1S_0$	22.300	184860
		$*3^3P_{2,1,0}$	23.007	185560
		$*3^3D_{3,2,1}$	23.074	186100
		$*3^1D_2$	23.074	186100
		3^1P_1	23.086	186200
23.70	191000	$*4^3S_1$	23.593	190290
		$*4^1S_0$	23.672	190930
		+ other $n = 4$ levels		

[a]Data mainly taken from A. R. Striganov and N. S. Sventitskii, *Tables of Spectral Lines of Neutral and Ionized Atoms* (Plenum, New York, 1968).

Table II. Energy levels and resonance potentials of neon. Transition to levels marked * from the ground state are forbidden by optical selection rules.[a]

Observed resonance potentials		Electron energy levels from optical spectroscopy designation			
(eV)	(cm^{-1})	LS	$J_c l_2$	(eV)	(cm^{-1})
16.70	134500		$*3s[1\frac{1}{2}]^0_2$	16.615	134040
			$3s[1\frac{1}{2}]^0_1$	16.671	134460
			$*3s'[\frac{1}{2}]^0_0$	16.716	134820
			$3s'[\frac{1}{2}]^0_1$	16.849	135890
18.65	150500	$^3S_1$	$*3p[\frac{1}{2}]_1$	18.38	148260
		$^3D_3$	$*3p[2\frac{1}{2}]_3$	18.555	149660
		$^3D_2$	$*3p[2\frac{1}{2}]_2$	18.57	149830
		$^3D_1$	$*3p[1\frac{1}{2}]_1$	18.61	150120
		$^1D_2$	$*3p[1\frac{1}{2}]_2$	18.64	150320
		$^1P_1$	$*3p'[1\frac{1}{2}]_1$	18.69	150770
		$^3P_2$	$*3p'[1\frac{1}{2}]_2$	18.70	150860
		$^3P_0$	$*3p[\frac{1}{2}]_0$	18.71	150920
		$^3P_1$	$*3p'[\frac{1}{2}]_1$	18.73	151040
		$^1S_0$	$*3p'[\frac{1}{2}]_0$	18.966	152970
19.75	159500		$*4s[1\frac{1}{2}]^0_2$	19.66	158600
			$4s[1\frac{1}{2}]^0_1$	19.689	158800
			$*4s'[\frac{1}{2}]^0_0$	19.76	159380
			$4s'[\frac{1}{2}]^0_1$	19.780	159540
20.10	162000		$*3d[\frac{1}{2}]^0_0$	20.020	161510
			$3d[\frac{1}{2}]^0_1$	20.027	161530
			$*3d[3\frac{1}{2}]^0_4$	20.034	161590
			$*3d[3\frac{1}{2}]^0_3$	20.034	161590
			$*3d[1\frac{1}{2}]^0_2$	20.037	161610
			$3d[1\frac{1}{2}]^0_1$	20.041	161640
			$*3d[2\frac{1}{2}]^0_2$	20.048	161700
			$*3d[2\frac{1}{2}]^0_3$	20.048	161700
			$*3d'[2\frac{1}{2}]^0_2$	20.136	162410
			$*3d'[2\frac{1}{2}]^0_3$	20.136	162410
			$*3d'[1\frac{1}{2}]^0_2$	20.115	162420
			$3d'[1\frac{1}{2}]^0_1$	20.140	162440
			$5s[1\frac{1}{2}]^0_1$	20.57	165907
Here selected levels only are listed			$6s[1\frac{1}{2}]^0_1$	20.95	168972
			$7s[1\frac{1}{2}]^1_1$	21.14	170504
			$8s[1\frac{1}{2}]^0_1$	21.26	171472

[a]Data mainly taken from A. R. Striganov and N. S. Sventitskii, *Tables of Spectral Lines of Neutral and Ionized Atoms* (Plenum, New York, 1968).

see transitions to 2^3S, 2^1S, and 2^3P—violating $\Delta S = 0$, $L = L' = 0$, and $\Delta S = 0$, respectively—and many other examples. Transitions to 3^1D and 3^3D are probably present ($\Delta J > 1$) although at lower intensity than for lower ΔJ values. Of particular interest is the direct observation of the 2^3S–2^1S energy difference with its implications in terms of the pairing energy of electrons.

Spectra obtained with this simple teaching apparatus are not too inferior to those observed with more elaborate electron impact methods. In curve (c) of Fig. 2 we reproduce results similar to those obtained by Brion and Olsen[7] in which SF_6, which has a high electron-capture cross section only for energies <0.02eV, is used to "scavenge" the low-energy electrons; the concentration of SF_6^- ions is measured in a negative-ion mass spectrometer. The performance of the resonance potentials tube when detecting He^+ ions is clearly far superior to methods using "electron tubes," due in part to emission stabilization.

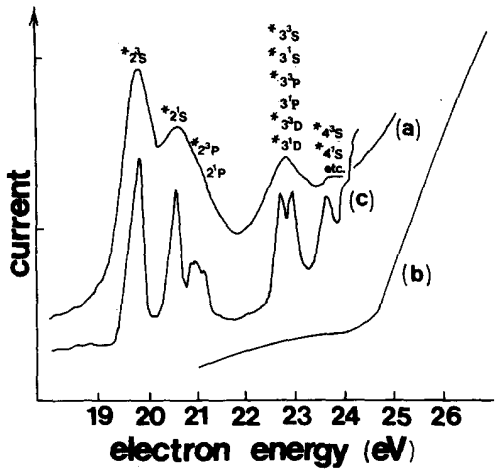

Fig. 2. Electron-impact spectra of helium: (a) this work; (b) He^+ current; (c) electron impact with SF_6 scavenging (after Brion and Olsen[7]).

Neon

In Fig. 3 we compare our resonance potentials (a) with those obtained using SF_6 scavenging (b) and high-resolution electron-energy-loss spectrometry (c).[8] The neon resonance potentials tube performs very well and results are quite similar to those obtained using the more complicated scavenging technique.[7] We have included curve (c) to enable some prediction to be made of the relative contributions of various transitions. In Table II we list a selection of energy levels for the neon atom and the corresponding resonance potentials we observe. The designations are generally in $J_c l_2$ notation and are of the form $nl'[K]^\circ_J$ where the l value of the optical electron is "dashed" only when $J_c = \frac{1}{2}$, otherwise $J_c = \frac{3}{2}$. The superscript ° recognizes odd parity, and its absence even parity. In addition LS term symbols are given for the $2p^5 3p$ configuration for reasons mentioned in Sec. III. We see the strong contributions of transitions from the ground state to the parity-forbidden $2p^5 3p$ configuration and most likely similar contributions to higher-p states. Examination of the LS term symbols for this group indicates more simply the presence of transitions forbidden by the $\Delta S = 0$ selection rule. The $^3P_{2,1,0}$ states are degenerate at the LS extreme as also are $^3D_{3,2,1}$ and we see ac-

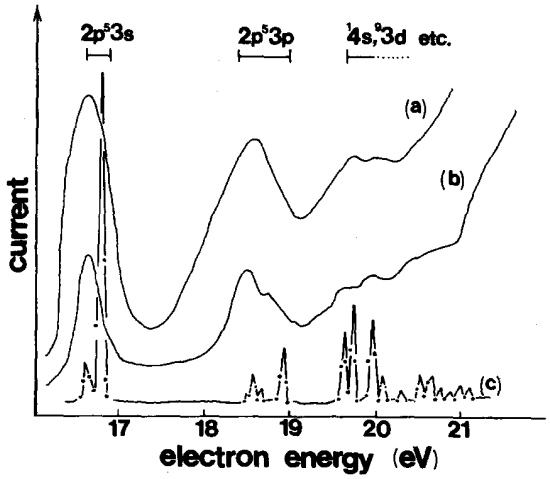

Fig. 3. Electron-impact spectra of neon: (a) this work; (b) with SF_6 scavenging (after Brion and Olsen[7]); (c) high-resolution trapped-electron excitation (after Roy and Carette[8]).

cording to Cowan and Andrew[5] the effects of predominantly core spin-orbit terms in splitting these levels. The peak at around 16.7 eV most probably involves predominantly the optically allowed transition from the ground state to $3s^2[1/2]_1^0$ but the detail of (c) indicates the presence of a contribution from all other states of the $2p3s$ configuration, thus including a $J = J' = 0$ and $\Delta J = 2$ transition. There are numerous other contributions which may be discussed in a similar way.

The neon tube may also be operated to collect Ne^+ ions. In this mode the performance in detecting the onset of ionization is again superior to methods using "electron tubes."

V. CONCLUSIONS

We have demonstrated that with relatively simple apparatus, resonance potentials tubes are capable of supplying interesting information concerning the energy levels of electrons in noble gases. In particular, emphasis can be placed on complementing emission spectra and on the operation of optical selection rules since many violations may be directly observed. In addition the implications of various coupling schemes in determining the patterns of levels for various configurations can be introduced to students. Finally, singlet–triplet energy differences can be resolved and serve as an interesting basis for a discussion of electron "pairing."

[1]R. B. Dineen and R. S. Nyholm, J. R. Inst. Chem. 110 (1963).

[2]A helium resonance potentials tube is available from Teltron Ltd., 32/36 Telford Way, London W3.

[3]It should be noted that because of the filled-shell ground state of the rare gases their behavior is formally similar to a two-electron system; despite this, the spin-orbit term of the "hole," for example, can greatly exceed that of the electron it "replaces." The term symbol for $J_c j_2$ coupling is presented here in the form $\{J_c, j_2\}$ $(J = \cdots)$.

[4]There are many excellent accounts of intermediate coupling, for example, E. U. Condon and G. H. Shortley, *The Theory of Atomic Spectra* (Cambridge University, Cambridge, 1935) and B. Edlen, *Handbuch der Physik, Vol. 27, Atomic Spectra* (Springer-Verlag, Berlin, 1964) provide additional discussion to that presented here.

[5]R. D. Cowan and K. L. Andrew, J. Opt. Soc. Am. **55**, 502 (1965).

[6]C. E. Moore, *Circular No. 467, Vol. 1* (National Bureau of Standards, Washington, D.C., 1949).

[7]C. E. Brion and L. A. R. Olsen, J. Phys. B **3**, 1020 (1970).

[8]D. Roy and J. D. Carette, Can. J. Phys. **52**, 1178 (1974).

Appendix D

"Determination of the rest-mass energy of the electron...", Am J. Phys Vol 45 No 11, Nov. 1977

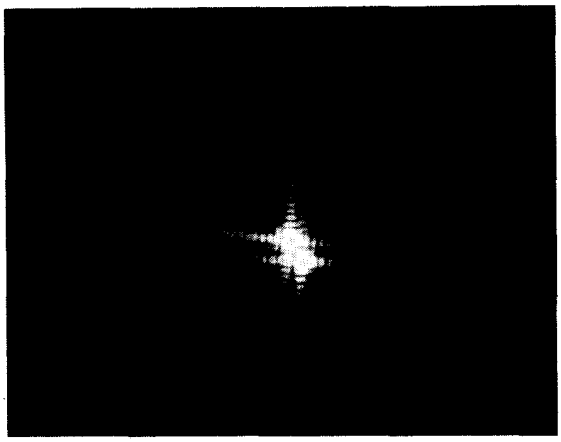

Fig. 1. The output of a misaligned double-beam interferometer illuminated through a square aperture.

this simple aligning technique. Such rotations cannot be tolerated in interferometric systems and may be troublesome also in other applications.

In noncoherent systems, rotational alignment is achieved by using some kind of reticle (i.e., cross hairs). Unfortunately, due to diffraction, a reticle does not solve the problem in a coherent system. We found it very useful to convert the whole laser beam into a "reticle." This can easily be done by inserting an aperture of some definite form in the beam in order to produce a diffraction pattern—the "reticle" of the desired form. For example, a circular aperture produces a set of concentric rings that are useful in accurate centering of the beam. In our laboratory[1] we used a square aperture in order to align an interferometric system with two laser beams exactly colinear and allowing no rotation between them. Figure 1 shows the output of the system with inaccurate alignment (a slight displacement of the beams was also introduced for clarity.

many cases this is adequate. However, when a larger number (over three) of reflections are involved they may introduce a rotation in the beam which is undetectable by

[1]J. Shamir, Appl. Opt. **15**, 120, (1976).

Determination of the rest-mass energy of the electron: a laboratory experiment

T.S. Mudhole and N. Umakantha
Department of Physics, Karnatak University, Dharwar, 580 003, India
(Received 23 October 1975; revised 9 December 1975)

The rest-mass energy of the electron is an important quantity in physics and it is desirable to have a laboratory experiment to determine it. This can be done by making use of the Compton scattering in which an incident photon of known energy shares energy and momentum with an electron at rest. It can be shown[1] that in a head-on collision with an incident photon of energy E_γ, the electron receives the maximum possible energy given by

$$T_{\max} = E_\gamma[1 + (m_0c^2/2E_\gamma)]^{-1} \quad (1)$$

and the back-scattered photon has the minimum possible energy given by

$$E'_\gamma = E_\gamma - T_{\max} = m_0c^2[2 + (m_0c^2/E_\gamma)]^{-1}, \quad (2)$$

where m_0 is the rest mass of the electron and c is the velocity of light. Thus, by experimentally determining either $T_{\max}$ or E'_γ for a known E_γ the electron rest-mass energy m_0c^2 can be determined.

This experiment can be done in any undergraduate laboratory which is equipped with a gamma-ray spectrometer consisting of a NaI($T1$) crystal coupled to a photomultiplier and a single- or multichannel analyzer to determine the pulse-height distribution due to monoenergetic gamma rays falling on the crystal. The photoelectric absorption of the incident photons lead to a peak called the photopeak whose maximum corresponds to the energy E_γ of the incident photons. The Compton scattered electrons have a continuous distribution of energy from zero to $T_{\max}$ and these lead to the so-called Compton distribution in the pulse-height spectrum. Because of the finite resolution of the crystal, the Compton distribution has at the higher energy end a rapidly falling part called the Compton edge. The pulse height corresponding to the midpoint of the Compton edge may be taken as corresponding to the electron energy $T_{\max}$. On the other hand, if the head-on collision takes place at the interface between the crystal and the glass envelope of the phototube, the electron would escape from the crystal and the back-scattered photon of energy E'_γ may undergo photoelectric absorption in the crystal. Such processes lead to a well-discernable peak called the back-scattered peak which is superposed on the continuous Compton distribution.[2] If, using a set of gamma sources of known energy, the spectrometer is calibrated so that the pulse height can be expressed in terms of energy, the pulse heights corresponding to the photopeak, the Compton edge, and the back-scattered peak can be directly expressed in terms of energy, and using Eqs. (1) and (2) the value of m_0c^2 can be determined.

We report the results we have obtained by using a NaI($T1$) crystal of 1-in. diam. and 1-in. height coupled to

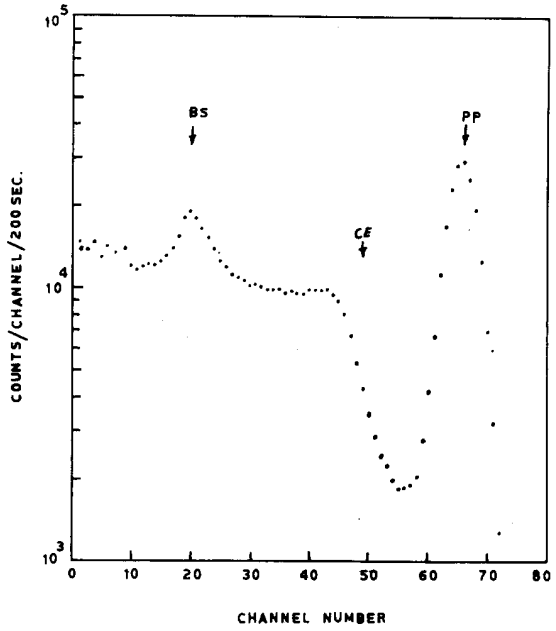

Fig. 1. A typical pulse-height distribution obtained with a ^{137}Cs source, where *BS*, *CE*, and *PP* indicate, respectively, back-scattered peak, the Compton edge, and the photopeak.

an RCA-6199 photomultiplier. The pulse-height distribution is obtained by using a multichannel analyzer. A typical pulse-height distribution is given in Fig. 1. The gamma sources used, their half-lives, the values of E_γ, T_{max}, and E'_γ are given in Table I. The sources are of 10 μCi. In column 6 we give the values of m_0c^2 obtained by using Eq. (1), and in column 7 the values obtained by using Eq. (2). The uncertainty in determining T_{max} and E'_γ from the observed pulse-height distribution is about $\pm 1/2$ channel, i.e., about ± 5 KeV. This leads to an error of about ± 20 KeV in the calculated rest-mass energy of the electron. The mean value of the rest-mass energy of the electron is found to be 516 ± 20 KeV which is close to the standard value of 511 KeV. Using the standard value of the velocity of light, the mass m_0 of the electron can be calculated. In our case it comes out to be $(9.20 \pm 0.35) \times 10^{-28}$ g comparable to the standard value of 9.108×10^{-28} g. Greater accuracy can be achieved by using a Ge(Li) detector, if available.

Table I. The values of the electron rest-mass energy (m_0c^2) calculated using the experimental values of the Compton edge (T_{max}) and the back-scattered peak (E'_γ) are given in columns 6 and 7, respectively, for the three gamma energies (E_γ) used. The error of ± 20 KeV corresponds to the uncertainty of $\pm 1/2$ channel (i.e., ± 5 KeV) in determining T_{max} and E'_γ from the pulse-height distributions. Mean value of $m_0c^2 = 516 \pm 20$ KeV.

Source	Halflife	E_γ KeV	T_{max} KeV	E'_γ KeV	m_0c^2 KeV	m_0c^2 KeV
^{137}Cs	30y	662	480	190	502	533
^{54}Mn	310d	840	640	200	525	525
^{65}Zn	245d	1114	910	210	499	517

We are grateful to the University Grants Commission for the financial assistance.

[1] R. D. Evans, *The Atomic Nucleus* (McGraw-Hill, New York, 1955), p. 672.

[2] J. H. Neiler and P. R. Bell, "The Scintillation Method," in *Alpha-, Beta-, and Gamma-Ray Spectroscopy*, edited by K. Siegbahn (North-Holland, Amsterdam, 1965), p. 245.

Half-life of thorium-232: a laboratory experiment

G. C. Chikkur and N. Umakantha
Department of Physics, Karnatak University, Dharwar-580 003, India
(Received 30 March 1976; revised 24 September 1976)

We report a simple laboratory experiment to estimate the half-life of ^{232}Th, which also familiarizes the students with the technique of absolute counting with a 4π geometry using a liquid scintillator.[1] The isotope has an abundance of 100% and its decay series is well known.[2] The longest lived product ^{228}Ra, has a half-life of 5.75 y. So, in any thorium sample which is more than about 35 y old, all the decay products would be nearly in secular equilibrium with thorium, leading to emission of six alpha particles in the energy range from 4 to 9 MeV and four beta particles belonging to beta spectra having endpoint energies from 0.012 to 2.25 MeV. In this experiment a known amount of thorium nitrate is dissolved in a liquid scintillator and a difference method is used to determine the counting rate due to alpha particles only. As there are six alpha emissions in the series, one-sixth of this counting rate gives the disintegration rate of thorium in the sample. From this, the half-life of thorium can be calculated. The experiment can be done in 3–4 h using a single or a multichannel analyzer, or even a scaler-discriminator setup.

A liquid scintillator solution is prepared by dissolving 25 mg of *p*-terphenyl in 5 cc of dioxane. Of this 2 cc is poured into a flat-bottomed Pyrex glass cell of 2 cm diam and 2 cm height and an exactly weighed quantity of 2 mg of anhydrous thorium nitrate, $Th(NO_3)_4 \cdot 4H_2O$, is dissolved in the solution. In our experiment, we have used a sample which was purchased by our department 20 y ago. The cell is mounted on an RCA 6199 photomultiplier and covered

Appendix E

Interactions of Electrons and Photons with Matter

27. PASSAGE OF PARTICLES THROUGH MATTER

Revised April 2006 by H. Bichsel (University of Washington), D.E. Groom (LBNL), and S.R. Klein (LBNL).

27.1. Notation

Table 27.1: Summary of variables used in this section. The kinematic variables β and γ have their usual meanings.

Symbol	Definition	Units or Value
α	Fine structure constant $(e^2/4\pi\epsilon_0\hbar c)$	$1/137.035\,999\,11(46)$
M	Incident particle mass	MeV/c^2
E	Incident particle energy γMc^2	MeV
T	Kinetic energy	MeV
$m_e c^2$	Electron mass $\times\ c^2$	$0.510\,998\,918(44)$ MeV
r_e	Classical electron radius $e^2/4\pi\epsilon_0 m_e c^2$	$2.817\,940\,325(28)$ fm
N_A	Avogadro's number	$6.022\,1415(10) \times 10^{23}$ mol^{-1}
ze	Charge of incident particle	
Z	Atomic number of absorber	
A	Atomic mass of absorber	g mol^{-1}
K/A	$4\pi N_A r_e^2 m_e c^2/A$	$0.307\,075$ MeV g^{-1} cm^2 for A = 1 g mol^{-1}
I	Mean excitation energy	eV (*Nota bene!*)
$\delta(\beta\gamma)$	Density effect correction to ionization energy loss	
$\hbar\omega_p$	Plasma energy $(\sqrt{4\pi N_e r_e^3}\ m_e c^2/\alpha)$	$28.816\sqrt{\rho\langle Z/A\rangle}$ eV$^{(a)}$
N_c	Electron density	(units of r_e)$^{-3}$
w_j	Weight fraction of the jth element in a compound or mixture	
n_j	$\propto$ number of jth kind of atoms in a compound or mixture	
—	$4\alpha r_e^2 N_A/A$	$(716.408$ g cm$^{-2})^{-1}$ for $A = 1$ g mol^{-1}
X_0	Radiation length	g cm^{-2}
E_c	Critical energy for electrons	MeV
$E_{\mu c}$	Critical energy for muons	GeV
E_s	Scale energy $\sqrt{4\pi/\alpha}\ m_e c^2$	21.2052 MeV
R_M	Molière radius	g cm^{-2}

$^{(a)}$ For ρ in g cm^{-3}.

$$= z_1\, x\, \theta_0/\sqrt{12} + z_2\, x\, \theta_0/2 \ ; \tag{27.18}$$

$$\theta_{\rm plane} = z_2\, \theta_0 \ . \tag{27.19}$$

Note that the second term for $y_{\rm\ plane}$ equals $x\,\theta_{\rm plane}/2$ and represents the displacement that would have occurred had the deflection $\theta_{\rm plane}$ all occurred at the single point $x/2$.

For heavy ions the multiple Coulomb scattering has been measured and compared with various theoretical distributions [34].

27.4. Photon and electron interactions in matter

27.4.1. ***Radiation length*** : High-energy electrons predominantly lose energy in matter by bremsstrahlung, and high-energy photons by e^+e^- pair production. The characteristic amount of matter traversed for these related interactions is called the radiation length X_0, usually measured in g cm^{-2}. It is both (a) the mean distance over which a high-energy electron loses all but $1/e$ of its energy by bremsstrahlung, and (b) $\frac{7}{9}$ of the mean free path for pair production by a high-energy photon [35]. It is also the appropriate scale length for describing high-energy electromagnetic cascades. X_0 has been calculated and tabulated by Y.S. Tsai [36]:

$$\frac{1}{X_0} = 4\alpha r_e^2 \frac{N_A}{A} \left\{ Z^2 \left[L_{\rm rad} - f(Z) \right] + Z\, L'_{\rm rad} \right\} \ . \tag{27.20}$$

For $A = 1$ g mol^{-1}, $4\alpha r_e^2 N_A/A = (716.408\ {\rm g\ cm^{-2}})^{-1}$. $L_{\rm rad}$ and $L'_{\rm rad}$ are given in Table 27.2. The function $f(Z)$ is an infinite sum, but for elements up to uranium can be represented to 4-place accuracy by

$$f(Z) = a^2 \left[(1+a^2)^{-1} + 0.20206 \right.$$
$$\left. -0.0369\, a^2 + 0.0083\, a^4 - 0.002\, a^6 \right] \ , \tag{27.21}$$

where $a = \alpha Z$ [37].

Table 27.2: Tsai's $L_{\rm rad}$ and $L'_{\rm rad}$, for use in calculating the radiation length in an element using Eq. (27.20).

Element	Z	$L_{\rm rad}$	$L'_{\rm rad}$
H	1	5.31	6.144
He	2	4.79	5.621
Li	3	4.74	5.805
Be	4	4.71	5.924
Others	> 4	$\ln(184.15\, Z^{-1/3})$	$\ln(1194\, Z^{-2/3})$

Although it is easy to use Eq. (27.20) to calculate X_0, the functional dependence on Z is somewhat hidden. Dahl provides a compact fit to the data [38]:

$$X_0 = \frac{716.4\ {\rm g\ cm^{-2}}\, A}{Z(Z+1)\ln(287/\sqrt{Z})} \ . \tag{27.22}$$

Results using this formula agree with Tsai's values to better than 2.5% for all elements except helium, where the result is about 5% low.

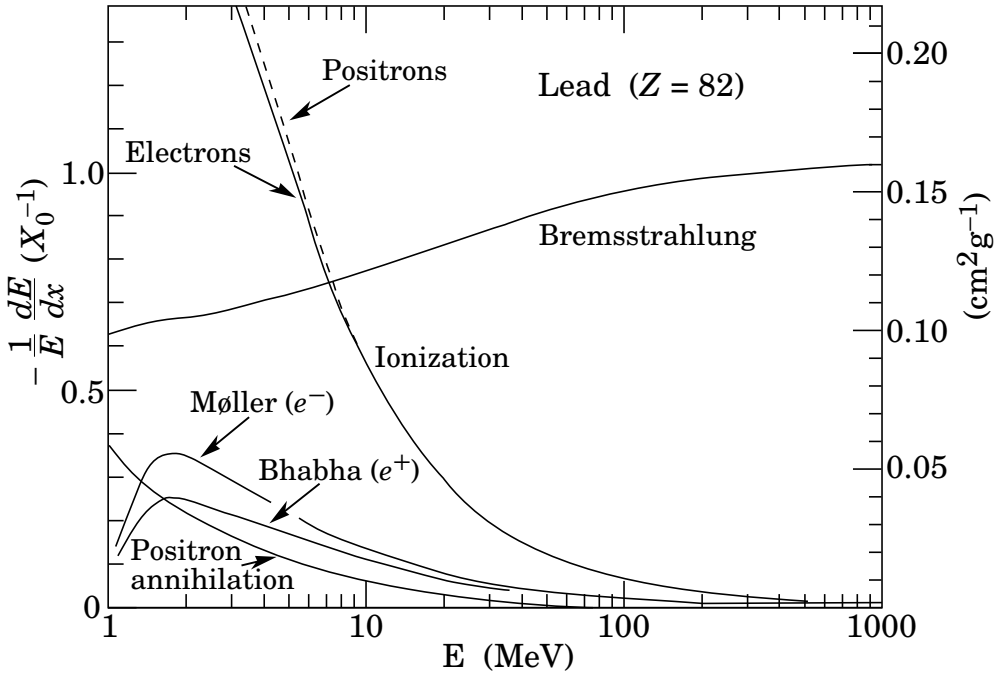

Figure 27.10: Fractional energy loss per radiation length in lead as a function of electron or positron energy. Electron (positron) scattering is considered as ionization when the energy loss per collision is below 0.255 MeV, and as Møller (Bhabha) scattering when it is above. Adapted from Fig. 3.2 from Messel and Crawford, *Electron-Photon Shower Distribution Function Tables for Lead, Copper, and Air Absorbers*, Pergamon Press, 1970. Messel and Crawford use $X_0(\mathrm{Pb}) = 5.82$ g/cm^2, but we have modified the figures to reflect the value given in the Table of Atomic and Nuclear Properties of Materials ($X_0(\mathrm{Pb}) = 6.37$ g/cm^2).

The radiation length in a mixture or compound may be approximated by

$$1/X_0 = \sum w_j/X_j \ , \tag{27.23}$$

where w_j and X_j are the fraction by weight and the radiation length for the jth element.

27.4.2. ***Energy loss by electrons*** : At low energies electrons and positrons primarily lose energy by ionization, although other processes (Møller scattering, Bhabha scattering, e^+ annihilation) contribute, as shown in Fig. 27.10. While ionization loss rates rise logarithmically with energy, bremsstrahlung losses rise nearly linearly (fractional loss is nearly independent of energy), and dominates above a few tens of MeV in most materials

Ionization loss by electrons and positrons differs from loss by heavy particles because of the kinematics, spin, and the identity of the incident electron with the electrons which it ionizes. Complete discussions and tables can be found in Refs. 7, 8, and 27.

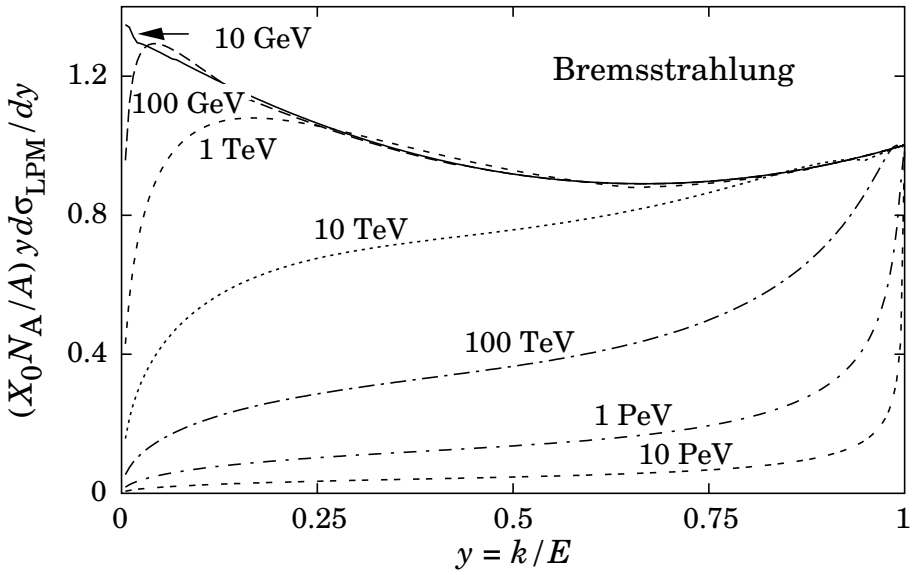

Figure 27.11: The normalized bremsstrahlung cross section $k\, d\sigma_{LPM}/dk$ in lead versus the fractional photon energy $y = k/E$. The vertical axis has units of photons per radiation length.

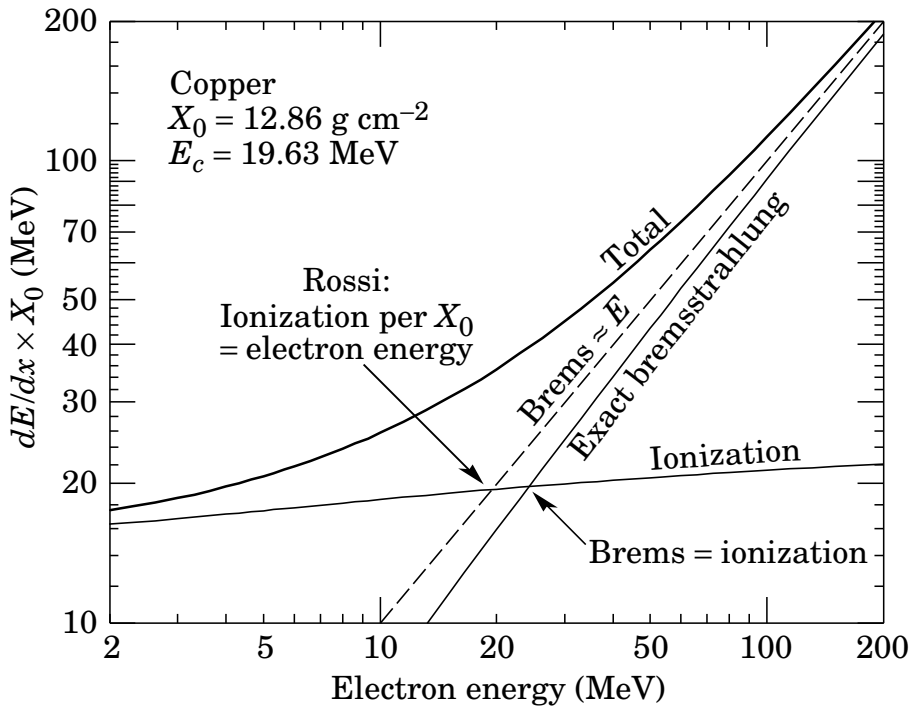

Figure 27.12: Two definitions of the critical energy E_c.

At very high energies and except at the high-energy tip of the bremsstrahlung

spectrum, the cross section can be approximated in the "complete screening case" as [36]

$$d\sigma/dk = (1/k)4\alpha r_e^2\{(\tfrac{4}{3} - \tfrac{4}{3}y + y^2)[Z^2(L_{\rm rad} - f(Z)) + Z\,L'_{\rm rad}] + \tfrac{1}{9}(1-y)(Z^2+Z)\}\ , \tag{27.24}$$

where $y = k/E$ is the fraction of the electron's energy transfered to the radiated photon. At small y (the "infrared limit") the term on the second line ranges from 1.7% (low Z) to 2.5% (high Z) of the total. If it is ignored and the first line simplified with the definition of X_0 given in Eq. (27.20), we have

$$\frac{d\sigma}{dk} = \frac{A}{X_0 N_A k}\left(\tfrac{4}{3} - \tfrac{4}{3}y + y^2\right)\ . \tag{27.25}$$

This cross section (times k) is shown by the top curve in Fig. 27.11.

This formula is accurate except in near $y = 1$, where screening may become incomplete, and near $y = 0$, where the infrared divergence is removed by the interference of bremsstrahlung amplitudes from nearby scattering centers (the LPM effect) [39,40] and dielectric suppression [41,42]. These and other suppression effects in bulk media are discussed in Sec. 27.4.5.

With decreasing energy ($E \lesssim 10$ GeV) the high-y cross section drops and the curves become rounded as $y \to 1$. Curves of this familar shape can be seen in Rossi [4] (Figs. 2.11.2,3); see also the review by Koch & Motz [43].

Except at these extremes, and still in the complete-screening approximation, the the number of photons with energies between $k_{\rm min}$ and $k_{\rm max}$ emitted by an electron travelling a distance $d \ll X_0$ is

$$N_\gamma = \frac{d}{X_0}\left[\frac{4}{3}\ln\left(\frac{k_{\rm max}}{k_{\rm min}}\right) - \frac{4(k_{\rm max} - k_{\rm min})}{3E} + \frac{(k_{\rm max} - k_{\rm min})^2}{2E^2}\right]\ . \tag{27.26}$$

27.4.3. ***Critical energy*** : An electron loses energy by bremsstrahlung at a rate nearly proportional to its energy, while the ionization loss rate varies only logarithmically with the electron energy. The *critical energy* E_c is sometimes defined as the energy at which the two loss rates are equal [44]. Berger and Seltzer [44] also give the approximation $E_c = (800\ {\rm MeV})/(Z + 1.2)$. This formula has been widely quoted, and has been given in older editions of this *Review* [45]. Among alternate definitions is that of Rossi [4], who defines the critical energy as the energy at which the ionization loss per radiation length is equal to the electron energy. Equivalently, it is the same as the first definition with the approximation $|dE/dx|_{\rm brems} \approx E/X_0$. This form has been found to describe transverse electromagnetic shower development more accurately (see below). These definitions are illustrated in the case of copper in Fig. 27.12.

The accuracy of approximate forms for E_c has been limited by the failure to distinguish between gases and solid or liquids, where there is a substantial difference in ionization at the relevant energy because of the density effect. We distinguish these two cases in Fig. 27.13. Fits were also made with functions of the form $a/(Z + b)^\alpha$, but α was found to be essentially unity. Since E_c also depends on A, I, and other factors, such forms are at best approximate.

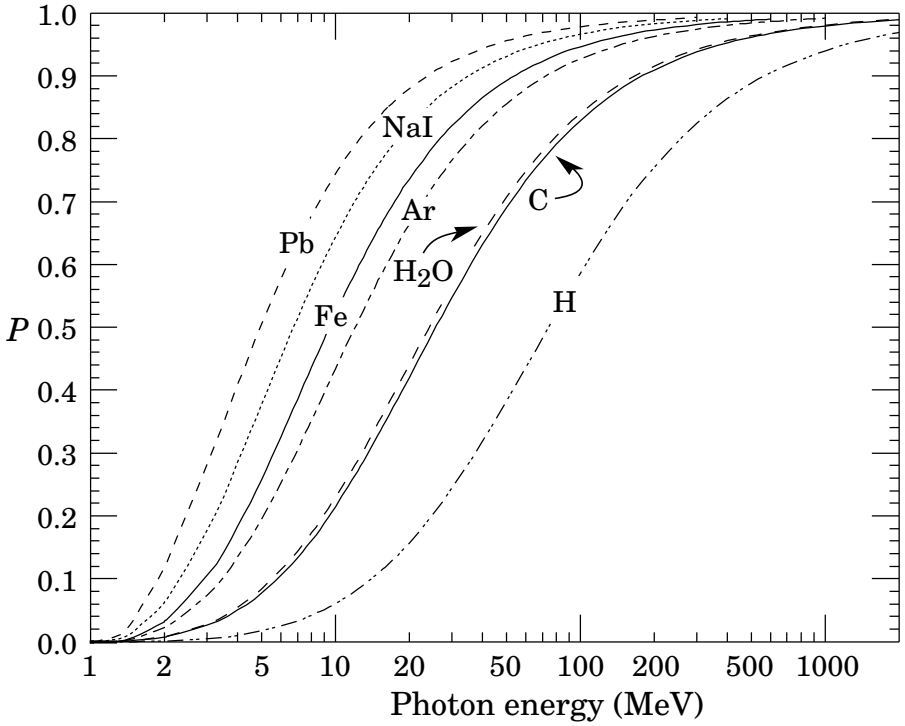

Figure 27.13: Electron critical energy for the chemical elements, using Rossi's definition [4]. The fits shown are for solids and liquids (solid line) and gases (dashed line). The rms deviation is 2.2% for the solids and 4.0% for the gases. (Computed with code supplied by A. Fassó.)

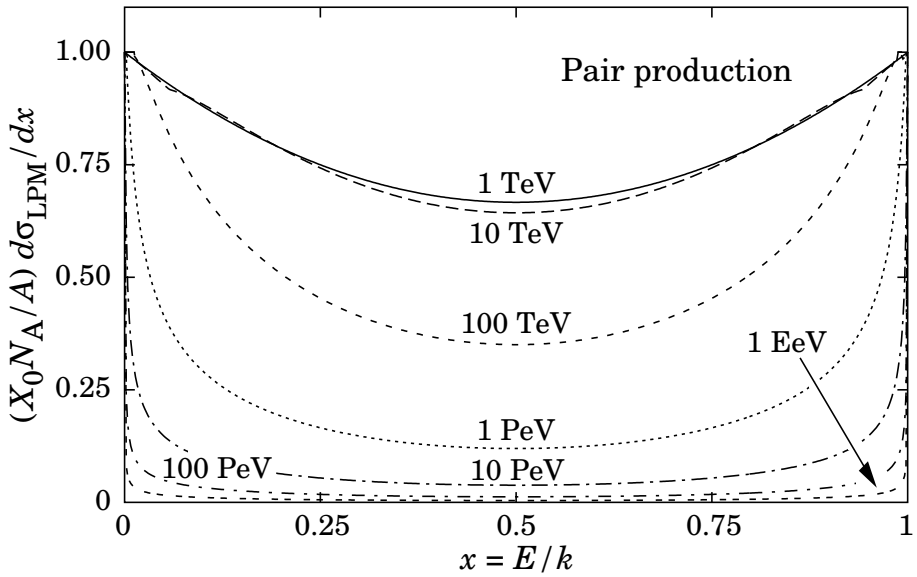

Figure 27.15: The normalized pair production cross section $d\sigma_{LPM}/dy$, versus fractional electron energy $x = E/k$.

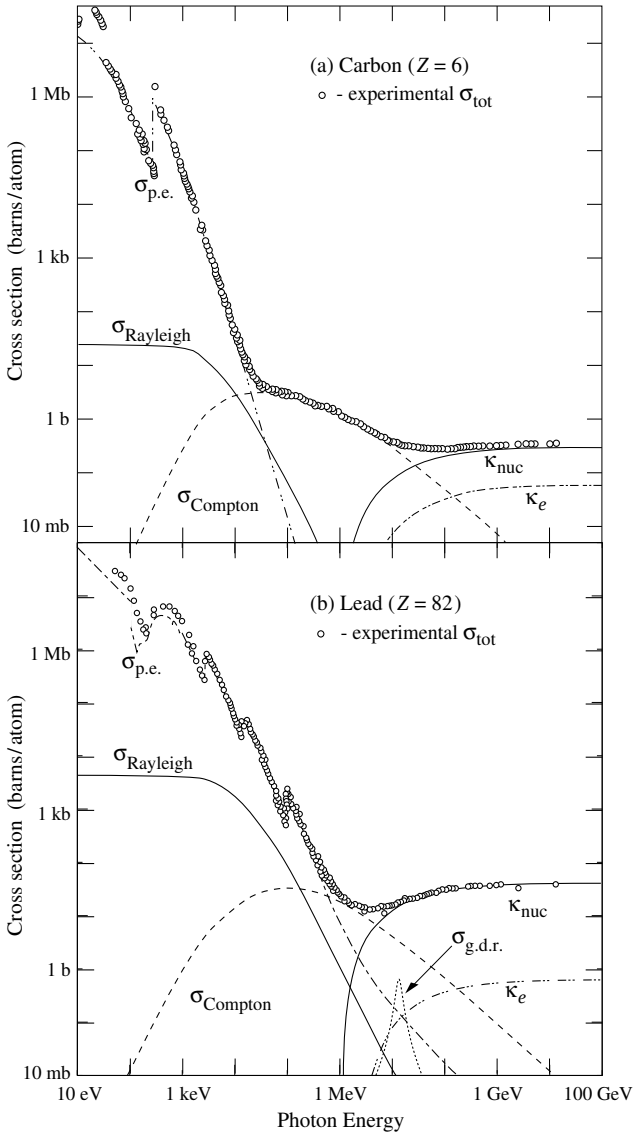

Figure 27.14: Photon total cross sections as a function of energy in carbon and lead, showing the contributions of different processes:

$\sigma_{\text{p.e.}}$ = Atomic photoelectric effect (electron ejection, photon absorption)

σ_{Rayleigh} = Rayleigh (coherent) scattering–atom neither ionized nor excited

σ_{Compton} = Incoherent scattering (Compton scattering off an electron)

κ_{nuc} = Pair production, nuclear field

κ_e = Pair production, electron field

$\sigma_{\text{g.d.r.}}$ = Photonuclear interactions, most notably the Giant Dipole Resonance [46]. In these interactions, the target nucleus is broken up.

Data from [47]; parameters for $\sigma_{\text{g.d.r.}}$ from [48]. Curves for these and other elements, compounds, and mixtures may be obtained from `http://physics.nist.gov/PhysRefData`. The photon total cross section is approximately flat for at least two decades beyond the energy range shown. Original figures courtesy J.H. Hubbell (NIST).

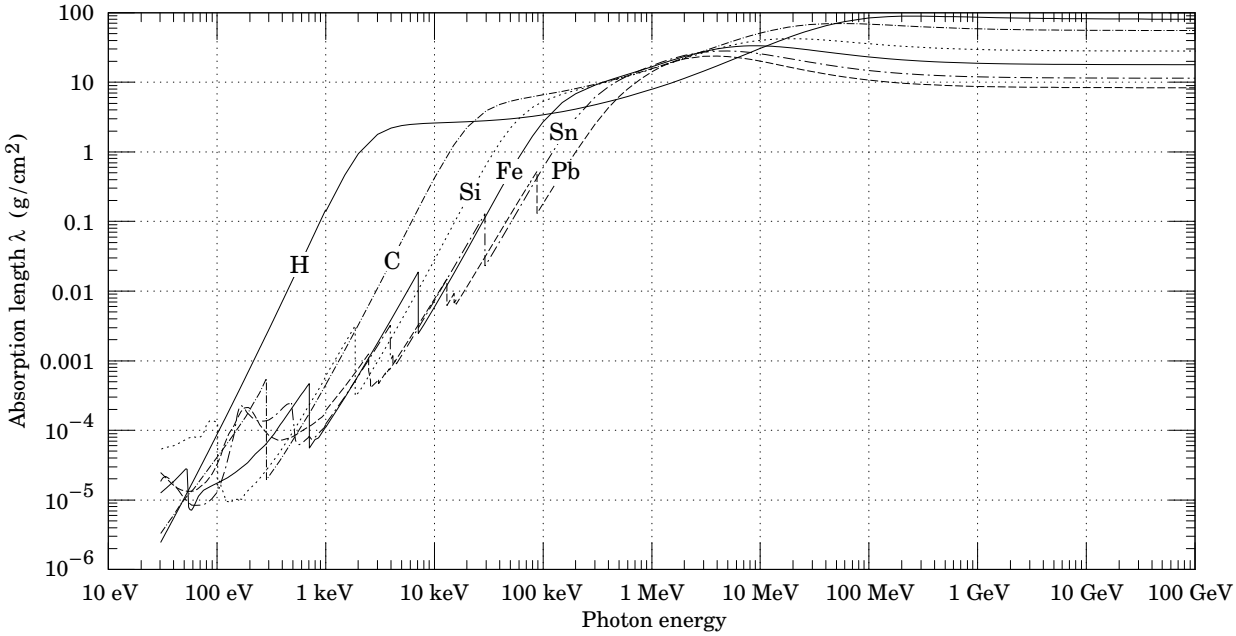

Figure 27.16: The photon mass attenuation length (or mean free path) $\lambda = 1/(\mu/\rho)$ for various elemental absorbers as a function of photon energy. The mass attenuation coefficient is μ/ρ, where ρ is the density. The intensity I remaining after traversal of thickness t (in mass/unit area) is given by $I = I_0 \exp(-t/\lambda)$. The accuracy is a few percent. For a chemical compound or mixture, $1/\lambda_{\rm eff} \approx \sum_{\rm elements} w_Z/\lambda_Z$, where w_Z is the proportion by weight of the element with atomic number Z. The processes responsible for attenuation are given in not Fig. 27.10. Since coherent processes are included, not all these processes result in energy deposition. The data for 30 eV $< E <$ 1 keV are obtained from `http://www-cxro.lbl.gov/optical_constants` (courtesy of Eric M. Gullikson, LBNL). The data for 1 keV $< E <$ 100 GeV are from `http://physics.nist.gov/PhysRefData`, through the courtesy of John H. Hubbell (NIST).

27.4.4. ***Energy loss by photons*** : Contributions to the photon cross section in a light element (carbon) and a heavy element (lead) are shown in Fig. 27.14. At low energies it is seen that the photoelectric effect dominates, although Compton scattering, Rayleigh scattering, and photonuclear absorption also contribute. The photoelectric cross section is characterized by discontinuities (absorption edges) as thresholds for photoionization of various atomic levels are reached. Photon attenuation lengths for a variety of elements are shown in Fig. 27.16, and data for 30 eV$< k <$100 GeV for all elements is available from the web pages given in the caption. Here k is the photon energy.

The increasing domination of pair production as the energy increases is shown in Fig. 27.17. Using approximations similar to those used to obtain Eq. (27.25), Tsai's

formula for the differential cross section [36] reduces to

$$\frac{d\sigma}{dx} = \frac{A}{X_0 N_A}\left[1 - \tfrac{4}{3}x(1-x)\right] \tag{27.27}$$

in the complete-screening limit valid at high energies. Here $x = E/k$ is the fractional energy transfer to the pair-produced electron (or positron), and k is the incident photon energy. The cross section is very closely related to that for bremsstrahlung, since the Feynman diagrams are variants of one another. The cross section is of necessity symmetric between x and $1-x$, as can be seen by the solid curve in Fig. 27.15. See the review by Motz, Olsen, & Koch for a more detailed treatment [49].

Eq. (27.27) may be integrated to find the high-energy limit for the total e^+e^- pair-production cross section:

$$\sigma = \tfrac{7}{9}(A/X_0 N_A)\ . \tag{27.28}$$

Equation Eq. (27.28) is accurate to within a few percent down to energies as low as 1 GeV, particularly for high-Z materials.

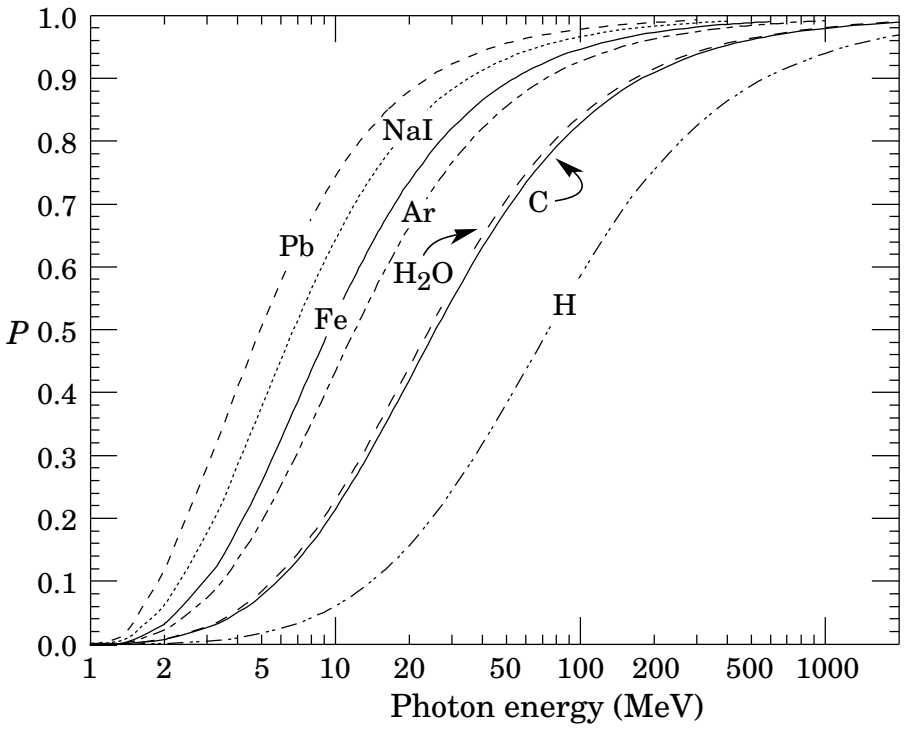

Figure 27.17: Probability P that a photon interaction will result in conversion to an e^+e^- pair. Except for a few-percent contribution from photonuclear absorption around 10 or 20 MeV, essentially all other interactions in this energy range result in Compton scattering off an atomic electron. For a photon attenuation length λ (Fig. 27.16), the probability that a given photon will produce an electron pair (without first Compton scattering) in thickness t of absorber is $P[1 - \exp(-t/\lambda)]$.

Appendix F

Radiation Dosages

29. RADIOACTIVITY & RADIATION PROTECTION

Revised Sept. 1996 by R.S. Donahue (LBNL) and A. Fassó (SLAC);
revised Sept. 2005 by J.C. Liu (SLAC) and S. Roesler (CERN).

29.1. Definitions

The International Commission on Radiation Units and Measurements (ICRU) recommends the use of SI units. Therefore we list SI units first, followed by cgs (or other common) units in parentheses, where they differ.

• **Unit of activity** = becquerel (curie):
1 Bq = 1 disintegration s^{-1} [$= 1/(3.7 \times 10^{10})$ Ci]

• **Unit of absorbed dose in any material** = gray (rad):
1 Gy = 1 joule kg^{-1} ($= 10^4$ erg $g^{-1} = 100$ rad)
$= 6.24 \times 10^{12}$ MeV kg^{-1} deposited energy

• **Unit of exposure**, A measure of photon fluence at a certain point in space integrated over time, in terms of ion charge of either sign produced by secondary electrons in a small volume of air about the point:
= 1 C kg^{-1} of air (roentgen; 1 R = 1 esu cm^{-3} in air = 2.58×10^{-4} C kg^{-1})
Implicit in the definition is the assumption that the small test volume is embedded in a sufficiently large uniformly irradiated volume that the number of secondary electrons entering the volume equals the number leaving (so-called charged particle equilibrium). This unit is somewhat historical, but appears on many measuring instruments.

• **Unit of equivalent dose** (for biological damage) = sievert [= 100 rem (**r**oentgen **e**quivalent for **m**an)]: Equivalent dose H_T (Sv) in an organ T is equal to the absorbed dose in the organ (Gy) times the radiation weighting factor w_R (formerly the quality factor Q, but w_R is defined for the radiation incident on the body). It expresses long-term risks (primarily cancer and leukemia) from low-level chronic exposure. It depends upon the type of radiation and other factors, as follows [1]:

Table 29.1: Radiation weighting factors.

Radiation	w_R
X- and γ-rays, all energies	1
Electrons and muons, all energies	1
Neutrons < 10 keV	5
10–100 keV	10
> 100 keV to 2 MeV	20
2–20 MeV	10
> 20 MeV	5
Protons (other than recoils) > 2 MeV	5
Alphas, fission fragments, & heavy nuclei	20